In vitro evaluation of 2-methoxyestradiol-bis-sulphamate and crude *Sutherlandia frutescens* extracts as possible anticancer agents

CHRISTIAAN JACOB JOHAN VORSTER

(23085534)

Submitted in fulfilment of the requirements for the degree

MAGISTER SCIENTIAE

IN

PHYSIOLOGY

IN THE

FACULTY OF HEALTH SCIENCES

SCHOOL OF MEDICINE

UNIVERSITY OF PRETORIA

PRETORIA

Supervisor: Prof AM Joubert

Summary

In the search for new and improved anticancer therapies, researchers have identified several potentially useful compounds. Two of these agents are 2-methoxyestradiol-bis-sulphamate and extracts of *Sutherlandia frutescens*, an indigenous plant occurring in the Western Cape, with aqueous extracts being used traditionally as an anticancer agent. The aim of this study was to evaluate these compounds for efficacy against the MCF-7 and MCF-12A cell lines. The influence of these compounds on cell numbers, morphology, cell cycle progression and induction of cell death were investigated. Time- and dose-dependent studies were conducted using a concentration range of 0.2 - 1.0 μM for 2ME-BM and 0.5 - 2.5 mg/ml aqueous *S. frutescens* extracts respectively. These studies revealed pronounced cell line-specific responses to 2ME-BM after 24 hours at a concentration of 0.4 μM, and for *S. frutescens* extracts after 48 hours at a concentration of 1 mg/ml. Further studies revealed decreased cell density and cell death-associated morphology in samples exposed to both 2ME-BM and *S. frutescens* extracts. This study demonstrated and quantified the differential effects of both 2ME-BM and aqueous *S. frutescens* extracts on the carcinogenic MCF-7 and non-carcinogenic MCF-12A cell lines. Further research into the actions of these possible anticancer agents is warranted.

Keywords: 2-methoxyestradiol-bis-sulphamate, *Sutherlandia frutescens*, cancer, ethnopharmacology, steroid sulphatase inhibitor, apoptosis, autophagy, physiology, anticancer, therapy

Research outputs

Peer-reviewed research articles

- Vorster C, Stander A, Joubert A. Differential signaling involved in *Sutherlandia frutescens*-induced cell death in MCF-7 and MCF-12A cells. J Ethnopharmacol. 2012; 140 (1): 123-30.
- Vorster C, Joubert A. *In vitro* effects of 2-methoxyestradiol-bis-sulphamate on cell growth, morphology and cell cycle dynamics in the MCF-7 breast adenocarcinoma cell line. Biocell. 2010; 34 (2): 71-79.
- Vorster C, Joubert A. *In vitro* effects of 2-methoxyestradiol-bis-sulphamate on the non-tumorigenic MCF-12A cell line. Cell Biochem Funct. 2010; 28(5): 412-419.
- Stander BA, Marais S, Stivaktas V, Vorster C, Albrecht C, Lottering M, Joubert AM. *In vitro* effects of *Sutherlandia frutescens* water extracts on cell numbers, morphology, cell cycle progression and cell death in a tumorigenic and a non-tumorigenic epithelial breast cell line. J Ethnopharmacol. 2009; 124 (1): 45-60.

Conferences contributions

2008:

- Oral presentation:
  - Physiology Society of South Africa (PSSA) conference (Pretoria)
  - South African Academy of Sciences (University of Pretoria, Pretoria)
- Poster presentation:
  - Indigenous Plant Use Forum (IPUF) (Graaff-Reinet)
  - University of Pretoria Medical Faculty Day (Pretoria)
  - CANSA Research in Action Conference (Emperor's Palace)

2009:

- Oral presentation:
  - University of Pretoria Medical Faculty Day, Pretoria
  - South African Academy of Sciences (University of Potchefstroom)

2010:

- Oral presentation:
  - South African Academy for Science and Technology conference (Onderstepoort, Pretoria)
- Poster presentation:
  - South African Society for Biochemistry and Molecular Biology (SASBMB) conference (Bloemfontein)
  - University of Pretoria Medical Faculty Day (Pretoria)

2011:

- Poster presentation:
  - South African Cell Death Society (SACDS) conference (Cape Town)

Awards received

2008:

- CANSA Research in Action conference: Student Poster Award

2011:

- Best publication by a young researcher: Category: Non-clinical (2010), Faculty of Health Sciences, University of Pretoria
- Best overall publication: Category: Non-clinical (2010), Faculty of Health Sciences, University of Pretoria

Acknowledgements

The following people deserve more credit than I can put into words. Thank you.

- Prof. Annie Joubert, for her infinite patience, understanding and wisdom, for her guidance, both intellectual and otherwise, and above all for her humanity.
- Prof. Dirk van Papendorp, for the opportunity to complete this project in his department.
- My parents, Jan and Nilia Vorster, for their financial support, their caring and their unwaivering faith in my abilities.
- My brother, Jan-Daniël Vorster, for his ever-present encouragement, his moral support and his understanding.
- The staff of the Department of Physiology, in particular Andre Stander, Sumari Marais and Michelle Visagie, for all the meaningful discussions, practical advice and camaraderie.
- Facilities:
    - Department Physiology (Laboratory).
    - Department Chemistry (2ME-BM synthesis).
    - Department Pharmacology (Flow cytometry).
- Funding
    - Cancer Association of South Africa (CANSA).
    - Medical Research Council (MRC).
    - National Research Foundation (NRF).
    - Struwig-Germeshuysen Trust.
    - University of Pretoria School of Medicine Research Committee (RESCOM).

Declaration of originality

Full names of student: Christiaan Jacob Johan Vorster

Student number: 23085534

Declaration

1. I understand what plagiarism is and am aware of the University's policy in this regard.

2. I declare that this dissertation is my own original work. Where other people's work has been used (either from a printed source, Internet or any other source), this has been properly acknowledged and referenced in accordance with departmental requirements.

3. I have not used work previously produced by another student or any other person to hand in as my own.

4. I have not allowed, and will not allow, anyone to copy my work with the intention of passing it off as his or her own work.

SIGNATURE OF STUDENT:

Table of Contents

List of Figures

All figures in this document were generated by the author (unless stated otherwise) using CellDesignerTM 4.0.1 (http://celldesigner.org), MarvinSketch from ChemAxon (http://www.chemaxon.com/product/marvin_land.html), Cyflogic 1.2.1 (CyFlo Ltd. - http://www.cyflogic.com), Zeiss AxioVision software (Carl Zeiss MicroImaging, Inc., NY, USA - www.http://microscopy.zeiss.com) and Corel Paint Shop Pro Photo XI 11.20 (http://www.corel.com).

List of Tables

List of Abbreviations

- 2ME2 - 2-methoxyestradiol
- 2ME-BM - 2-methoxyestradiol-bis-sulphamate
- A2780 - A2780 ovarian carcinoma cell line
- AIDS - acquired immunodeficiency syndrome
- AIF - apoptosis-inducing factor
- AMP - adenosine monophosphate
- AMPK - adenosine monophosphate kinase
- ANOVA - analysis of variance
- AO - acridine orange
- Akt - serine/threonine kinase (protein kinase B)
- *APC* - adenomatosis polyposis coli gene
- APC/C - anaphase promoting complex or cyclosome

- Apo-2L - APO-2 ligand (apolipoprotein 2 ligand)
- Atg - autophagy-related protein
- ATM - ataxia telangiectasia mutated
- ATR - ataxia telangiectasia and Rad3 related
- Bax - Bcl-2-associated X protein
- Bcl-2 - B-cell lymphoma 2 protein
- BRCA1 - breast cancer 1, early onset protein
- *BRCA1* - breast cancer 1, early onset gene
- BRMS1 - breast cancer metastasis suppressor 1 protein
- BSA - bovine serum albumin
- Bub1 - budding uninhibited by benzimidazoles 1 protein
- Bub2 - budding uninhibited by benzimidazoles 2 protein
- Bub3 - budding uninhibited by benzimidazoles 3 protein
- C57BL/6J - C57 black 6 mice
- CAK - CDK-activating kinase
- cdc2 - cell division cycle 2 protein
- cdc14 - cell division cycle 14 protein
- cdc20 - cell division cycle 20 protein
- cdc25 - cell division cycle 25 protein
- CDK - cyclin-dependent kinase protein
- CHO - Chinese hamster ovary cancer cell line
- Cip - calf intestinal alkaline phosphatase protein

- c-Myc - myelocytomatosis oncogene
- *c-Sis* - platelet-derived growth factor 2 (PDGF2) proto-oncogene
- DEPTOR - DEP domain-encoding mTOR-interacting protein
- DHEA - dehydroepiandrosterone
- DHEA-S - dehydroepiandrosterone sulphate
- DIC - differential interference contrast
- DMEM - Dulbecco's modified Eagle's medium
- DMSO - dimethylsulphoxide
- DNA - deoxyribonucleic acid
- DNA-PK - DNA-dependent protein kinase
- DR4 - death receptor 4
- DR5 - death receptor 5
- DU-145 - DU-145 prostate cancer cell line
- E1A - human Y-chromosome haplogroup E1A
- E1S - oestrone sulphate
- E_2 - estradiol
- E2F - transcription factor E2F
- EGF - epidermal growth factor
- EGFR - epidermal growth factor receptor
- EndoG - endonuclease G
- ER - estrogen receptor
- Fas - Fas ligand (TNF ligand superfamily, member 6)

- FBS - fetal bovine serum
- FCS - fetal calf serum
- FITC - fluorescein isothiocyanate
- FL1 - forward scatter detector 1 (laser detector)
- FL3 -forward scatter detector 3 (laser detector)
- FoxO3 - forkhead box O3
- GβL - G protein beta subunit-like (MTOR associated protein, LST8 homolog)
- GADD45 - growth arrest and DNA damage
- GDP - guanine diphosphate
- GI_{50} - concentration inhibiting growth in 50% of cells
- GnRH - gonadotropin-releasing hormone
- GTP - guanine triphosphate
- GTPase - guanine triphosphate hydrolase enzyme
- H&E - haematoxylin and eosin
- HIF-1 - hypoxia-inducible factor 1
- HIF-1α - hypoxia-inducible factor 1 alpha subunit
- HIV - human immunodeficiency virus
- HUVEC - human umbilical cord vein endothelial cell
- IC_{50} - inhibitory concentration in 50% of cells
- IGF - insulin-like growth factor
- IGF-BP3 - insulin-like growth factor binding protein 3
- IgG - immunoglobulin G

- IL-1 - interleukin 1
- IL-7 - interleukin 7
- INK4 - inhibitor of cyclin-dependent kinase 4
- JNK1 - Jun N-terminal kinase 1
- Kip - kinase inhibitor protein
- LC3 - microtubule associated protein light chain 3
- LC3B - microtubule associated protein light chain 3 subunit B
- LNCaP - androgen-sensitive human prostate adenocarcinoma cell line
- Mad1 - mitotic arrest deficient 1 protein
- Mad2 - mitotic arrest deficient 2 protein
- Mad3 - mitotic arrest deficient 3 protein
- MAP-kinase - mitogen-activated protein kinase
- MAP4K3 - mitogen-activated protein kinase kinase kinase kinase 3
- MCF-7 - Michigan Cancer Foundation 7, breast adenocarcinoma cell line
- MCF-12A - Michigan Cancer Foundation 12A, breast epithelial cell line
- MDA-MB-231 - M.D. Anderson, metastatic breast 231 cell line
- Mdm-2 - murine double minute 2 protein
- MDR - multiple drug resistant
- MO - medium only
- MOMP - mitochondrial outer membrane permeabilization
- MPF - mitosis promoting factor
- MPT - mitochondrial permeability transition

- mTOR - mammalian target of rapamycin
- mTORC1 - mammalian target of rapamycin complex 1
- mTORC2 - mammalian target of rapamycin complex 2
- Myc - myelocytomatosis viral oncogene protein
- Myt1 - myelin transcription factor 1
- *MYC* - myelocytomatosis viral oncogene, coding for Myc protein
- NO - nitric oxide
- Noxa - Phorbol-12-myristate-13-acetate-induced protein 1
- p15 - cyclin-dependent kinase 4 inhibitor B (*CDKN2B*)
- p16 - cyclin-dependent kinase inhibitor 2A (*CDKN2A*)
- p18 - cyclin-dependent kinase 4 inhibitor 2C (*CDKN2C*)
- p19 - cyclin-dependent kinase 4 inhibitor 2D (*CDKN2D*)
- p21 - cyclin-dependent kinase inhibitor 1A (*CDKN1A*)
- p27 - cyclin-dependent kinase inhibitor 1B (*CDKN1B*)
- p53 - protein 53, tumor protein 53
- p57 - cyclin-dependent kinase inhibitor 1C (*CDKN1C*)
- p53AIP1 - p53-regulated apoptosis-inducing protein 1
- PBS - phosphate buffered saline
- PC3 - PC3 human prostate cancer cell line
- PDGF - platelet derived growth factor
- PEST - proline, glutamic acid, serine and threonine peptide sequence
- PI - propidium iodide

- PI-3K - phosphatidyl-inositol-3 kinase
- PIG3/8 - p53-inducible gene protein 3/8
- PlasDIC - polarization-optical transmitted light differential interference contrast
- PRAS40 - proline-rich AKT1 substrate
- pRb - retinoblastoma protein
- PRR5 - proline-rich 5 (renal)
- PS - phospatidyl-serine
- PTEN - phosphatase and tensin homolog protein
- PUMA - p53-upregulated modulator of apoptosis
- Raf - proto-oncogene serine/threonine-protein kinase
- raptor - regulatory-associated protein of mTOR
- Ras - rat sarcoma protein
- *RAS* - gene coding for rat sarcoma protein
- *RB1* - retinoblastoma gene, coding for pRB
- REDD1 - regulated in development and DNA damage 1 protein
- RNA - ribonucleic acid
- RNAse - ribonuclease
- rictor - rapamycin insensitive companion of mTOR
- ROS - reactive oxygen species
- R-point - restriction point
- RRAG - Ras-related GTP-binding protein
- *S. frutescens* - *Sutherlandia frutescens* (subspecies *microphylla*)

- Sin1 - stress-activated MAP kinase-interacting protein 1
- Src - sarcoma proto-oncogenic tyrosine kinase
- STS - steroid sulphatase inhibitor
- TEM - transmission electron microscopy
- TGF-α - transforming growth factor alpha
- TGF-β - transforming growth factor beta
- TNF - tumor necrosis factor
- *TP53* - protein 53 gene, coding for p53
- TRAIL - TNF-related apoptosis-inducing ligand
- TSC2 - tuberous sclerosis complex 2
- ULK1/2 - UNC-51 like kinase 1/2
- VEGF - vascular endothelial growth factor
- Vps34 - vacuolar protein sorting 34
- Waf1 - cyclin-dependent kinase inhibitor 1
- wee1 - wee1 serine threonine kinase

Chapter 1 - Literature review

1.1. Cancer as a disease

Cancer is one of the largest health risks in modern society, with approximately 12 million new cases reported and in excess of 7 million deaths attributed to cancer during 2008 worldwide [1] placing a significant burden on healthcare [2], an effect most notable in developing countries [3]. In 2009 Statistics South Africa reported in excess of 35 000 deaths (approximately 6% of the total deaths in South Africa) attributable to various neoplasms [4].

Cancer is a disease in which a single cell displays uncontrolled division as a result of the loss of tumor suppressor genes (e.g. *TP53* coding for p53 protein [5, 6], *APC* coding for adenomatous polyposis coli protein [7], *RB1* coding for retinoblastoma protein [8]) or the activation of proto-oncogenes [9] due to risk factors (figure 1). This genetically defective tumor cell can then divide without the normal cell cycle checkpoints, leading to an accumulation of mutations in the subsequent generations of cells. Cancers can often become invasive or metastatic, with individual cells becoming detached from the original tumor and degrading the extracellular matrix to spread to and invade other adjacent and remote parts of the body, forming secondary tumors.

There are several risk factors for cancer [10, 11, 12, 13, 14, 15], including carcinogens and mutagens (lifestyle factors (*e.g.* smoking [16, 17], alcohol [18]), chemicals (polycyclic aromatic hydrocarbons [19], nitrosamines [20], reactive aldehydes [21]), radiation and genetic predisposition (*e.g. BRCA1* mutation [22]). Mutagens are substances that cause cancer directly through damaging the genetic material, while carcinogens can cause cancer by any means (deoxyribonucleic acid (DNA) damage, disruption of normal metabolic processes).

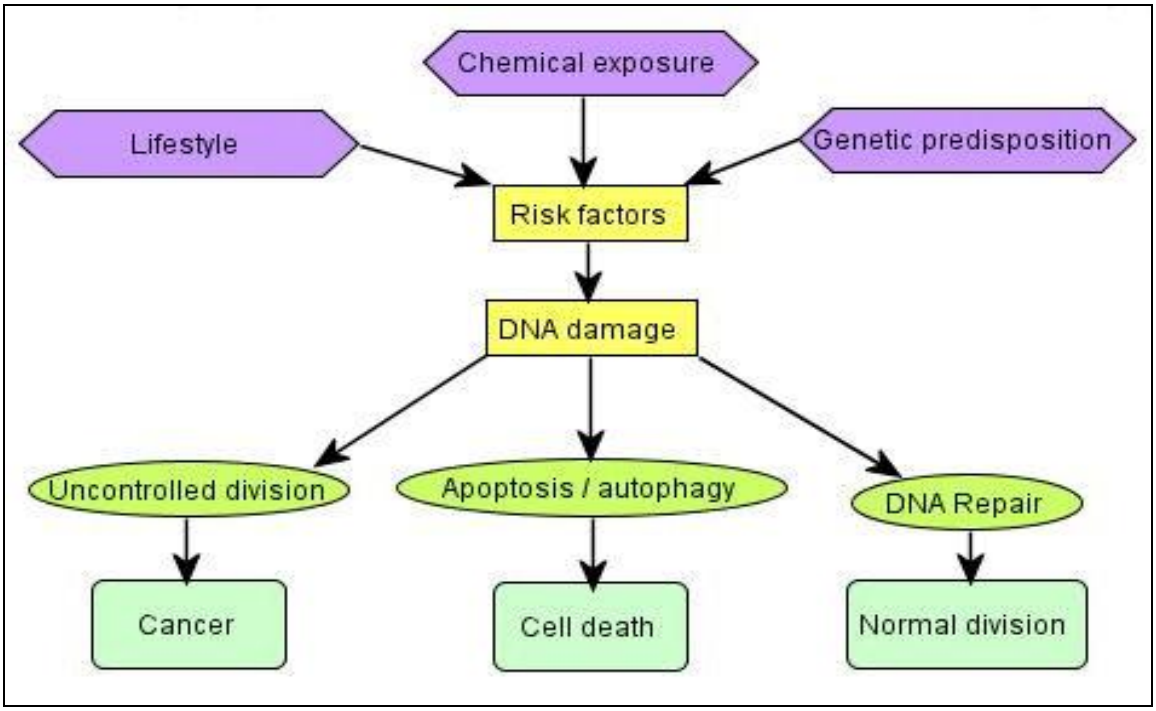

Figure 1: Diagrammatic representation of the various factors mediating formation of tumorigenic cells (diagram by author created with CellDesignerTM 4.0.1 - http://celldesigner.org)

1.1.1. Genetic basis of cancer

The genetics of cancer generally involves two classes of genes, namely oncogenes and tumor-suppressor genes. Recent research has indicated that microRNAs (miRNAs – noncoding RNAs) can influence the expression of several classes of genes involved in cell growth and division, including proto-oncogenes and tumor suppressor genes [23].

Proto-oncogenes [24, 25, 26, 27] are genes which, when mutated (then termed oncogenes) or hyper-expressed, cause cells to become resistant to normal cell cycle checkpoint machinery and continue to divide and escape programmed cell death even in the presence of a defective cell division cascade [28]. A single mutated proto-oncogene usually does not cause a tumor cell to form, requiring mutations in additional genes before checkpoint machinery can be completely abrogated. There are several different classes of proto-oncogenes, usually grouped together according to normal physiological function. Some examples will briefly be discussed, and a short summary is given in table 1.

Mitogens are pro-division factors, examples of which include platelet-derived growth factor (PDGF) [29] and insulin-like growth factor (IGF) [30]. Transcription factors are proteins which bind to target DNA sequences, thus controlling the expression (transcription) of a specific gene. A prominent example of a transcription factor is myelocytomatosis oncogene [31] (c-Myc, coded by the *MYC* gene) which plays roles in cell division and growth, cellular differentiation and programmed cell death [32, 33, 34]. The serine/threonine

kinases are a class of phosphorylative enzymes with a multitude of physiological functions. The examples most relevant to cancer physiology are the cyclin-dependent kinases [35, 36, 37, 38], which regulate the normal replicative process by forming active complexes with the various cyclins, as discussed later (section 1.2). Tyrosine kinases [39, 40, 41] are enzymes similar to serine threonine kinases, but with different specificity, playing various roles in cellular growth, differentiation and signaling. Notable examples of tyrosine kinases include epidermal growth factor receptor (EGFR) [42, 43, 44] and the sarcoma proto-oncogenic tyrosine kinase (Src) family proteins [45, 46, 47]. The guanine triphosphate hydrolase enzymes (GTPase enzymes) are a class of hydrolytic enzymes specifically targeted to guanosine triphosphate, fulfilling a host of functions in processes including cell division [48], cellular signaling and cellular transport [49]. The rat sarcoma (Ras) protein is a small GTPase which, through several distinct signaling cascades, influences processes such as cellular adhesion, cell division and cell death [50, 51, 52, 53].

Table 1: Examples of proto-oncogenes and their physiological functions

Type	Examples	Normal function
Mitogens	c-*Sis* (mutated PDGF B-chain gene)	Induces cell proliferation, over-expression causes uncontrolled division
Transcription factors	*MYC*	Regulation of pro-proliferative protein transcription
Serine/threonine kinases	Cyclin-dependent kinases (CDK's)	Phosphorylation of the OH-group of serine or threonine residues on effector molecules (e.g. cyclins, Raf etc.)
Tyrosine kinases	Epidermal growth factor receptor (EGFR), Src-family proteins	Phosphorylation of tyrosine residues on various effector molecules (e.g. Ras, PI3K etc.)
GTPases	Ras protein	Hydrolyses GTP to GDP to control activation of regulatory proteins

Tumor-suppressor genes inhibit the accumulation of transformation inducing gene mutations by repairing DNA damage or activating programmed cell death in case of irreparable damage by means of apoptosis or autophagy. Tumor-suppressor gene products generally protect the cell from a single, critical step in the formation of cancer, though there are exceptions (e.g. p53). Examples of tumor-suppressor proteins include the proteins involved in the DNA-damage checkpoints [54, 55], inhibitors of cell cycle machinery proteins [56] and those proteins involved in the initiation of programmed cell death (e.g. apoptosis / autophagy initiating proteins). Some examples are summarized

here, with a short overview presented in table 2. Further details of tumor suppressor genes relevant to this study are discussed in sections 1.2 and 1.3.

Several tumor suppressor genes act to suppress genes involved in active cell division. Defects in these genes promote uncontrolled expression of pro-mitotic factors and subsequent cell division. Examples of such tumor suppressors include CDK-activating kinase (CAK) [57, 58] and cell division cycle 25 protein (cdc25) [59]. Other tumor suppressor genes produce proteins that function in the cell cycle checkpoints, such as retinoblastoma protein (pRb) [8, 60], tumor protein 53 (p53) [61, 62], breast cancer 1, early onset protein (BRCA1) [22, 63] and cyclin-dependent kinase inhibitor 1A (p21) [64]. These proteins and their functions are discussed in section 1.2. Some tumor suppressor genes have functions in the regulation of cell death, such as phosphatase and tensin homolog (PTEN) [65, 66], which has roles in cell division and cell death, while other tumor suppressor genes such as breast cancer metastasis suppressor 1 (BRMS1) [67] play roles in cell adhesion (and thus metastasis of existing tumors).

Table 2: Functions of selected tumor suppressor genes

Category	Examples	Description
Gene repression	CAK, Cdc25	Suppression of genes / proteins required for continuation of cell cycle
Cell cycle checkpoints	pRb, p53, BRCA1, p21	Genes / proteins involved in cell cycle checkpoint machinery
Cell death	PTEN	Genes / proteins critical for initiation of programmed cell death in response to irreparable DNA damage
Cell adhesion	BRMS1	Genes / proteins involved in normal cell adhesion and contact inhibition, properties which have to be abrogated for metastasis to occur

1.1.2. Current treatment options

Currently available cancer treatment options will not be discussed in full, since it falls outside the scope of this study. However, a cursory understanding of the processes involved and their respective shortfalls will serve to underline the necessity of ongoing basic research into potential cancer therapies. Thus a brief discussion is provided.

The treatment for cancer is selected on the grounds of type, location and advancement of the individual tumor. Treatment options include chemotherapy [68], surgery [69, 70], hormonal therapy [71] and radiation [72, 73], with more recent breakthroughs adding monoclonal antibody treatment [74] and immunotherapy [75] to the arsenal. Surgical procedures utilized to treat cancer involve physical removal of the cancerous cells from the body [69]. These interventions are only effective in the case of defined, solid tumor masses in operable locations, and range from relatively minor procedures such as the removal of small, benign skin cancers [76] to procedures as complex and dangerous as radical mastectomy [77] or brain surgery.

Radiation therapy functions by targeting ionizing radiation to the localization of the tumor, which does significant damage to cellular DNA by means of molecular ionization. Damage to the genome is so severe that the targeted cells can no longer produce the necessary metabolic processes to sustain life and thus die. Examples of radiation therapy includes external beam radiotherapy [72] (several beams of radiation are targeted onto the

tumor from different angles, intersecting inside the tumor and thereby maximizing DNA damage there), and brachytherapy (a radiation source is placed inside or near the tumor, localizing the damaging effects to a comparatively small area) [78].

Hormonal therapy involves manipulation of normal hormone balance in order to inhibit the growth of specific types of tumors, known as hormone-dependent cancers [71]. Treatment can be subdivided into several categories, including hormonal synthesis inhibition (aromatase inhibitors [79], gonadotropin-releasing hormone (GnRH) analogs [80]), receptor antagonism (estrogen receptor modulators, androgen antagonists [81]) and hormonal supplementation. A brief summary with examples is given in table 3.

Table 3: Summary of treatment modalities for hormonal cancer therapy

Treatment	Examples	Description
Aromatase inhibitors	Aminoglutethimide, testolactone	Inhibit the aromatase enzyme, which is responsible for estrogen production
GnRH analogs	Goserelin, leuprolide	Lower estrogen levels by mimicking gonadotropin-releasing hormone, thus causing pituitary hyper stimulation
Estrogen receptor modulators	Tamoxifen, raloxifene	Block the estrogen receptor without causing activation
Androgen antagonists	Flutamide, bicalutamide	Inhibit androgen receptor activation
Hormone supplementation	Megestrol, fluoxymesterone, diethylstilbetrol, ocreotide	Hyper-stimulation of molecular pathways, leading to inhibition of tumor growth

Chemotherapy [68] is the treatment of cancer by chemical substances which exert either cytotoxic or cytostatic effects on the rapidly dividing cancer cells. It can be described as poisoning the cancer cells by deregulation of cell division, or mitosis. Although chemotherapy has a high rate of success in destroying cancer cells, normal and healthy cells are also severely affected by these drugs, most notably the cells which normally divide quickly, leading to side-effects profiles which can be nearly as damaging as the cancer itself [82]. Despite the development of chemotherapeutic resistant cancer, for lack of a better alternative, chemotherapy has been the mainstay of cancer therapy over the past decades [83]. A brief summary of chemotherapeutic classification and examples of specific drugs in each class is given in table 4.

Table 4: Examples of currently used chemotherapeutic agents and their mechanisms of action

Type	Examples	Description
Alkylating agents	Cisplatin, cyclophosphamide, chlorambucil	Alkylate nucleophilic groups on biologically relevant molecules, inhibiting functionality and thus causing cell death
Antimetabolites	Azathioprine, mercaptopurine	Molecular resemblance to purines or pyrimidines, incorporated into DNA, leading to loss of function
Anthracyclines	Doxorubicin, daunorubicin	Intercalates into DNA and RNA and disrupts molecular integrity, also inhibits topoisomerase and generates free oxygen radicals
Alkaloids	Taxol, vincristine, docetaxel	Plant-derived molecules, interfere with microtubule dynamics
Topoisomerase inhibitors	Topotecan, etoposide	Interferes with DNA replication by inhibition of topoisomerase isoforms

Immunotherapy [84] is a relatively recent addition to the arsenal of cancer therapies. It relies, in principle, upon the natural ability of the human body to recognize and mount an immune response against cancer cells [85, 86]. Monoclonal antibody treatment stems from a related field of research, relying on the use of monoclonal antibodies directed against extracellular markers found on some cancer cells. The monoclonal antibody binds to these markers, effectively designating the cancer cell for destruction by the immune system [87, 88].

Even though significant advances in cancer therapy has been made in recent years, all available cancer therapies retain significant and often near-fatal side-effects profiles, while being fully effective in only a small percentage of cases. It has thus become increasingly important to evaluate the cancer-cell specificity of potential drugs *in vitro* during the search for new anti-cancer therapies with improved side-effects profiles.

1.2. Potential anticancer compounds evaluated in this study

1.2.1. 2-Methoxyestradiol-bis-sulphamate

It has been reported that the natural metabolite of estradiol (E_2), namely 2-methoxyestradiol (2ME2) (figure 2), is a mitogen antagonist and tubulin poison that hinders cell proliferation and induces apoptosis in a large diversity of non-tumor and tumor cell lines *in vitro* (breast, prostate, colon and renal cell carcinoma cell lines) [89, 90, 91, 92, 93] and suppresses growth in certain murine tumors *in vivo* [94, 95, 96, 97]. In addition, this 17-ß-estradiol derivative has been shown to exert anti-inflammatory and anti-angiogenic effects [98, 97]. It can be synthesized from estrone using the 9 step procedure described by Prakasham *et al.* (2012) [99] or obtained commercially. Since phase I clinical trials have shown 2ME2 to be orally active and well tolerated it was patented as PANZEM® by EntreMed (Rockville, USA), and was subsequently included in human phase II clinical trials against breast cancer, prostate cancer and in patients suffering from multiple myeloma, renal cell carcinoma, as well as rheumatoid arthritis [100, 101, 102].

The possible molecular targets of 2ME2 include hypoxia-inducible factor-1α (HIF-1α), mammalian target of rapamycin (mTOR), transforming growth factor β (TGF-β) [103] and tubulin. HIF-1α is a subunit of HIF-1, a transcription factor which is normally activated during hypoxia to facilitate transcription of genes involved in angiogenesis, oxygen

transport, glucose metabolism, growth factor signaling, apoptosis, invasion and metastasis, and acts upon p53, murine double minute (Mdm-2) and vascular endothelial growth factor (VEGF) [104]. mTOR is a protein kinase influenced by the nutritional environment of the cell, growth factors (epidermal growth factor (EGF), IGF) and stress hypoxia. mTOR regulates the rate of protein synthesis (and thus cell growth), CDK synthesis, HIF-1 activation and cytoskeletal organization [105]. 2ME2 implements both its anti-angiogenic and antimitotic effects regardless of the cell's hormone receptor status and is accountable for abnormal mitotic spindle formation and mitotic accumulation in both estrogen receptor (ER) positive- and ER negative cells [94, 96, 97].

Hitherto, several studies have increased our knowledge of how 2ME2 exerts its pleiotropic effects [106, 107], however, the molecular mechanisms of action are not yet completely elucidated and research continues actively [89, 108]. Current research aims to refine the structures surrounding the steroid nucleus of the molecule to provide higher efficacy and lower toxicity [97], and to increase bioavailability by utilizing novel delivery systems [108]. Newman *et al.* (2006) [109] showed that bioavailability was among the parameters which could be improved by sulphamoylation of 2ME2. These sulphamoylated derivatives have improved bioavailability, plasma half-life and potency both *in vitro* (MDA-MB-231, MCF-7 cell lines) [110] and *in vivo* (female C57BL/6J mice) [111] when compared to 2ME2, causing irreversible cell cycle arrest.

One of the most successful sulphamoylated analogues of 2ME2 has been 2-methoxyestradiol-bis-sulphamate (2ME-BM). The molecule was created by the addition of sulphamate groups on carbons 3 and 17 (figure 2), and was originally developed as a steroid sulphatase (STS) inhibitor [110, 112, 113, 114]. STS inhibitors are intended to target hormone-dependent cancers by interfering with the conversion of oestrone sulphate (E1S) to oestrone and the hydrolysis of dehydroepiandrosterone sulphate (DHEA-S) to dehydroepiandrosterone (DHEA), which is reduced to 5-androstenediol [115].

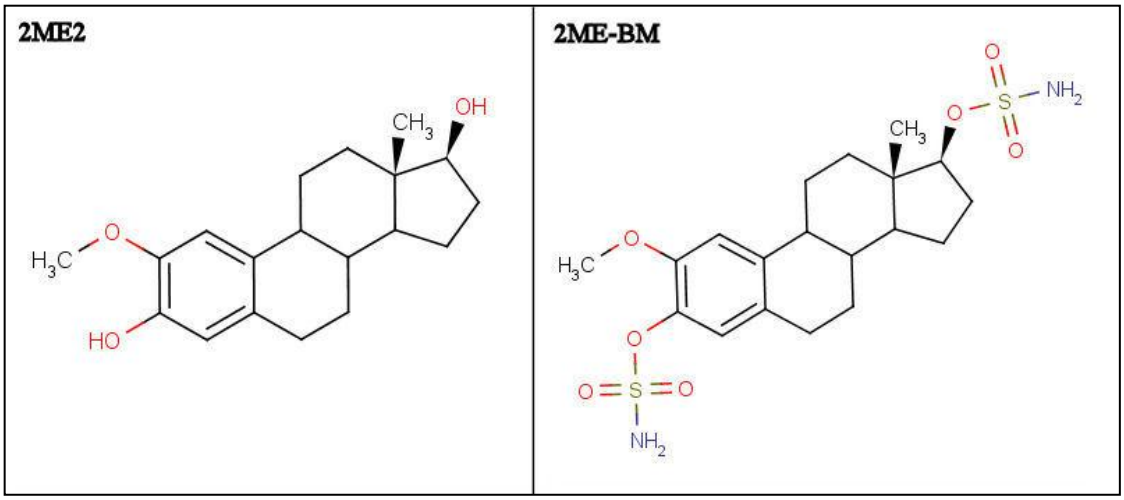

Figure 2: Chemical structures of 2ME2 and 2ME-BM (drawings by author using MarvinSketch software available from ChemAxon at http://www.chemaxon.com/product/marvin_land.html.)

2ME-BM has been shown to possess higher oral bioavailability [116, 117, 118] and high resistance to metabolic degradation [109] when compared to 2ME2 [111]. These characteristics are, in all probability, related to the sulphamate group added to the

original 2ME2 molecule, enabling the molecule to bind to carbonic anhydrase II in erythrocytes and thus escape first-pass inactivation by the liver.

2ME-BM irreversibly [119] inhibits cancer cell proliferation, tumor growth and angiogenesis [101, 115, 116, 117] in *in vitro* and *in vivo* [111, 118, 120] breast cancer models in both ER positive and negative tumors, as well as multiple drug resistant (MDR) cell lines [116]. A significantly decreased concentration of drug which inhibits cell growth in 50% of the population (IC_{50} value) was observed when growth inhibitory results from 2ME-BM are compared to those of 2ME [111, 119]. Literature has shown that this inhibition of proliferation is, at least in part, due to the ability of 2ME-BM to bind to the colchicine-binding site of tubulin, disrupting microtubule stability and thus causing both a G_2/M-phase cell cycle arrest and Bcl-2 phosphorylation (inactivation) and the subsequent induction of autophagy and apoptosis [118, 119, 121].

In view of these results, it became clear that research needs to be conducted in order to fully characterize the intracellular events responsible for these effects and that, in view of the enhanced potencies associated with sulphamoylated 2ME2 derivatives in traditionally resilient ER alpha negative [122] and MDR cells, these analogues hold considerable therapeutic potential for the treatment of both hormone-dependent and hormone-independent breast cancers.

1.2.2. *Sutherlandia frutescens*

Another area of cancer research which has made significant contributions toward improved cancer treatments is ethnopharmacology. Humans have a long-standing tradition of using plants and plant products as remedies for a variety of ailments, with specific formulations (teas, powders etc.) passed down mostly through oral history (of specific relevance in an African context). The more recent scientific study of natural products and molecular derivations of compounds found in these products has yielded approximately 60% of all used chemotherapeutic agents [123] and current research efforts combine several fields of specialization (e.g. anthropology, botany, chemistry and molecular biology) [124].

One of the traditional preparations which has recently shown promise is aqueous extracts of *Sutherlandia frutescens* (tribe Galegeae, Fabaceae) (figure 3), a shrub indigenous to South Africa, Lesotho, southern Namibia and southeastern Botswana [125]. It is used traditionally as a tea (aqueous extract) to treat a variety of ailments ranging from cancer and diabetes to intestinal disease [126, 127], and more recently to improve the overall health of HIV/AIDS patients [128, 129, 130, 131], and has been cultivated and commercialized on small scale since 1990. More recently, Phyto Nova (Pty) Ltd (http://www.phyto-nova.co.za/) has started large scale cultivation and export.

Figure 3: *Sutherlandia frutescens* plants showing leaves, flowers, pods and dried plant material. (Image adapted from: van Wyk BE, Albrecht C. A review of the taxonomy, ethnobotany, chemistry and pharmacology of Sutherlandia frutescens (Fabaceae) [125]).

Although *in vitro* research to evaluate the effects of *S. frutescens* on various disease states is available, the molecular mechanisms of action are still very poorly characterized. Plant extracts (water, ethanol, methanol, acetone, methylene dichloride) have demonstrated antiproliferative [126], anti-HIV [129], antidiabetic [132], anti-inflammatory, antibacterial [133], analgesic, anticonvulsant and antithrombotic activities.

Research into the chemical constitution of the plant has shown that *S. frutescens* contains large amounts of amino acids (notably L-arginine and L-canavinine), pinitol, flavonol glycosides and triterpenoid saponins [125]. L-canavanine replaces the structurally related amino acid L-arginine during protein synthesis, leading to non-functional proteins and

induction of apoptosis via Bcl-2 mediated caspase-3 induction [134], a signalling pathway which presents the further possibility of autophagy induction. L-arginine is a direct precursor of nitric oxide (NO) which has cytostatic and pro-apoptotic effects [135]. Pinitol is metabolised to D-chiro-inositol (3-0-methyl-1,2,4-cis-3,5,6-trans-hexahydroxycyclohexanol) which has insulin-like activity, affecting glucose transport [136]. Flavonol glycosides inhibit cytochrome P450 enzymes responsible for lipid and steroid catalysis [137], while triterpenoid saponin metabolites exert cytotoxic effects on tumor cells [138], inhibiting microtubule dynamics [139]. As discussed in section 1.4.1, apoptosis is a form of cell death characterized by nuclear condensation, membrane blebbing and cellular fragmentation, while autophagy comprises cellular self-digestion through the formation of acidic intracellular lysosomes. It has been demonstrated in our laboratory that ethanolic extracts of *S. frutescens* induce an S-phase cell cycle arrest, apoptosis and autophagy in cultured breast adenocarcinoma cells [140], while Chinkwo (2005) [126] showed that apoptosis induction occurred with the involvement of flip-flop translocation of the membrane protein phosphatidylserine.

It is suspected that ethanolic and aqueous extracts of *S. frutescens* have significantly different chemical constituents and would thus have different effects on the cellular physiology of both normal and transformed cells. The conditions of plant cultivation and method of extraction are also important parameters in the effects achieved by *S. frutescens* extracts. These variable aspects and the diverse effects produced by *S. frutescens* extracts indicate that a combination of compounds, rather than a single active ingredient, is responsible for the cytotoxic effects observed. Given the widespread

traditional use and therapeutic potential of *S. frutescens*, further research into the exact mechanisms involved in the induced cell death and the possible active ingredients of *S. frutescens* is warranted.

1.3. Overview of the cell cycle

The cell cycle is the progression of intracellular events necessary for replication of normally dividing cells. The process of division is divided into two main phases, namely interphase and mitosis. During interphase a cell grows, expands and functions, replicating its organelles, accumulating nutrients, increasing its cytoplasmic volume and eventually duplicating its genetic material. During mitosis the cell divides its cytoplasm and organelles, and splits into two new cells, each of them exiting mitosis and re-emerging into interphase. Both of these phases are further subdivided into distinct periods, each with its own unique events and characteristics (figure 4).

During interphase, a cell is termed as being in the G_0 phase if it is metabolizing the raw materials necessary for physiological function, but no longer actively dividing. A cell can also exit the cell cycle either permanently (senescence) or temporarily (quiescence), a level of differentiation at which cellular replication no longer takes place, or is no longer possible. However, if a cell is still actively dividing, it will continue through the cell cycle and pass sequentially though the G_1, S, G_2 and M phases (figure 4), each of which involves several checkpoints to ensure that successful replication can take place.

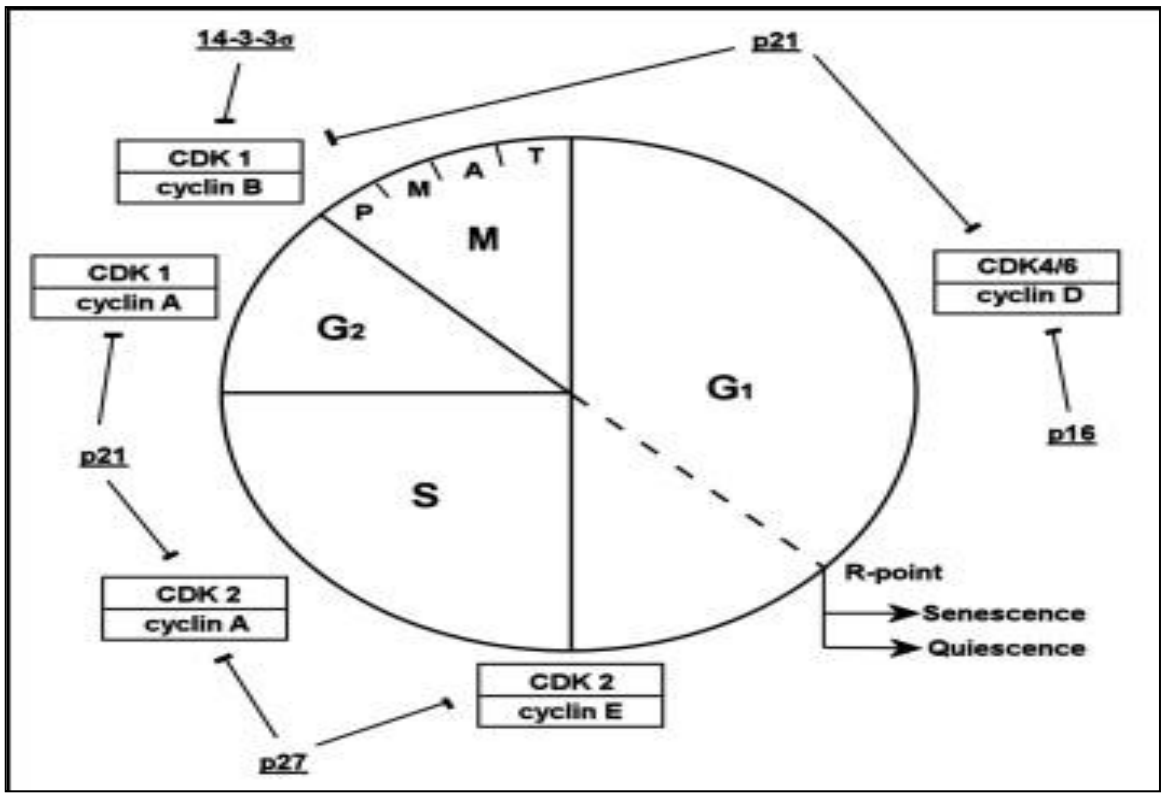

Figure 4: Normal cell cycle, showing the different phases (G_1, S, G_2, M), the CDK-cyclin complexes involved in each phase and the main inhibitors of each CDK-cyclin complex. (Diagram generated by the author using Corel Paint Shop Pro Photo XI)

During the G_1 phase the cell grows and metabolizes at a high rate, synthesizing the enzymes necessary for progression into the next phase, and this phase is characterized by an increase in cell volume and preparation for DNA replication (including the G_1-DNA-damage checkpoint). During the first part of the G_1 phase the cell is prompted by tissue-specific internal and external growth factors (mitogens), for example EGF, PDGF, IGF, transforming growth factors alpha and beta (TGF-α / TGF-β) and the interleukins (IL-1 to IL-7). After a certain point, however, progression of the cell through the cycle becomes

growth factor independent (i.e. withdrawal of growth factors no longer causes cessation of cell growth). This checkpoint, occurring after approximately two-thirds of the G_1 phase is called the restriction point (R-point), and is regulated largely by the E2F protein family (figure 4). Beyond this point the cell is committed to progress through the entire cycle culminating in division, and is no longer able to revert to quiescence. It is thus clear that the R-point is the critical decision point in the normal progression of the cell cycle, with the remaining checkpoints ensuring that replication is executed correctly.

During the S phase the cell's genetic material is duplicated, causing the aneuploid DNA-content (between 2N and 4N) that denominates this phase. The S-phase is characterized by DNA duplication, histone synthesis and quality control through the actions of a DNA-damage checkpoint to ensure the integrity of the genome during replication.

Organelle replication and the G_2-DNA damage checkpoint follow in the G_2 phase. During the G_2/M phase transition tubulin microtubules (composed of α- and β-subunits) are synthesized to segregate the chromosomes during metaphase of the M-phase. Interference with microtubule function is thus a promising target in combating rapidly dividing cancer cells.

The M phase (mitosis) contains the spindle attachment checkpoint and is subdivided into prophase (polarization of centrosomes and fragmentation of nuclear envelope), metaphase (chromosomes on metaphase plate), anaphase (chromatids separated), and telophase (reformation of nuclei, division of cytoplasm).

The subsequent interphase encompasses the G_1, S and G_2 phases. The cell is then back in G_1 phase, from where it can again follow any of the three available paths (quiescence, senescence or division).

1.3.1. Cell cycle regulation

The normal cell cycle has a complex mechanism of control, regulated by cyclin dependent kinases (CDK's) and cyclin proteins. Once the decision to proceed to mitosis is made (R-point) the control of progression through the subsequent phases is taken over by these protein complexes (also termed the "cell cycle clock machinery"). CDK's are serine/threonine protein kinases that are activated and targeted to the nucleus by forming complexes with the various isoforms of cyclin proteins. These complexes phosphorylate various target proteins (*e.g.* pRb), leading to the correct sequence of events for normal cell replication. The levels of the CDK's remain relatively constant throughout the cell cycle, with the cyclin of the previous phase being broken down (ubiquitination timed by proline, glutamic acid, serine and threonine peptide sequences (PEST-sequences) in cyclins) before synthesis of the next phase's cyclin. The $CDK_{4,6}$/cyclin D-complex is found throughout the G_1 phase, with the CDK_2/cyclin E-complex being responsible for the G_1/S transition. The S/G_2 transition is mediated by the CDK_2/cyclin A-complex, and the G_2/M transition by the CDK1(cdc2)/cyclin B-complex. Intricate positive and negative feedback mechanisms (e.g. cdc25-phosphatase, wee1-kinase etc.) as well as other stimulatory (e.g. MAP-kinase pathway) and inhibitory (p16 and p21 protein families, 14-3-3σ etc.) proteins regulate the activity of the CDK/cyclin complexes, ensuring that the complexes are activated only at the appropriate time and localization. The various cell cycle checkpoints also exert their effect on the progression of the cell cycle mostly though

inhibiting or stimulating the CDK/cyclin complexes or their regulatory proteins. This effect is mostly mediated through the actions of p53, probably the single most important cell cycle regulatory protein.

1.3.2. Cell cycle checkpoints

The function of these checkpoints is to halt progression until the damage that caused activation can be repaired, or induce apoptosis if the damage is irreparable. There are two essential checkpoint mechanisms monitoring the cell cycle: the DNA damage checkpoint (G_1/S phase transition, S phase, G_2 phase and metaphase) and the spindle-assembly checkpoint (during metaphase of mitosis). Factors that stimulate p53-activation, and would thus activate the G_1/S or G_2 checkpoints include oncogenic stimuli (E1A, c-Myc, E2F-1, Ras), hypoxia / hypoglycemia, DNA-damage (ATM/ATR, DNA-PK) and BRCA1.

1.3.2.1. G_1/S DNA damage checkpoint

The G_1/S checkpoint is effected through inhibition of the CDK4,6/cyclin D1-complex and the CDK2/cyclin E-complex. These two complexes phosphorylate pRb, sequestering it from its role as E2F-inhibitor during the G_1-phase. Once pRb is phosphorylated, the E2F-elongation factor is free to participate in the transcription of genes required for the G_1/S phase transition. The inhibitors of the CDK/cyclin complexes involved are the INK4-inhibitors ($p16^{INK4A}$, $p15^{INK4B}$,

p18^{INK4C} and p19^{INK4D}) and the downstream targets of p53, the Cip/Kip family proteins (p21$^{Waf1/Cip1}$, p27^{Kip1} and p57^{Kip2}) (figure 5).

1.3.2.2. S phase DNA damage checkpoint

The S phase checkpoint is unique in that it induces arrest not only in response to DNA damage of exogenous origin, but also in case of double strand breaks or replication fork stalls that originate during normal replication. It can operate to repair damage to DNA without interrupting DNA replication or cause DNA-polymerase to skip the replication of a damaged segment until repair is complete. It shares many of the proteins and pathways of the G_1/S and G_2 phase DNA damage checkpoints, including p53. The checkpoint is activated via a complex mechanism involving claspin and ATM/ATR (figure 5).

1.3.2.3. G_2 DNA damage checkpoint

The G2-checkpoint is executed through inhibition of the CDK1/cyclin B-complex, an effect mediated by the PI-3K family proteins (DNA-PK, ATM, ATR), and p21. The checkpoint operates by the inhibition of the CDK/cyclin-complex by p53, directly through the action of p21, and additionally by transcriptional up-regulation of downstream target genes (GADD45, 14-3-3σ). In the absence of active CDK1/cyclin B-complex, the cell is arrested in the G_2 phase (figure 5).

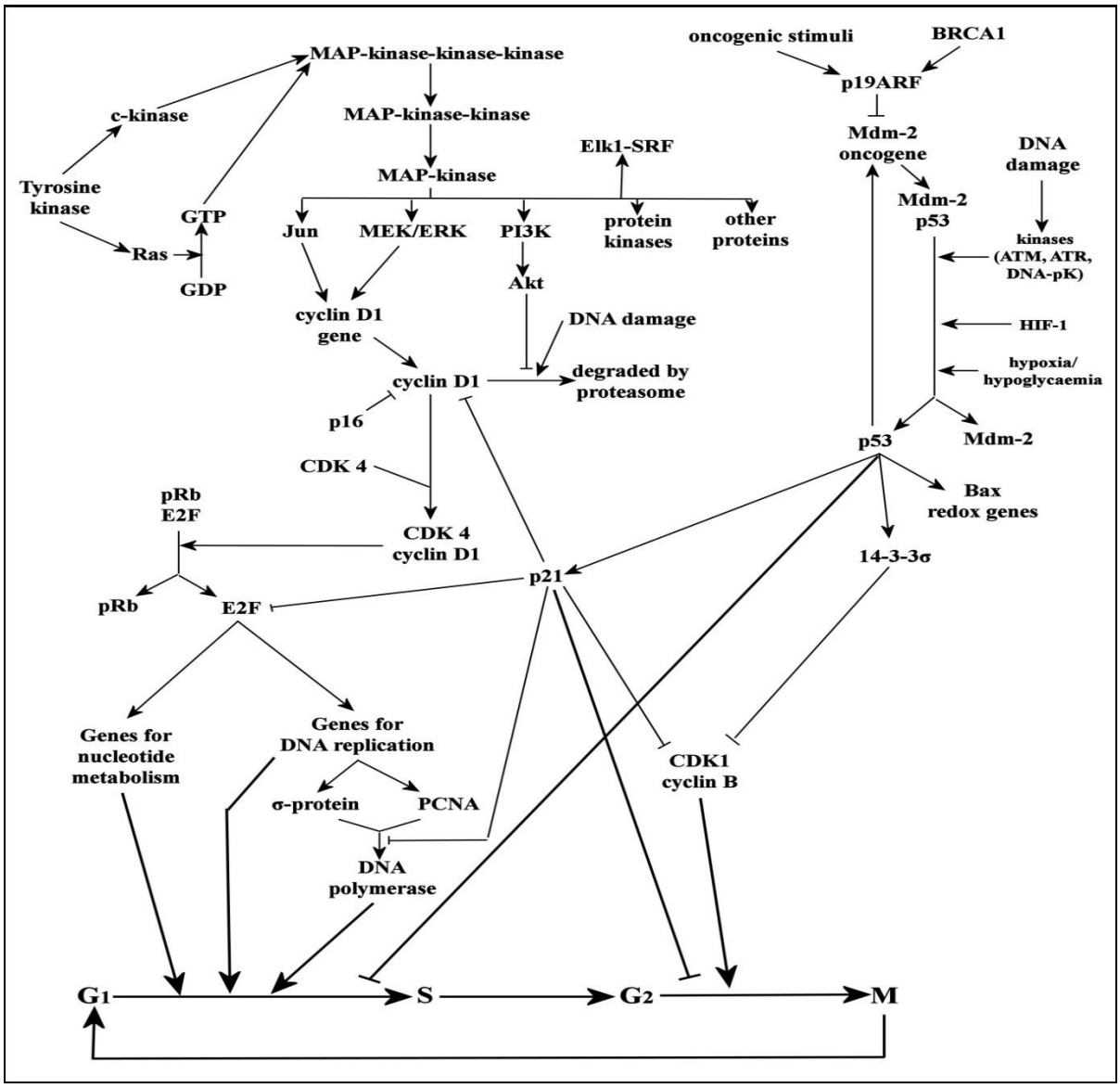

Figure 5: Summary of the molecular mechanisms involved in the DNA-damage checkpoints. The main regulatory molecules are p21 and p53, governing cell cycle progression through various effector molecules and regulatory pathways in response to inputs related to DNA integrity, nutritional status and growth factor signals. (Diagram generated by the author using Corel Paint Shop Pro Photo XI)

1.3.2.4. Spindle assembly checkpoint

The spindle assembly checkpoint [141] is active during the M phase and arrests cells in metaphase if damage is present. It is activated by damage to the chromosomes, and not by incorrect spindle formation. This checkpoint is mediated by Mad2 in association with Bub1, Bub3, Mad1 and the anaphase promoting complex or cyclosome (APC/C) [142], although p53 plays a role in its activation (figure 6). The APC/C is an ubiquitin ligase which is involved in chromosome segregation and progression to anaphase.

Extensive DNA damage leads to one or more defective kinetochores, which cannot maintain proper attachment to the spindle fibers. These unattached kinetochores are the initiators of the signal transduction cascade leading to the block in anaphase initiation through the activation of Mad2, a protein localized on the kinetochores. A conformational change in Mad2 allows it to form a complex including Mad1, Mad2, Mad3, Bub1 and Bub3, and bind to cdc20, an activator of APC/C, thus inhibiting chromosome segregation [143, 144]. The APC/C complex is also inhibited through the actions of Bub2, which inhibits cdc14, a promoter of APC/C activity during the exit from anaphase. Although plant cells can sometimes escape the spindle assembly checkpoint and continue through cell division with improper chromatid segregation, it is uncommon for mammalian cells to overcome this checkpoint, and its prolonged activation usually leads to the initiation of apoptosis through p53 activation [145].

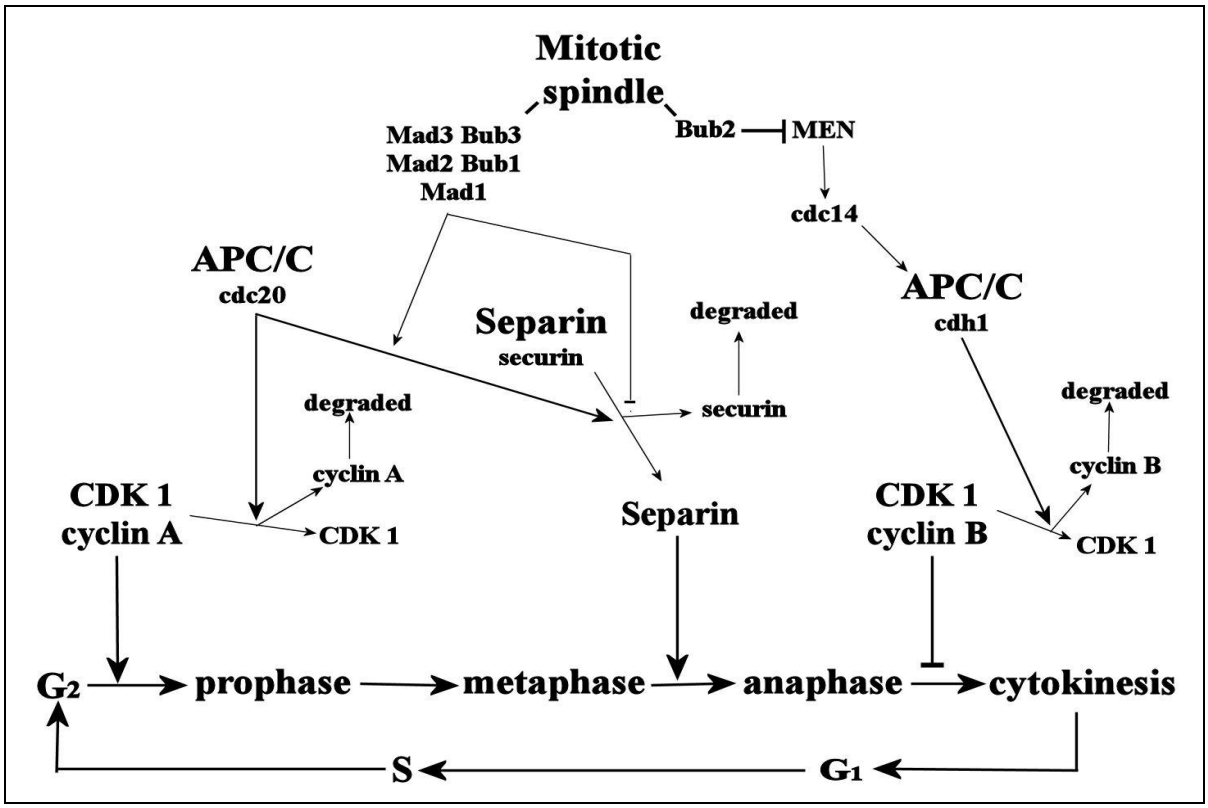

Figure 6: A schematic representation of the molecular machinery involved in the spindle assembly checkpoint. The main regulators are the APC/C complexes, separin-securin interaction and the CDK-cyclin complexes. (Diagram generated by the author using Corel Paint Shop Pro Photo XI)

1.4. Types of cell death

There exist several different, though interlinked, mechanisms of cell death (figure 7), each with its own distinct causes, effects and molecular mechanisms of action. Apoptosis is characterized by condensation of the chromatin and nuclear fragmentation, membrane blebbing and the formation of apoptotic bodies and is executed through the activation of effector caspases. Mitotic catastrophe involves nuclear fragmentation and the formation of multiple micronuclei, abnormal activation of the CDK1/cyclin B1 complex and lowered securin and survivin levels, with the early stages being caspase independent. Autophagy can be seen as a survival mechanism whereby the cell digests itself through lysosomal activity, and is characterized by the formation of autophagosomes and the lack of caspase involvement. Necrosis is uncontrolled at molecular level, and can be identified by the clumping and random degradation of DNA, the swelling and eventual rupture of the cell membrane and general organelle disintegration.

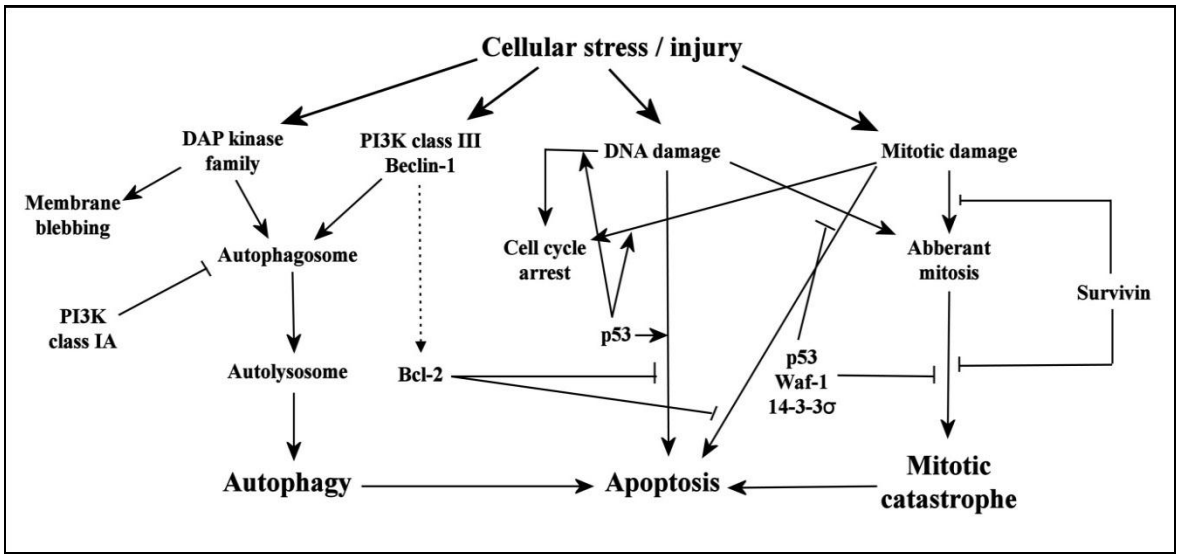

Figure 7: Schematic representation of the general interactions between different types of cell death. Autophagy, apoptosis and mitotic catastrophe can be initiated through distinct, interacting pathways with p53 and the PI3 kinases providing for cross-talk. (Diagram generated by the author using Corel Paint Shop Pro Photo XI)

1.4.1. Apoptosis

Apoptosis can be described as cellular suicide. It is a mechanism of cell death that is activated in response to irreparable damage to the cell's genome or structure. Apoptosis must, however, not be confused with accidental death (tissue injury), programmed/specialized cell death (e.g. cornification of skin), oncosis (characterized by cellular swelling), autophagy (cellular self-digestion) or necrosis (post-mortem changes to cells). The mitochondria [146] and p53 plays a central role in the cell's decision to initiate apoptosis. When activated, p53 induces pro-apoptotic gene transcription through receptor-mediated signaling (IGF-BP3, Fas, TRAIL[DR4/DR5] death receptors), and genes regulating apoptotic effector proteins (BAX, p53AIP1,

Noxa, PUMA, PIG3/8) and causing the release of reactive oxygen species (ROS). Death receptors (TNF gene-receptors) can induce apoptosis even in the absence of endogenous p53 activation. Morphologically, apoptosis is characterized by cell shrinkage, active blebbing of the plasma membrane, condensation and margination of chromatin and nuclear and cellular fragmentation. The membrane-bound cellular fragments are then phagocytosed by the surrounding cells and in particular phagocytes. The intracellular changes leading to apoptosis constitute an interplay of cytosolic and mitochondrial events (both pro-apoptotic and anti-apoptotic signals [147, 148]), with the release and activation of caspases (specialized protease enzymes) being the mechanism of self-destruction. As demonstrated in figure 8 the process of apoptosis can be divided into caspase-dependent and caspase-independent mechanisms.

Caspase-dependent apoptosis [149] occurs through the actions of the caspase family of enzymes. Caspases are subdivided into two categories. The initiator caspases (caspases 8, 9, 10 and 12) [150, 151, 152, 153] are activated by the intrinsic (mitochondrial mediated) or extrinsic (death-receptor mediated) pathways [154, 155], and function to activate the effector caspases (caspases 3, 6 and 7) [156, 157, 158], which are the enzymes responsible for cell death through the cleaving of various substrates.

The intrinsic pathway [159] is activated by the release of cytochrome *c* [160] from the mitochondria, forming the apoptosome complex (containing caspase 9), activating the

initiator caspases and commencing the apoptotic cascade. Interestingly, caspase 9 is also involved in cell survival through autophagy [161]. Mitochondrial cell death signaling and cytochrome *c* release is controlled by the Bcl-2 protein family [162, 163].

The extrinsic pathway [164, 165] is mediated through signaling mechanisms involving membrane-bound death receptors (e.g. Apo2L, TRAIL) [166, 167, 168] and caspase 8, and is initiated by extracellular cytokine signaling.

Caspase-independent apoptosis is initiated when apoptosis-inducing factor (AIF) [169, 170] and endonuclease G (EndoG) are translocated from the mitochondria to the nucleus [169]. AIF is a mitochondrial protein with both pro-apoptotic and pro-survival functions [171] depending on cellular localization. When contained within the mitochondria, AIF has a pro-survival role and functions in reactive oxygen species control [170, 172] through regulation of respiratory chain complex 1 [173]. When released from the mitochondria during mitochondrial outer membrane permeabilization (MOMP) however, AIF translocates to the nucleus and binds to DNA, causing condensation of chromatin and DNA cleavage [174, 175]. Mitochondrial EndoG is similarly released from the mitochondria and translocated to the nucleus where it causes DNA fragmentation [176]. However, the exact roles of and importance in apoptosis of both AIF and EndoG are still being elucidated and discussed [177].

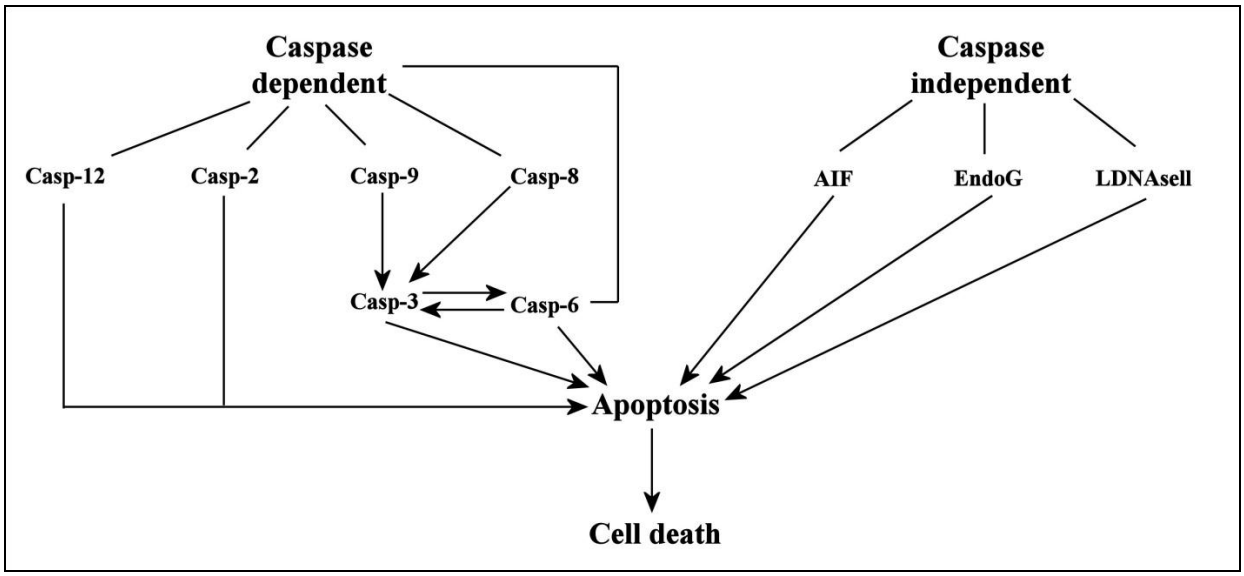

Figure 8: Caspase-dependent *vs*. caspase-independent induction of apoptosis. Caspase dependent apoptosis is induced through the effects of initiator and effector caspases, while caspase independent apoptosis is mediated mainly through the AIF, EndoG and LDNAsell proteins. (Diagram generated by the author using Corel Paint Shop Pro Photo XI)

1.4.2. Autophagy

The term autophagy (literally translating to self-eating) refers to a highly conserved metabolic process encompassing three distinct pathways (macroautophagy, microautophagy and chaperone-mediated autophagy) which lead to lysosomal degradation of organelles, portions of cytoplasm and proteins [178]. This process has a homeostatic role during normal cellular function through the degradation of old and damaged cellular components and their release into the cytosol for re-use [179, 180]. Under stressful conditions (nutrient starvation, hypoxia, oxidative stress, pathogen infection, carcinogenesis, radiation, or anticancer drug treatment) [181, 182, 183, 184] the rate at which autophagy occurs is dramatically increased in which case autophagic processes take on a cytoprotective role [185]. If, however, the stimulus exceeds the adaptive capability of the cell, autophagy can lead to cell death [178], with cross-talk to apoptotic mechanisms [186, 187, 188]. It has been suggested that autophagy can represent both a pro-survival and pro-death process [189] depending on the specific environmental conditions, and thus use of the term "autophagic cell death" has been discouraged, with the more accurate term of "cell death with autophagy" being used in recent scientific literature [190]. Supraphysiological autophagy has been reported in several disease states, including cancer, neuronal degeneration disorders and aging [178], and it has been shown that autophagy can confer chemoresistance to certain types of cancer cells. However, overstimulation of this pathway is being targeted as a potential novel mechanism by which to affect cancer cell death in cell lines resistant to apoptosis induction [191, 192]. Various traditional anticancer compounds have been shown to cause

autophagy induction (antiestrogens, radiation, resveratrol etc.), while autophagy inhibiting drugs in combination with chemotherapeutic agents have been shown to either increase or decrease cell death, depending on cell type and drug combinations [193]. Autophagy refers to a group of processes initiated when organelles, proteins or portions of cytoplasm are sequestered into double-membraned vesicles, or autophagosomes [194]. This autophagosome then fuses with a lysosome leading to the formation of autolysosomes, the contents of which are enzymatically degraded and released back into the cytosol through specialized pores.

1.4.2.1. Autophagic signaling

There exist several autophagic signaling pathways, each with its own unique molecular machinery and process (figure 9). Mammalian target of rapamycin plays a central role in the regulation and initiation of autophagy [195], integrating the input from signaling pathways linked to nutrient and growth factor status, apoptotic signaling and reactive oxygen species (ROS) signaling [196], with significant overlaps and cross-talk existing between these pathways [197]. mTOR forms two major complexes relating to autophagy signaling: the mTORC1 complex acting as the major inhibitor of autophagy, and the mTORC2 [198] complex which inhibits autophagy through the actions of protein kinase B (Akt) on the pro-apoptotic forkhead box O3 (FoxO3) in skeletal muscle [195].

The anti-apoptotic mTORC1 complex is composed of several protein subunits, including mTOR, regulatory-associated protein of mTOR (raptor), proline-rich AKT1 substrate (PRAS40), DEP domain-encoding mTOR-interacting protein (DEPTOR) and G protein beta subunit-like protein (GβL). It functions as the master inhibitor of autophagy by keeping the pro-apoptotic UNC-51 like kinase 1/2 (ULK1/2) complex in a phosphorylated, inactive state. Formation of mTORC1 complex is promoted by signaling pathways related to nutrient status, growth factors and insulin, and inhibited by cellular stress, starvation and rapamycin [195]. The mTORC2 complex is composed of the mTOR, rictor, stress-activated MAP kinase-interacting protein 1 (Sin1), PRR5, DEPTOR and GβL subunits and functions to inhibit autophagy in skeletal muscle through the actions of FoxO3 and Akt [195].

Several distinct signaling pathways are involved in regulating mTORC control over autophagy (figure 9). The availability of amino acids regulates mTOR activity through the actions of mitogen-activated protein kinase kinase kinase kinase 3 (MAP4K3), phosphatidyl-inositol-3 kinase (PI-3K) and IGF in conjunction with Akt, the Ras-related GTP-binding protein (RRAG) GTPase enzyme family and reactive oxygen species (ROS) released from mitochondria [195]. mTORC complexes can also be regulated through the adenosine monophosphate kinase (AMPK) pathway during glucose deficiency through the actions of tuberous sclerosis complex 2 (TSC2) [199]. The regulated in development

and DNA damage 1 (REDD1) protein regulates mTOR in response to hypoxia or endoplasmic reticulum stress [200].

1.4.2.2. Autophagosome activity

Autophagosome formation can begin once the inhibition of autophagy by the mTORC complexes is abrogated by cellular stress or starvation (figure 9). The *de novo* formation of autophagosomes is initiated in a membrane core organelle known as the isolation membrane or phagophore [201, 202]. Yeast cells display a single phagophore assembly site [203, 204] while mammalian cells display multiple sites of phagophore assembly [205, 206]. However, the origins of autophagosome membranes are not well understood and are the subject of continuing research [207]. An initial Bcl-2 regulated 208 Beclin-PI3K complex (including vacuolar protein sorting 34 (Vps34) and p150) forms and starts to assemble the double-membraned vesicle [209,208], creating a cup-shaped structure termed a preautophagosome, which then begins to engulf and sequester cytoplasm and organelles [210]. A complex comprising the microtubule-associated protein light chain 3-I (LC3), autophagy-related protein 5 (Atg5), Atg12 and Atg16L proteins is involved in the expansion of the autophagosome membrane, with Atg5, Atg12 and Atg16L being removed from the membrane upon completion while LC3 is degraded along with the rest of the autophagosome and its contents [211]. During this process of membrane expansion LC3-I is lipidated and modified to the membrane-bound LC3-II [210]. Once the autophagosome is complete it fuses with a lysosome, facilitating the

degradation of the autophagosomal contents by the lysosomal hydrolase enzymes [212]. Once an autophagosome has fused with a lysosome the resultant structure is known as an autolysosome [201]. The molecules which result from autolysosomal degradation can be released back into the cytosol for reuse through specialized membrane pores known as permeases [212].

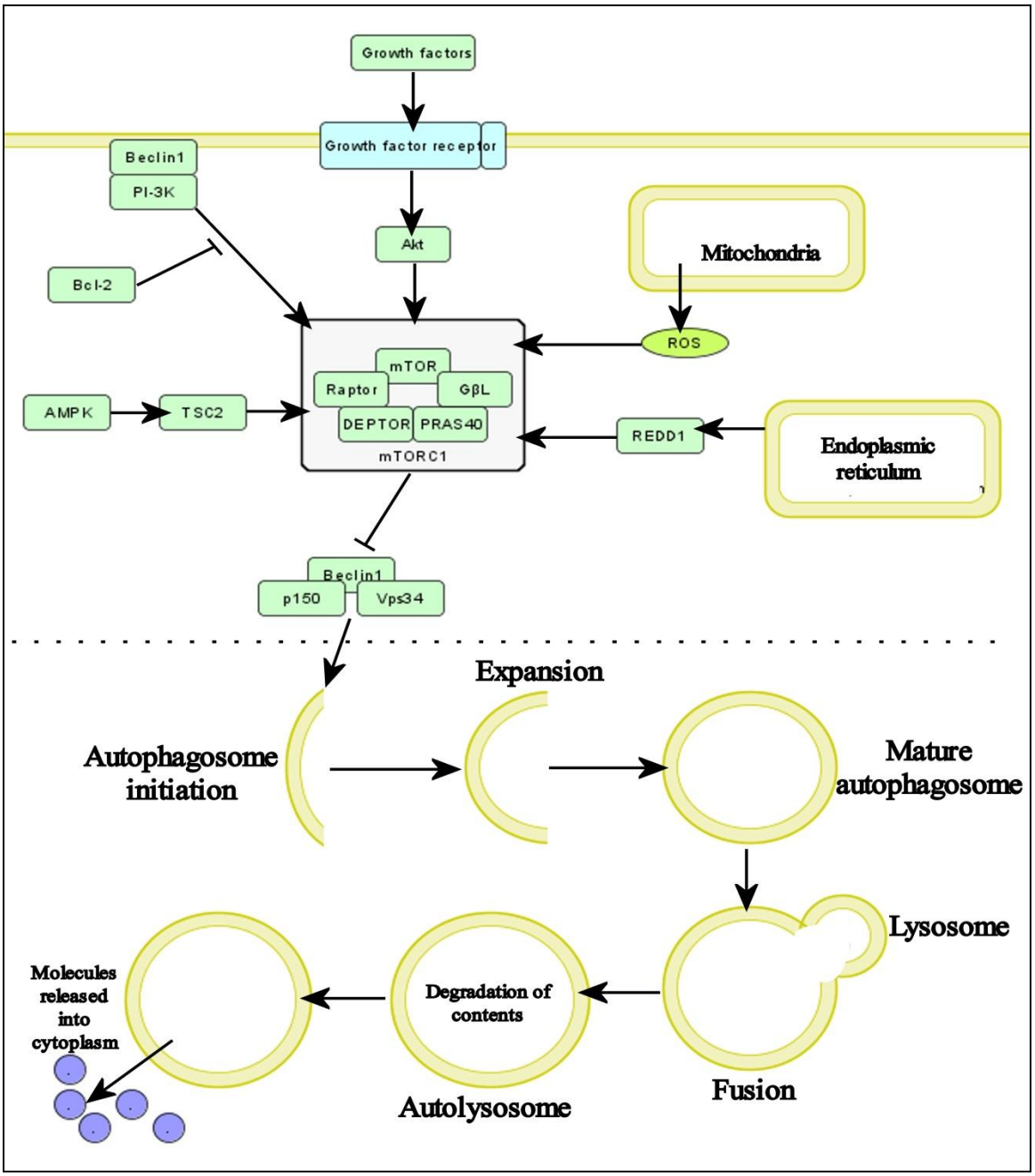

Figure 9: Autophagic induction signaling and autophagosome activity. The various pro- and anti-autophagic signals are integrated by the mTORC1 complex, which causes or inhibits autophagosome initiation and subsequent autophagy. (Diagram generated by the author using CellDesignerTM 4.0.1 - http://celldesigner.org and Corel Paint Shop Pro Photo XI).

1.5. Aims and Objectives

1.5.1. Aim

This study aimed to evaluate 2-methoxyestradiol-bis-sulphamate and crude *Sutherlandia frutescens* extracts *in vitro* as possible anticancer agents.

1.5.2. Objectives

The objectives of this study were to evaluate 2-methoxyestradiol-bis-sulphamate and crude *Sutherlandia frutescens* extracts as possible anticancer agents in the MCF-7 and MCF-12A cell lines using the following techniques:

- Spectrophotometry - crystal violet assays were used for quantification of growth inhibition and determination of optimal time-and dose parameters for further studies.

- Microscopy - light-, fluorescence- and transmission electron microscopic techniques were used to qualitatively evaluate cellular structure, cell cycle progression and cell death induction through autophagy and apoptosis.

- Flow cytometry - evaluation of cell cycle progression, cyclin B1 levels, mitochondrial membrane permeability, Annexin V externalization and LC3 localization through flow cytometry provided quantitative investigation of the intracellular events leading to the observed morphological changes and cell death.

1.5.3. Hypothesis

2-methoxyestradiol-bis-sulphamate and crude *Sutherlandia frutescens* extracts exert anticancer activity *in vitro*, and have differential effects on the tumorigenic MCF-7 and non-tumorigenic MCF-12A cell lines.

Chapter 2 - Materials and methods

2.1. Cell lines and culture techniques

2.1.1. Materials

The MCF-7 cell line was derived from a pleural effusion of human breast adenocarcinoma which is commercially available and was purchased from Highveld Biological Pty. (Ltd.) (Sandringham, SA). The MCF-12A cell line is a non-tumorigenic epithelial cell line produced by long-term culture of normal mammary tissue. These cells were a gift from Prof. Parker (Department of Medical Biochemistry, University of Cape Town, CT, SA). Dulbecco's Modified Eagle's Medium (DMEM), Ham's-F12 medium, trypsin, insulin, fetal calf serum (FCS), penicillin, endothelial growth factor, cholera toxin, streptomycin, fungizone, dimethyl sulphoxide, actinomycin D, flasks, plates, pipette tips and all other required materials were obtained from Sigma (St. Louis, USA) or Highveld Biological (Pty) Ltd. (Sandringham, SA) unless otherwise specified.

2.1.2. Methods

MCF-7 cells were cultured in DMEM supplemented with 10% FCS, penicillin (100µg/l), streptomycin (100µg/l) and fungizone (250µg/l. MCF-12A cells were cultured in a specialized medium containing DMEM, Ham's-F12 medium, fetal bovine serum, insulin, endothelial growth factor and cholera toxin. All cells were cultured at 37^{o}C in a humidified, 5% carbon dioxide environment. After seeding of an appropriate number of cells, flasks and plates were left overnight to allow for cell attachment. All experiments included the appropriate controls in the form of cells propagated in growth medium only

(MO), cells exposed to equivalent amounts of the vehicle dimethyl sulphoxide (DMSO) or distilled water (H_2O), as well as positive controls for apoptosis (actinomycin D) and autophagy (cells starved by culturing in 20% medium and 80% phosphate buffered saline). The DMSO vehicle has previously been shown to be non-toxic at the concentrations utilized (0.01% - 0.04% v/v). For each experiment, culture medium was changed before exposure.

2.2. Synthesis of 2-methoxyoestradiol-bis-sulphamate samples

Since 2ME-BM is not commercially available the estradiol-bis-sulphamate precursors and 2ME-BM were synthesized by Prof. R. Vleggaar from the Department of Chemistry at the University of Pretoria (Pretoria, SA).

2.3. Preparation of aqueous *Sutherlandia frutescens* extracts

2.3.1. Materials

Dried leaves and small twigs of *Sutherlandia frutescens* (family: Fabaceae, subspecies *Microphylla*) were purchased from Ms. Eilleen Menne of Karoo Herbs (De Aar, South Africa). Specimens of *S. frutescens* were harvested and air-dried in the shade.

2.3.2. Methods

Finely powdered *S. frutescens* leaves and twigs (0.5 g) were autoclaved and subsequently mixed to a final volume of 10ml with deionized boiling water and left overnight at room

temperature. The extract was centrifuged for 10min at 1000 × *g* (2500 rpm) and the supernatant was removed and filtered using a 0.2µm filter providing a stock solution extract of 0.05 g/ml as previously described [140].

2.4. Spectrophotometry

2.4.1. Materials

96-Well plates, glutaraldehyde, crystal violet and Triton-X100 were obtained from Sigma (St. Louis, USA) or Highveld Biological (Pty) Ltd. (Sandringham, SA). Absorbance measurements were made using a Bio-Tek Instruments ELX-800 Universal Microplate Reader.

2.4.2. Methods

Time- (24, 48 and 72 hours of exposure) and dose-dependent studies were conducted using a concentration range of 0.2 - 1.0 µM for 2ME-BM and 0.5 - 2.5 mg/ml aqueous *S. frutescens* extracts respectively to determine inhibition of cell proliferation and to select the optimal exposure parameters for this specific study. The concentrations and exposure times chosen for subsequent studies were selected to maximize the effects of the test compounds, while retaining a sufficient number of cells for effective assays. The crystal violet assay is a method for spectrophotometrically detecting the amount of DNA in a sample by measuring crystal violet dye uptake into the nuclei of cells in a monolayer culture, enabling researchers to calculate the number of cells in a certain sample by comparing the absorbance values of resolubilized dye to reference samples with known

cell numbers [213] [214]. Cells were seeded at 5 000 cells per well in 96-well plates and incubated overnight to ensure attachment. Cells were subsequently exposed to different concentrations of 2ME-BM or *S. frutescens* (and appropriate controls respectively) for 24, 48 and 72 hours, after which the experiment was terminated by removal of the medium and subsequent fixation of cells by glutaraldehyde. After 15 minutes, glutaraldehyde was replaced by crystal violet and cells were stained for a further 30 minutes. The plates were washed under slowly running tap water to remove excess stain and left to dry overnight. Crystal violet was then solubilized by addition of 200µl of Triton-X100 and incubation at room temperature for 30 minutes [215]. After mixing, 100µl of the solution was transferred to a clean 96-well plate and the absorbance was determined at 460 nm (with reference wavelength at 630 nm). Baseline values were determined before exposure to 2ME-BM and *S. frutescens* in order to quantify starting cell numbers by determining the cell numbers in untreated, test-identical samples at the time of exposure. The GI_{50} value was determined using the formula [(Tt - Tz) / (C - Tz)] x 100 = 50 (where C = medium only control value, Tt = Test sample value and Tz = baseline value).

2.5. Microscopy

2.5.1. Differential Interference Contrast Microscopy

2.5.1.1. Materials

Photomicrographs were taken at 100X and 400X magnification using a Zeiss inverted Axiovert CFL40 microscope and a Zeiss Axiovert MRm monochrome camera (Carl Zeiss MicroImaging, Inc., NY, USA).

2.5.1.2. Methods

Differential interference contrast microscopy (DIC) [216] (also called Nomarski Interference Contrast) was used to non-invasively evaluate the qualitative status of living cell populations. This technique utilizes a beam of polarized light being split into two beams, polarized at 90^{o} to each other with each taking a slightly different path through the sample. The optical density of the sample causes a different phase change in each of the two beams before they are recombined, leading to interference. The result is a three-dimensional relief indicating variations in optical density of the sample. DIC photomicrographs were taken of cells prior to fixation for haematoxylin and eosin staining.

2.5.2. Light microscopy

2.5.2.1. Materials

Haematoxylin, eosin, 6-well plates, coverslips, Bouin's fixative, ethanol, xylene and Entellan resin were obtained from Sigma (St. Louis, USA) or Highveld Biological (Pty) Ltd. (Sandringham, SA). Qualitative evaluation was conducted and photomicrographs were taken at 100X and 400X magnification with a Zeiss inverted Axiovert CFL40 microscope and a Zeiss Axiovert MRm monochrome camera (Carl Zeiss MicroImaging, Inc., NY, USA).

2.5.2.2. Methods

Haematoxylin and eosin (H&E) cell staining was conducted as a standard microscopic technique for qualitative evaluation of cellular morphology and in order to calculate the mitotic indices for quantitation of the cell cycle phase shift and abnormal morphology [217]. Haematoxylin [218] stains the nuclei of cells dark blue, while eosin [219] visualizes the cytoplasm and other eosinophilic structures in different shades of pink. Cells were seeded on heat-sterilized coverslips at 250 000 cells per well in 6-well plates and allowed to attach overnight. Cells were then exposed to 0.4µM 2ME-BM or 1mg/ml *S. frutescens* and appropriate controls respectively for 24 or 48 hours, after which coverslips were removed and fixed with Bouin's fixative for 30 minutes and 70% ethanol for a further 20 minutes. Coverslips were rinsed with tap water, stained with haematoxylin for 20 minutes, rinsed with tap water and 70% ethanol and stained with eosin for 7 minutes. Coverslips were then dehydrated stepwise with ethanol (70%, 96%, 100%) and xylene, after which they were mounted on

microscope slides with Entellan resin and allowed to dry overnight. Mitotic index counts were performed by microscopic examination of slides prepared for haematoxylin and eosin light microscopy in order to quantify the observed effects [220]. Cells were divided into the different phases of the cell cycle based on cellular and nuclear morphology. Where cells could not be categorized due to excessive fragmentation, highly unusual nuclear morphology or lack of clear nuclear material they were defined and counted as abnormal. One thousand cells in total were counted per slide and data was converted to represent the percentages of cells in each defined category.

2.5.3. Fluorescence microscopy

2.5.3.1. Materials - Autophagic lysosome detection

Hoechst 33342, propidium iodide (PI) and acridine orange (AO) were obtained from Sigma (St. Louis, USA). Wells were examined under a Zeiss inverted Axiovert CFL40 microscope camera (Carl Zeiss MicroImaging, Inc., NY, USA) and photomicrographs were taken with a Zeiss Axiovert MRm monochrome camera using different fluorescence filters to distinguish between the stains and composited with Zeiss AxioVision software. Zeiss filter 2 was used for Hoechst 33342 (blue emission) stained cells, Zeiss filter 9 for acridine orange-stained (green emission) cells and Zeiss filter 15 for propidium iodide (red emission) stained cells. Images were composited with Zeiss AxioVision software.

2.5.3.2. Methods - Autophagic lysosome detection

A fluorescent dye staining method was utilized in order to determine the effects that 2ME-BM and *S. frutescens* have on acidic vesicular organelle formation. Acridine orange [221] is a lysosomotropic fluorescent compound that serves as a tracer for acidic vesicular organelles including autophagic vacuoles and lysosomes [222]. Cells undergoing autophagy will have an increased tendency for AO staining when compared to viable cells. Hoechst 33342 is a fluorescent dye that can penetrate intact cell membranes of viable cells and cells undergoing apoptosis and stains the nucleus [223, 224]. PI concentrates in cells with damaged membranes (i.e. dead cells). Fluorescent triple staining with Hoechst 33342/acridine orange/propidium iodide was conducted in order to examine the cells for possible intracellular markers of autophagy. Cells were seeded at 250 000 cells per well in 6-well plates and allowed to attach overnight. Cells were then exposed to 2ME-BM, *S. frutescens* or appropriate controls in fresh medium for 24 h and 48 h respectively, after which cells were incubated with 0.9 µM Hoechst 33342 and 50 µM acridine orange in phosphate buffered saline for 30 min at 37^{o}C. Subsequently 12 µM propidium iodide was added for a further 5 min, after which the cells were washed twice with phosphate buffered saline (PBS). Samples were examined under a Zeiss inverted Axiovert CFL40 microscope and photomicrographs were taken.

2.5.3.3. Materials - Tubulin cytoskeleton

The primary monoclonal mouse anti-human IgG1 tubulin-alpha antibody (clone DM1A, catalogue number IMG-80196), manufactured by IMGENE (Alexandria, VA,

USA), was purchased from BIOCOM Biotech (Pty) Ltd. (Pretoria, Gauteng, South Africa). The secondary donkey anti-mouse IgG antibody labeled with Alexa Fluor 488 (catalogue number A-21202), manufactured by Invitrogen (Carlsbad, CA, USA), was purchased from The Scientific Group (Johannesburg, South Africa). Photomicrographs were taken using a Zeiss LSM 510 Meta Confocal microscope (University of Pretoria Microscopy Unit).

2.5.3.4. Methods - Tubulin cytoskeleton

Microtubules are intracellular filaments consisting of alpha- and beta-subunits which perform vital functions in the cytoskeletal structure, intracellular transport and mitotic cell division. As 2ME-BM has been shown to disrupt microtubule stability by binding to the colchicine binding site of tubulin, fluorescence-labeled antibodies to tubulin were used to demonstrate the disruptive effects of 2ME-BM on the intracellular microtubule network and mitotic spindle formation. Cells were seeded into 6-well plates (350 000 cells per well), allowed to attach overnight and subsequently exposed to 0.4µM 2ME-BM or appropriate controls respectively for 24 hours. The medium was then removed and cells were washed twice for 2 minutes using a pH controlled (pH=7) cytoskeletal buffer (CB) containing 10mM ethylene glycol tetraacetic acid, 4mM magnesium sulphate heptahydrate, 60mM 1,4-piperazinediethanesulfonic acid and 27mM 4-(2-hydroxyethyl)-1-piperazineethanesulfonic acid. Cells were fixated for 15 minutes with a 0.3% glutaraldehyde in CB solution at 37^{o}C and washed three times with CB before membrane permeabilization with a 1% Triton X-100 in CB solution (15 minutes at room temperature). After subsequent wash steps (once with

CB, twice with PBS) unreacted aldehydes were removed using two 10 minute washes with freshly prepared 1 mg/ml sodium borohydride in distilled water. Cells were washed with PBS and non-specific antibody-binding sites were blocked by a blocking buffer – a PBS solution containing 10% fetal bovine serum (FBS) and 0.05% Triton X-100 (60 minutes at room temperature). Tubulin was subsequently bound by the primary antibody by incubating cells with a PBS cocktail containing the primary tubulin antibody (1:50 dilution), 2% bovine serum albumin (BSA) and 1% Triton X-100 for 90 minutes at 37^{o}C. Unbound primary antibodies were removed by washing with blocking buffer, after which the bound primary antibodies were labeled with the secondary anti-mouse IgG Alexa Fluor 488 antibodies in blocking buffer (90 minutes at 37^{o}C). After being washed twice with blocking buffer and twice with PBS containing 0.05% Triton X-100, nuclei were counterstained with a 1µg/ml solution of 4',6-diamidino-2-phenylindole (DAPI) in PBS and subsequently washed with PBS before photomicrographs were taken.

2.5.4. Transmission Electron Microscopy

2.5.4.1. Materials

All analytical grade chemicals used were obtained from Sigma (St. Louis, USA) or Highveld Biological (Pty) Ltd. (Sandringham, SA). Other materials and equipment required were provided by the Microscopy Unit of the University of Pretoria, where the electron micrographs were taken.

2.5.4.2. Methods

Transmission electron micrographs were acquired in order to examine the ultrastructural changes associated with 2ME-BM exposure. Cells were seeded at 750 000 cells per flask in 25cm^2 flasks and allowed to attach overnight. Cells were subsequently exposed to 2ME-BM and appropriate controls respectively for 24 hours. Samples were then trypsinized and resuspended in 1 ml growth medium. The cells were subsequently fixed with glutaraldehyde (2.5% in 0.075 M phosphate buffer) for 1 hour, washed with phosphate buffer and fixed with 0.25% aqueous osmium tetroxide for 30 minutes. After washing with distilled water the cells were dehydrated stepwise using 30%, 50%, 70%, 90% and 100% ethanol before being infiltrated with and embedded in Quetol (50% Quetol in ethanol for 1 hour, then 100% Quetol^{TM} for 4 to 6 hours) [215]. Sections were cut using a diamond ultramicrotome and placed on copper grids. Samples were further contrasted with aqueous 4% uranyl acetate and Reynolds lead citrate before electron micrographs were taken.

2.6. Flow cytometry

Flow cytometry is a technique which uses hydro-dynamic focusing to pass the cells in a suspension sample by a set of fluorescence and laser detectors one at a time, enabling them to be counted and the fluorescence emissions quantified. In this manner, a large volume of cells can be analyzed for a specific fluorescent probe. In this study, flow cytometry was used to confirm the observed cell death and cell cycle disturbances and to investigate the intracellular events causing these aberrations. Cells were seeded at 750 000 cells per flask in 25cm^2 flasks and allowed to attach overnight. For cell cycle analyses, results are expressed as percentage of the cells in each phase. Generated data was analyzed using Cyflogic software (CyFlo Ltd. - http://www.cyflogic.com/). Cells were exposed to 2ME-BM, *S. frutescens* or appropriate controls respectively for 24 or 48 hours, after which the following protocols were followed:

2.6.1. Cell cycle progression and cyclin B analysis

2.6.1.1. Materials

The fluorescein isothiocyanate (FITC)-conjugated cyclin B1 antibody reagent set from BD Pharmingen (Rockville, USA) was utilized. Analyses were conducted using a Beckman Coulter Cytomics FC500 instrument (Beckman Coulter Inc., Fullerton, CA, USA).

2.6.1.2. Methods

Cell cycle progression can be measured in flow cytometric analyses by utilizing PI, a fluorescent dye that binds to DNA. The amount and distribution of PI within a specific cell can be correlated to its current position in the cell cycle (*i.e.* G_1, S, G_2 or M phase), yielding valuable information about the general condition of a population of cells. Since 2ME2 has been shown to induce a G_2/M phase block in treated cells, the effects of 2ME-BM and aqueous *S. frutescens* extracts on cell cycle dynamics were investigated respectively contributing to the identification of targeted cellular pathways. Cyclin B forms part of the mitosis-promoting factor (MPF) and is broken down directly after the G_2/M phase transition, thus the levels of cyclin B will be elevated during a G_2/M phase block. Considering the above-mentioned effects of 2ME2 on the cell cycle, cyclin B is a potential, as yet unconfirmed target for 2ME-BM. Cyclin B was marked with a fluorescent antibody and the protein levels were determined by means of flow cytometry. Cells were trypsinized and fixated with 10 ml ice-cold 70% ethanol and stored at 4ºC for 24 hours. After 24 hours, cells ($1x10^6$) were washed with PBS and incubated with either FITC-conjugated mouse immunoglobulin G (IgG) as a control or FITC-conjugated cyclin B1 antibody (1:400 dilution) for 30 min at room temperature. Cells were then washed and resuspended in 0.5 ml PBS containing 40 µg/ml propidium iodide and 100 µg/ml RNase A for 30 min at 4°C. Propidium iodide staining was added in order to simultaneously analyze DNA-based cell cycle dynamics. Data from at least 10 000 cells were analyzed with CXP software (Beckman Coulter South Africa (Pty) Ltd) and Cyflogic software

(CyFlo Ltd. - http://www.cyflogic.com/). Aggregated and aneuploid cells were removed from analysis by visual inspection. For cyclin B1 analyses, fluorescence of the FITC-conjugated isotypic control was normalized to 1% on a logarithmic forward scatter 3 (FL3-log) *vs*. linear forward scatter 1 (FL1-lin) dot-plot. FITC-conjugated cyclin B1 fluorescence of control and exposed MCF-7 cells were measured utilizing the normalized area of the dot-plot.

2.6.2. Apoptosis detection

2.6.2.1. Materials

Annexin V-FITC staining kit was purchased from BIOCOM Biotec Pty (Ltd) (Clubview, South Africa). Propidium iodide was obtained from Sigma (St. Louis, USA). Analyses were conducted using a Beckman Coulter Cytomics FC500 instrument (Beckman Coulter Inc., Fullerton, CA, USA).

2.6.2.2. Methods

The induction of apoptosis by 2ME-BM and aqueous *S. frutescens* extracts were investigated by means of Annexin V binding. Annexin V is a calcium-dependent phospholipid binding protein with a high affinity for phosphatidylserine (PS) [225]. During the early stages of apoptosis, phosphatidylserine is externalized on the plasma membrane and can be selectively bound by fluorescent-labeled Annexin V. Cells were co-stained with propidium iodide in order to evaluate membrane integrity according to the method proposed by Moore *et al*. (1998) [226]. Trypsinized cells

($1x10^6$) were suspended in binding buffer and centrifuged at 300 x g for 10min to remove supernatant. Cells were subsequently exposed to 10µl of Annexin V-FITC in 100µl of binding buffer for 15 minutes at room temperature, after which cells were centrifuged and resuspended in 500µl of binding buffer. Propidium iodide solution (5µl of 100µg/ml) was added immediately before analysis. Data was obtained from a logarithmic plot of the forward scatter detector 1 (FL1) for FITC and the forward scatter detector 3 (FL3) for propidium iodide. Cellular debris and cell clumps were removed from analysis by visual gating of data. Data from at least 10 000 cells were analyzed with CXP software (Beckman Coulter South Africa (Pty) Ltd) and Cyflogic software (CyFlo Ltd. - http://www.cyflogic.com/).

2.6.3. Mitochondrial permeability

2.6.3.1. Materials

The MitoCapture™ Mitochondrial Apoptosis Detection Kit was obtained from BIOCOM Biotech Pty (Ltd) (Clubview, South Africa). Analyses were conducted using a Beckman Coulter Cytomics FC500 instrument (Beckman Coulter Inc., Fullerton, CA, USA).

2.6.3.2. Methods

The induction of apoptosis via the mitochondrial pathway causes the outer membranes of mitochondria to become water permeable, leading to the release of pro-apoptotic factors into the cytosol during an event known as the mitochondrial permeability transition (MPT) or MOMP. This effect can be observed by using a

cationic fluorescent dye which aggregates and polymerizes in normal mitochondria but is released from permeabilized mitochondria, remaining in its monomeric form in the cytoplasm. The dye gives of red fluorescence in the PI channel (617 nm emission) when it is polymerized (in mitochondria) and green fluorescence in the FITC channel (521 nm emission) in its monomeric form (in cytoplasm). Trypsinized cells were centrifuged, washed with PBS and resuspended in 1ml of pre-warmed incubation buffer containing 1µl of MitoCapture^{TM} solution. Cells were incubated at 37^{o}C and 5% CO_2 for 20 minutes, centrifuged, resuspended in 1ml of incubation buffer and analyzed immediately. Data was collected using a logarithmic plot of the forward scatter detector 1 (FL1). Cellular debris and cell clumps were removed from analysis by visual gating of data. Data from at least 10 000 cells were analyzed with CXP software (Beckman Coulter South Africa (Pty) Ltd) and Cyflogic software (CyFlo Ltd. - http://www.cyflogic.com/).

2.6.4. Autophagosome detection

2.6.4.1. Materials

The rabbit polyclonal DyLight488-conjugated anti-LC3B antibody was obtained from BIOCOM Biotech Pty (Ltd). Formaldehyde, methanol, Triton-X100, propidium iodide and BSA was obtained from Sigma (St. Louis, USA) or Highveld Biological (Pty) Ltd. (Sandringham, SA). Analyses were conducted using a Beckman Coulter Cytomics FC500 instrument (Beckman Coulter Inc., Fullerton, CA, USA).

2.6.4.2. Methods

Autophagy is a process by which the cell digests organelles, proteins and portions of cytoplasm by fusing double-membraned cytoplasmic inclusions (termed autophagosomes) to lysosomes (containing digestive enzymes). During the formation of autophagosomes cytosolic LC3-I is converted to LC3-II by conjugation to phosphatidylethanolamine and associated with the autophagosomal membrane. The amount of LC3 and its cellular localization can thus be utilized to quantify the induction of autophagy. Trypsinized cells were washed with PBS, centrifuged and fixed at 4^{o}C in 3ml of PBS containing 0.01% formaldehyde for 10 minutes. Cells were then centrifuged, washed with PBS and resuspended in 1ml of methanol (-20^{o}C) for 15 minutes at 4^{o}C. Cells were centrifuged, washed with PBS and resuspended in 0.5ml of PBS containing 0.05% Triton-X100, 1% BSA, 40µg/ml propidium iodide and 0.5µg/ml of rabbit polyclonal DyLight488-conconjugated anti-LC3B antibody (1:200 dilution) for 2 hours at 4^{o}C. Cells were centrifuged, washed with PBS containing 0.05% Triton-X100 and 1% BSA and analyzed immediately. Data was collected using a logarithmic plot of the forward scatter detector 1 (FL1). Cellular debris and cell clumps were removed from analysis by visual gating of data. Data from at least 10 000 cells were analyzed with CXP software (Beckman Coulter South Africa (Pty) Ltd) and Cyflogic software (CyFlo Ltd. - http://www.cyflogic.com/).

2.7. Statistical Analysis

2.7.1. Qualitative data

Representative data from qualitative experiments (light-, fluorescence- and electron microscopy) are shown. Each of these experiments was comprised of three independent replicates, containing test samples, control samples (vehicle control, positive control) and samples propagated in medium only.

2.7.2. Quantitative data

Spectrophotometric experiments were repeated thrice, with each experiment comprising six biological replicates of each test or control group. Flow cytometric analyses were composed of three independent experiments, each containing test samples and appropriate controls. The data obtained were statistically analyzed for significance using the analysis of variance (ANOVA)-single factor model followed by a two-tailed Student's *t*-test. Means are presented in bar charts, with T-bars referring to standard deviations. *P*-values < 0.05 were regarded as statistically significant and are marked with asterisks. For flow cytometric data at least 10 000 - 30 000 events were counted per sample using the Beckman Coulter Cytomics FC500 instrument with CXP software (Beckman Coulter South Africa (Pty) Ltd). Replicate data was normalized by gating the supplier-provided isotypic controls to 1% during analyses. Further analyses and visualization of flow cytometric data were conducted using Cyflogic software (CyFlo Ltd. - http://www.cyflogic.com/).

Chapter 3 - Results

3.1.Spectrophotometry

3.1.1. Crystal violet - 2-methoxyestradiol-bis-sulphamate

Crystal violet spectrophotometric growth assays were performed in order to determine the concentration at which the cytostatic and cytotoxic effects of 2ME-BM would be most pronounced, facilitating the subsequent studies into the molecular mechanisms involved in these effects. Results showed a time-and dose-dependent decrease in cell numbers with exposure to 2ME-BM (figure 10). The GI_{50} value was determined by calculating the drug concentration at which the control sample showed a 50% increase in growth above the test sample, taking into account the number of cells in each sample at the time of exposure. All subsequent experiments included an exposure time of 24 hours at 0.4µM for 2ME-BM since these parameters presented the most significantly differential GI_{50} values in tumorigenic MCF-7 cells (66% of control) when compared to the non-tumorigenic MCF-12A breast epithelial cell line (93% of control). This allowed for efficient analysis of the differential effects of 2ME-BM in these cell lines. Cell growth was inhibited to approximately 60% in MCF-7 samples (0.4µM - 1µM) and approximately 90% in MCF-12A samples (0.2µM - 1µM) after 24 hours, irrespective of 2ME-BM concentration, indicating that cellular effects of 2ME-BM are mediated within 24 hours after exposure, with the exponential growth of control sample cells explaining the logarithmic nature of the 48- and 72 hour datasets and confirming the irreversible and primarily cytostatic nature of these effects[227 228].

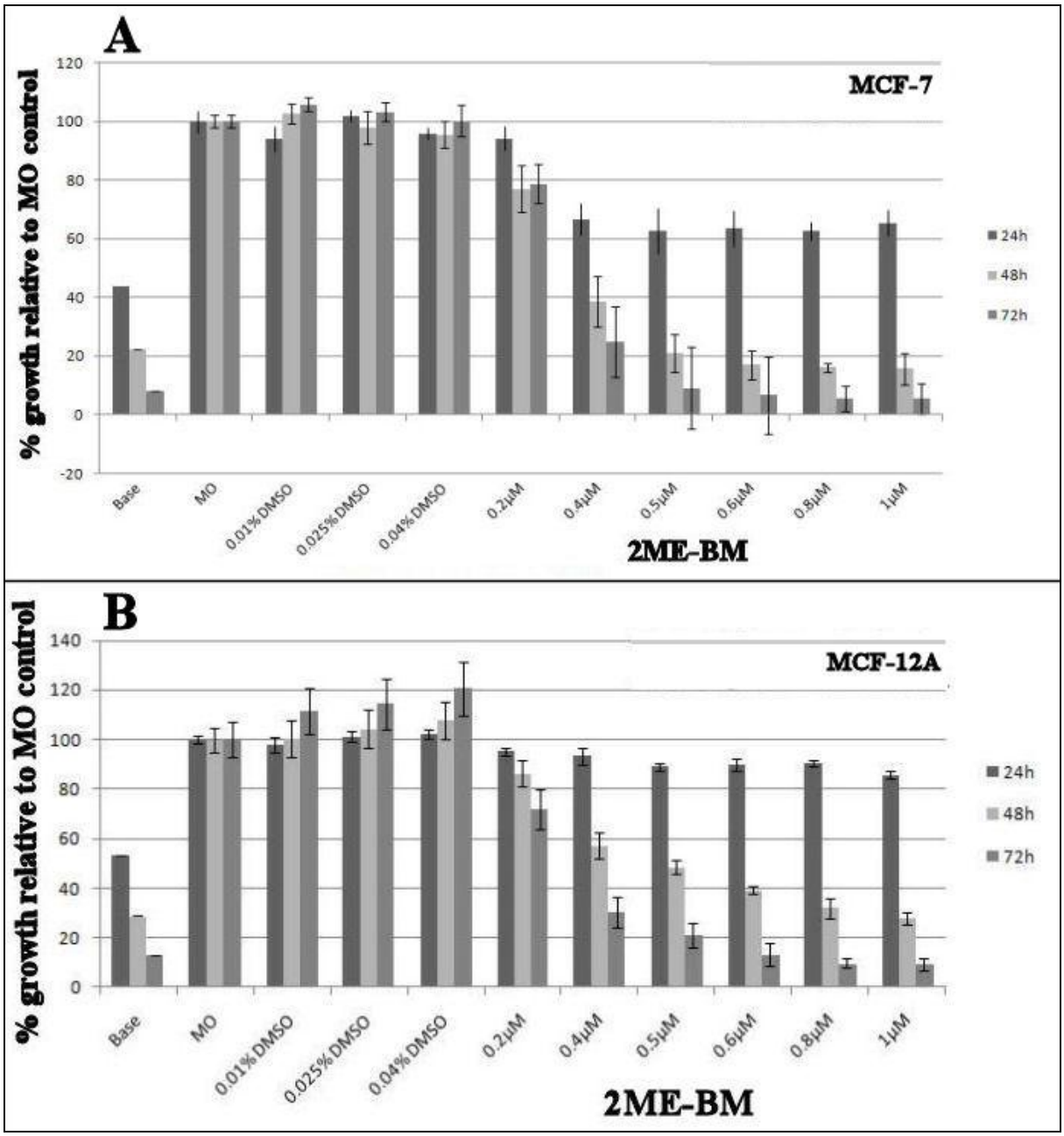

Figure 10: GI_{50} values derived from crystal violet proliferation assay results for MCF-7 (A) and MCF-12A (B) cells, showing a time- and dose-dependent inhibition of cell growth by 0.2µM - 1µM 2ME-BM over 24, 48 and 72 hours. The most pronounced cell line-specific response to 2ME-BM exposure when MCF-7 samples were compared to MCF-12A samples were observed after 24 hours at a concentration of 0.4µM.

3.1.2. Crystal violet - *S. frutescens*

Crystal violet spectrophotometric growth assays were to determine the concentration of aqueous *S. frutescens* extract at which the effects on intracellular signaling would be most pronounced, ensuring that meaningful results could be obtained from the subsequent studies. A time-and dose-dependent decrease in cell numbers was observed in response to *S. frutescens* exposure (figure 11). The GI_{50} value was determined (as previously discussed) by calculating the drug concentration at which the control sample showed a 50% increase in growth above the test sample, taking into account the number of cells in each sample at the time of exposure. A concentration of 1mg/ml *S. frutescens* and an exposure time of 48 hours were selected for further analysis, since these were the GI_{50} parameters calculated for the MCF-7 breast adenocarcinoma cell line (51% of control), while the MCF-12A non-tumorigenic cell line was significantly less affected (93% of control). All subsequent studies were conducted using these experimental parameters. Low concentrations of *S. frutescens* stimulated cell growth after 24 hours in both cell lines, both cell lines showed a nearly linear decrease in growth with increased concentration after 48 hours. Along with the significant growth recovery observed in the MCF-7 cell line after 72 hours, these results suggest a primarily cytotoxic mechanism of action for aqueous *S. frutescens* extracts [229].

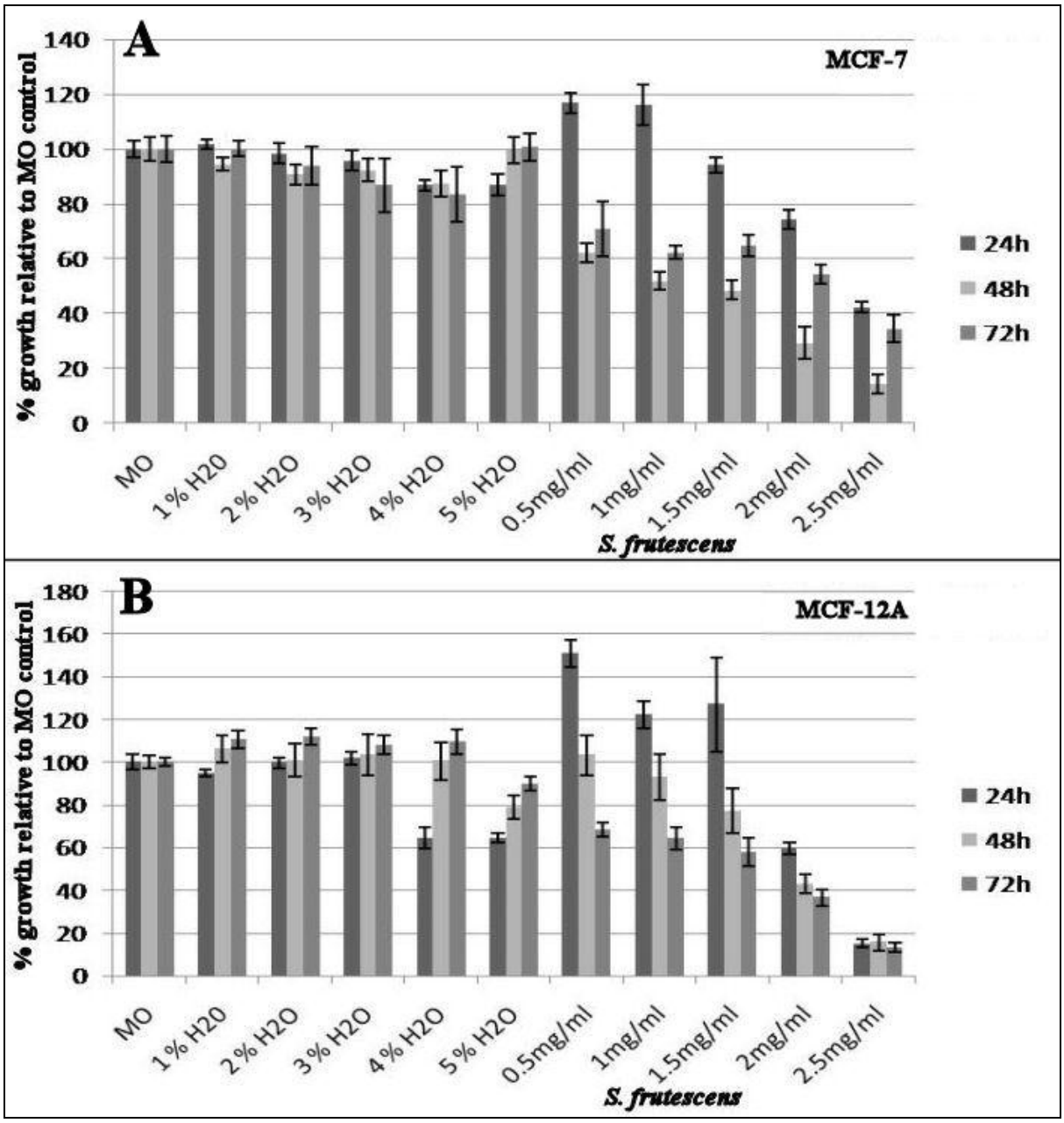

Figure 11: GI_{50} values derived from crystal violet proliferation assay results for MCF-7 (A) and MCF-12A (B) cells, showing a time and dose dependent inhibition of cell growth by aqueous 0.5mg/ml - 2.5mg/ml *S. frutescens* extracts. The most pronounced cell line-specific response to *S. frutescens* exposure when MCF-7 samples were compared to MCF-12A samples were observed after 48 hours at a concentration of 1 mg/ml.

3.2.Microscopy

3.2.1. Differential interference contrast microscopy - 2-methoxyestradiol-bis-sulphamate

Polarization-optical transmitted light differential interference contrast (PlasDIC) microscopy was used to evaluate the condition of living cell samples during culture and prior to experiments as cell numbers, cell density and morphological characteristics can be qualitatively observed without preparation or fixation that could interfere with normal cellular function. Photomicrographs showed a decrease in cell numbers and density in samples exposed to 2ME-BM when compared to vehicle control samples in both MCF-7 and MCF-12A (figure 12) cell lines, with qualitative assessment of samples at low magnification showing the carcinogenic MCF-7 cell line to be more susceptible. The increased number of detached, rounded cells and decreased cell density observed in samples exposed to 2ME-BM are indicative of the metaphase cell cycle blockade previously observed. Furthermore, cells displaying apoptotic characteristics and fragmentation were observed in exposed samples, showing that cell death is being initiated[227 228].

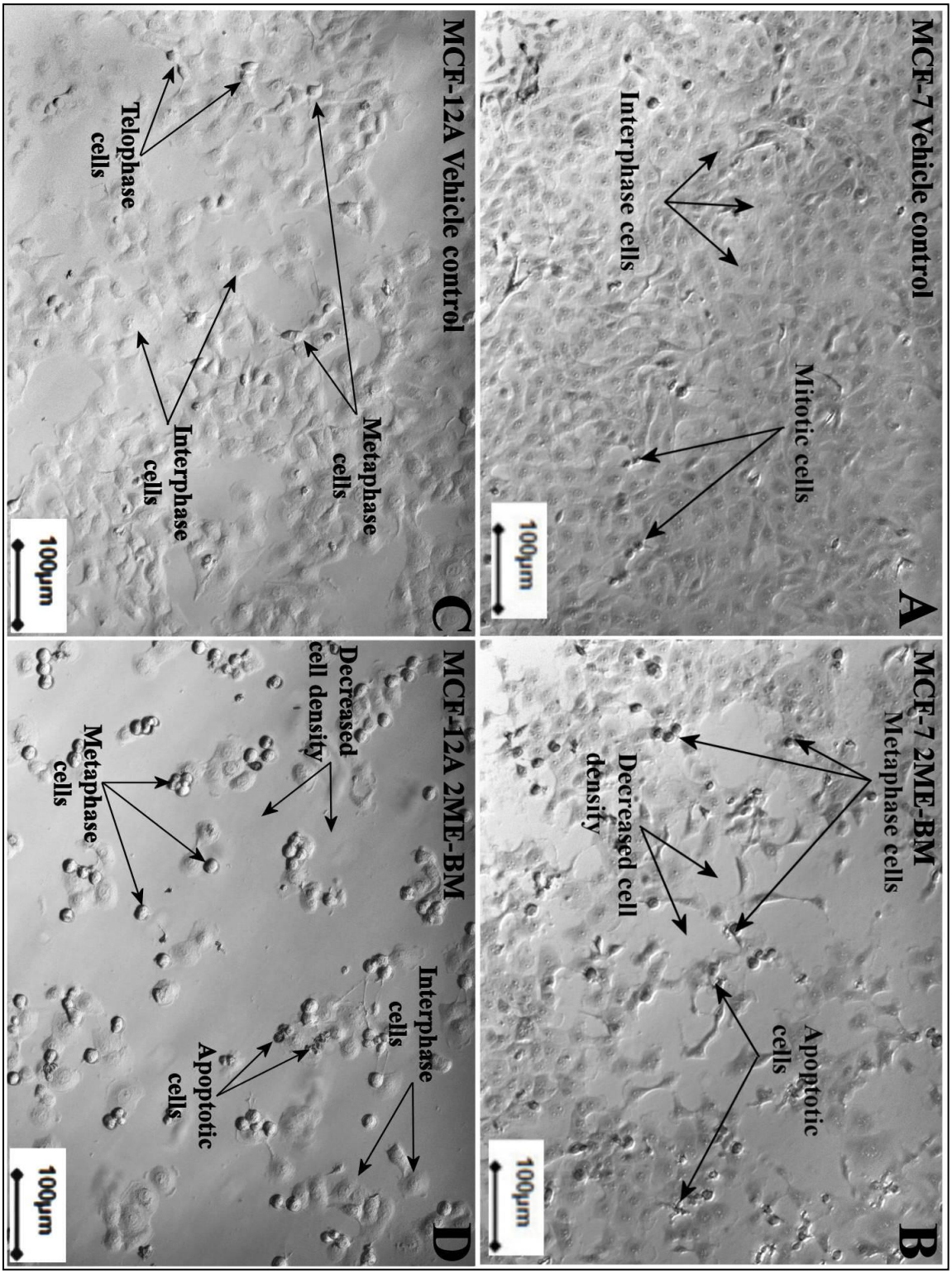

Figure 12: PlasDIC microscopic images (100X magnification) of MCF-7 (A, B) and MCF-12A (C, D) cells exposed to DMSO as a vehicle control (A, C) and 2ME-BM (B, D). A decrease in cell density, apoptotic changes and cellular damage in 2ME-BM exposed samples (B, D) of both cell lines were observed.

3.2.2. Differential interference contrast microscopy - *S. frutescens*

PlasDIC microscopy was used to evaluate the condition of living cell samples during culture and prior to experiments as cell numbers, cell density and morphological characteristics can be qualitatively observed without preparation or fixation that could interfere with normal cellular function. Photomicrographs revealed a decrease in cell numbers and density in *S. frutescens*-treated samples when compared to vehicle control samples in the MCF-7 cell line, while only a slight increase in cytoplasmic vacuolization and some changes in nuclear morphology were observed in the MCF-12A cell line (figure 13). The MCF-7 breast adenocarcinoma samples appear to be more susceptible to *S. frutescens* exposure, with an increase in the number of cell fragments and cells displaying apoptotic characteristics and stressed cell morphology being observed[229].

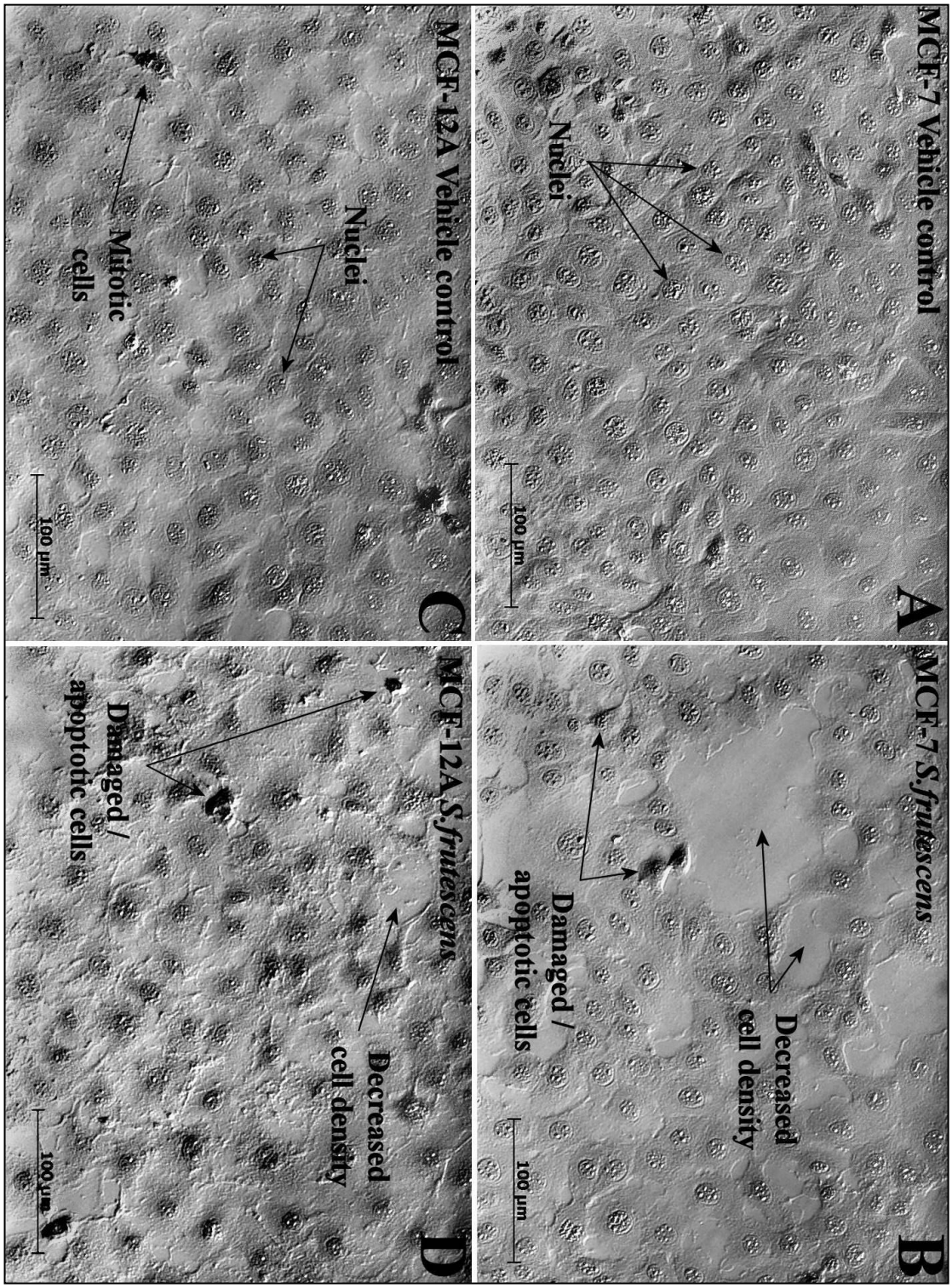

Figure 13: PlasDIC microscopic images (100X magnification) of MCF-7 (A, B) and MCF-12A (C, D) cells exposed to vehicle control (H_2O) and aqueous *S. frutescens* extracts. A decrease in cell density, morphological changes and cellular damage was noted in *S. frutescens* exposed samples (B, D) of both cell lines.

3.2.3. Haematoxylin and Eosin staining - 2-methoxyestradiol-bis-sulphamate

Haematoxylin and eosin (H&E) staining is a standard laboratory method for qualitative evaluation of cell samples, enabling the visualization of intracellular structures and revealing cell cycle status and nuclear morphology. Qualitative analysis by microscopy revealed no significant differences between samples treated with medium only and the vehicle control. A sharp decrease in cell density and significant morphological changes were observed in response to 2ME-BM exposure. Apoptotic (condensed nuclei, cytoplasmic blebbing) and abnormal cells (aberrant cytoplasmic and nuclear morphology) were observed in exposed samples, in addition to an increase in the number of cells in metaphase (figure 14). These effects were more prominent in the MCF-7 cell line when compared with the MCF-12A cell line, and can be explained by the previously discussed cytostatic effects of 2ME-BM on tubulin polymerization. 2ME-BM binds to the colchicine binding site of tubulin, thus interfering with the segregation of chromosomes after metaphase, and forcing the cells into apoptotic cell death[227 228].

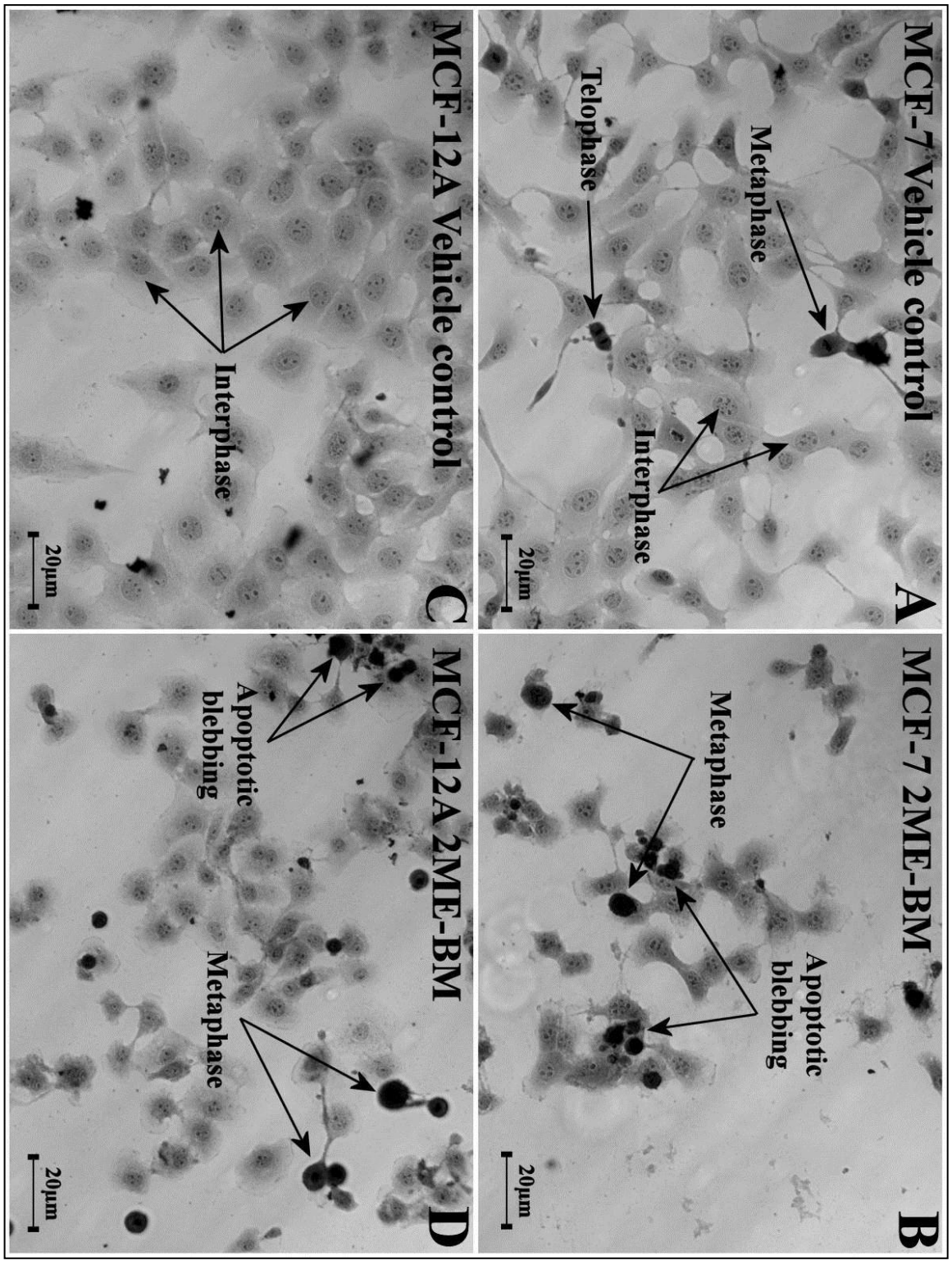

Figure 14: Photomicrographs of MCF-7 (A, B) and MCF-12A (C, D) cells exposed to DMSO as a vehicle control (A, C) and 2ME-BM (B, D) respectively. A decrease in cell density, increased number of metaphase cells and cell death associated morphological changes were observed in 2ME-BM-exposed samples (B, D).

3.2.4. Mitotic indices - 2-methoxyestradiol-bis-sulphamate

Mitotic index counts were performed on samples prepared for haematoxylin and eosin (H&E) microscopy in order to quantify the observed disturbances. Quantitative analyses showed distinct increase in the number of apoptotic and abnormal cells in samples exposed to 2ME-BM, as well as well-defined perturbations of mitotic dynamics (figure 15). Cells (1000 per slide) were counted and numbers were converted to percentages. Interphase cells are not included in the figures for clarity. A large increase in the number of apoptotic and abnormal cells, as well as metaphase cells was observed in 2ME-BM exposed samples, in conjunction with a decrease in all other phases, while vehicle control (DMSO) samples showed only minor deviations from medium only (MO) samples. These effects were observed in both the MCF-7 and MCF-12A cell lines. Nearly no cells progressed further than metaphase in treated samples[227 228].

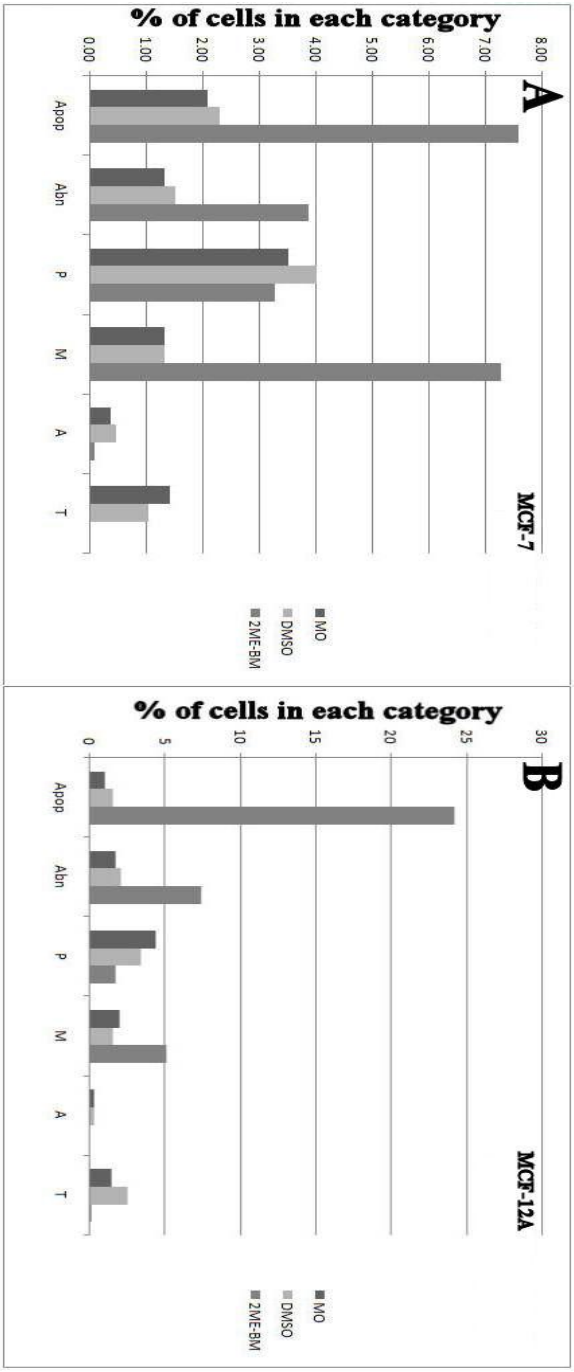

Figure 15: Graphs showing the results of mitotic index counts performed on haematoxylin and eosin-stained slides of MCF-7 (A) and MCF-12A (B) cell line samples exposed to medium only (MO), vehicle control (DMSO) and 2ME-BM respectively. In addition to a clear metaphase arrest a large increase in the number of apoptotic or abnormal cells was observed in samples exposed to 2ME-BM. (Apop - apoptosis; Abn - abnormal; P - prophase; M -metaphase; A - anaphase; T - telophase)

3.2.5. Haematoxylin and Eosin staining - *S. frutescens*

Haematoxylin and eosin (H&E) staining is a standard laboratory method for qualitative evaluation of cell samples, enabling the visualization of intracellular structures and revealing cell cycle status and nuclear morphology. Qualitative analysis by haematoxylin and eosin staining revealed decreased cell density and morphological changes in response to *S. frutescens* exposure in both cell lines, with this effect being more prominent in the MCF-7 breast adenocarcinoma cell line. Cells displaying apoptotic characteristics (hypercondensed chromatin, membrane blebbing) and aberrant morphology or cellular fragmentation were also observed in exposed samples (figure 16). Results seem to indicate that *S. frutescens* exerts a nonspecific cytotoxic effect on cells of both cell lines[229].

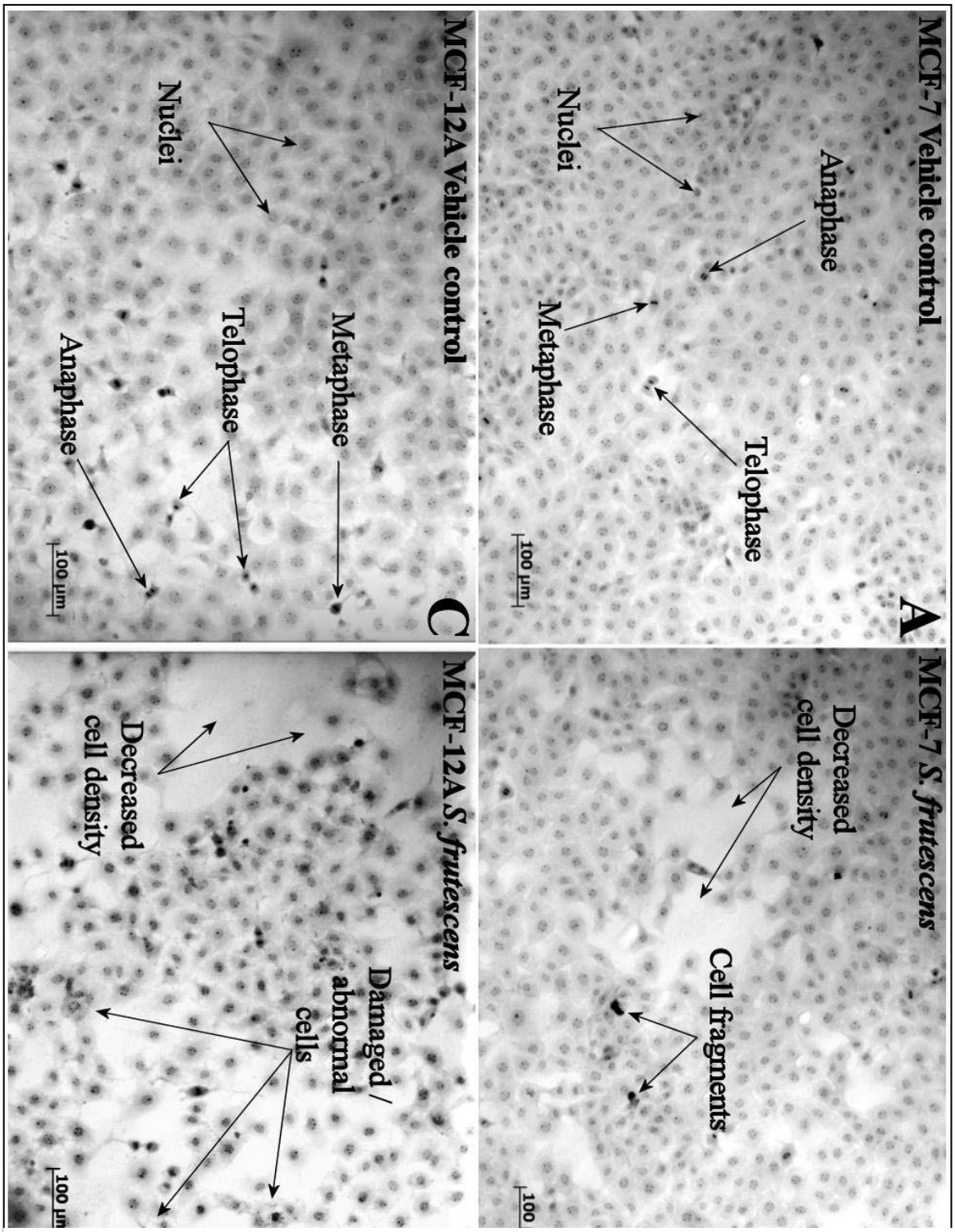

Figure 16: Photomicrographs of MCF-7 (A, B) and MCF-12A (C, D) cells exposed to H_2O as a vehicle control (A, C) and aqueous *S. frutescens* extracts (B, D) respectively. Decreased cell density and an increased number of cells displaying aberrant and apoptotic morphological characteristics were observed in the samples exposed to *S. frutescens* extracts (B, D).

3.2.6. Mitotic indices - *S. frutescens*

Mitotic index counts were performed on samples prepared for H&E microscopy in order to quantify the observed disturbances. Quantitative analyses showed a slight increase in the number of apoptotic and abnormal cells in *S. frutescens*-exposed samples of both MCF-7 and MCF-12A cell lines, as well as perturbations of mitotic dynamics in the MCF-7 breast adenocarcinoma cell line (figure 17). MCF-7 samples exposed to *S. frutescens* exhibited a marked decrease in the percentage of cells in prophase, metaphase, anaphase and telophase. This effect was observed to a much lesser extent in the MCF-12A cell line, and is possibly due to the increased number of cells in the apoptotic and abnormal fractions. Cells (1000 per slide) were counted and absolute counts were converted to percentages. For clarity of comparison, interphase cells are not shown[229].

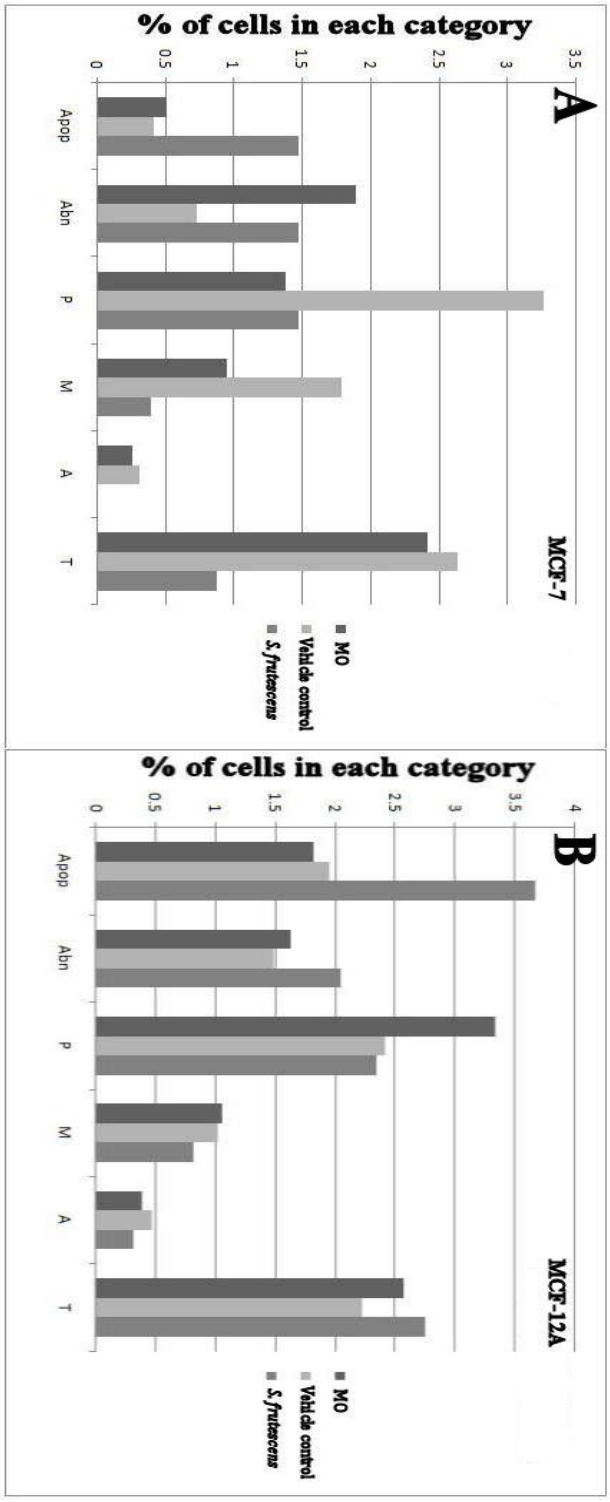

Figure 17: Graphs showing the results of mitotic index counts performed on haematoxylin and eosin-stained slides of MCF-7 (A) and MCF-12A (B) cell line samples exposed to medium only (MO), vehicle control (H_2O) and *S. frutescens* respectively. Exposed samples showed an increase in apoptotic and abnormal cells, and no significant influence on mitotic progression was observed. (Apop - apoptosis; Abn - abnormal; P - prophase; M -metaphase; A - anaphase; T - telophase)

3.2.7. Fluorescence microscopy - 2-methoxyestradiol-bis-sulphamate

Fluorescent stains were used for qualitative investigation of the effects on autophagic processes and cytoskeletal organization, specifically microtubule structure. In addition to confirming the marked decrease in cell density and increase in metaphase cells, fluorescent triple-staining with Hoechst 33342, PI and AO revealed a large increase in the amount of acidic intracellular lysosomes (as indicated by the increased density of bright green intracellular granules in figure 18), indicative of supraphysiological cellular autophagic activity in response to 2ME-BM exposure in both MCF-7 and MCF-12A cell lines. Furthermore, cells with compromised membranes and apoptotic blebbing were observed in MCF-7 samples exposed to 2ME-BM, confirming the presence of cells in both early- and late-stage apoptosis. Investigation of the cytoskeletal tubulin structure revealed significant cytoskeletal changes in response to 2ME-BM exposure in both cell lines, with the MCF-7 cell line more strongly affected (figure 19). Tubulin filaments appear to be shortened and malformed in exposed samples, which is in concurrence with previous studies showing that 2ME-BM interferes with tubulin polymerization by binding to the colchicine binding site of the tubulin molecule[227 228].

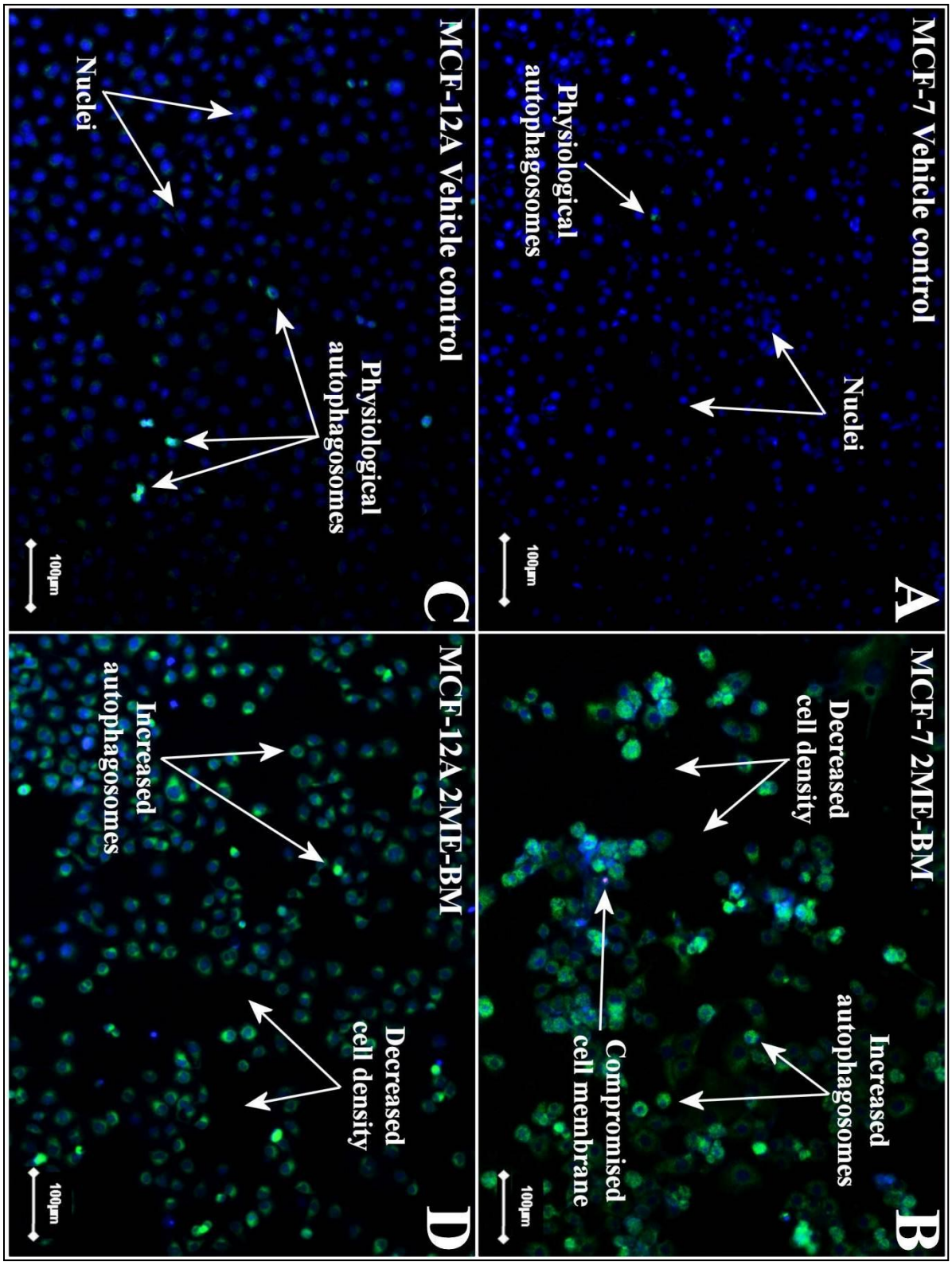

Figure 18: Fluorescence photomicrographs of MCF-7(A, B) and MCF-12A (C, D) cells exposed to DMSO as a vehicle control (A, C) and 2ME-BM (B, D) respectively, stained with a combination of Hoechst 33342, propidium iodide and acridine orange. The larger blue dots are cell nuclei, green granules are intracellular autophagosomes and red/pink dots indicate cells with compromised plasma membranes (i.e. dead/dying cells). A decrease in cell density and an increased amount of autophagic lysosomes were visible in 2ME-BM exposed samples (B, D).

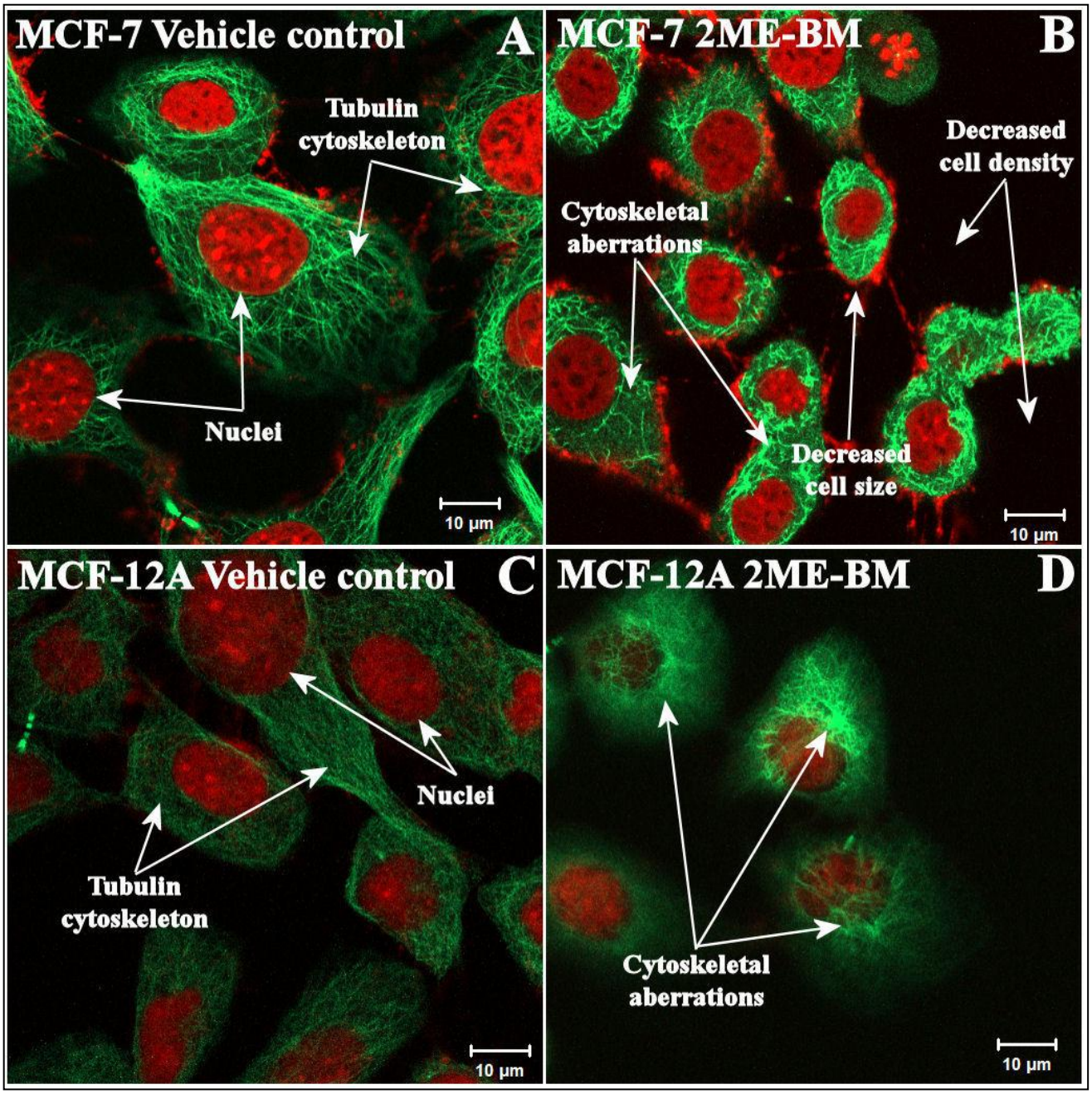

Figure 19: Confocal fluorescence micrographs of MCF-7 (A, B) and MCF-12A (C, D) cells exposed to DMSO as a vehicle control (A, C) and 2ME-BM (B, D) respectively. Red areas are cell nuclei and green fibers are tubulin filaments. Significant ultrastructural changes and decreased cell size and density were observed in samples exposed to 2ME-BM (B, D).

3.2.8. Fluorescence microscopy - *S. frutescens*

Fluorescent stains were used for qualitative investigation of the effects on autophagic processes. Fluorescent triple-staining with Hoechst 33342, PI and AO showed a marked increase in the amount of acidic intracellular vacuoles in the MCF-7 breast adenocarcinoma samples exposed to *S. frutescens* (increase in green acridine orange fluorescent intensity) (figure 20). MCF-7 samples were more severely affected when compared to the non-carcinogenic MCF-12A cell line[229].

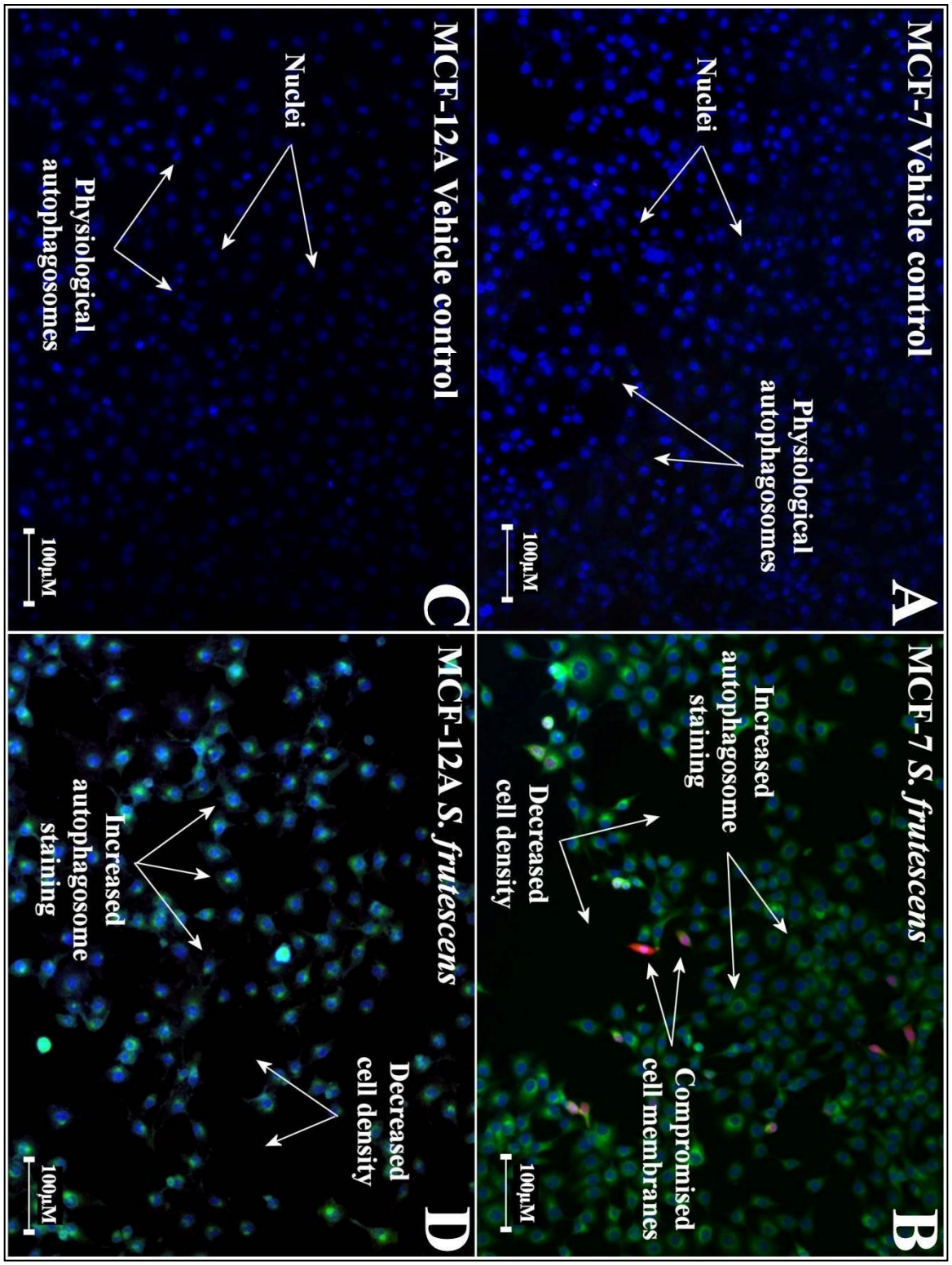

Figure 20: Fluorescence photomicrographs of MCF-7 (A, B) and MCF-12A (C, D) cells exposed to H_2O as a vehicle control (A, C) and aqueous *S. frutescens* extracts (B, D) respectively, stained with a combination of Hoechst 33342, propidium iodide and acridine orange. The larger blue dots are cell nuclei, green granules are intracellular autophagosomes and red/pink dots indicate cells with compromised plasma membranes (i.e. dead/dying cells). A decrease in cell density and an increase in the amount of intracellular autophagosomes were noted in *S. frutescens*-exposed samples (B, D).

3.2.9. Transmission Electron Microscopy - 2-methoxyestradiol-bis-sulphamate

Cellular ultrastructure and intracellular morphology was visualized by means of transmission electron microscopy (TEM), revealing evidence of apoptotic and autophagic processes occurring in cells exposed to 2ME-BM (figure 21). Membrane blebbing, hypercondensed chromatin, nuclear and plasma membrane fragmentation and autophagic lysosomes were observed in exposed MCF-7 samples. These changes are indicative of the activation of autophagic mechanisms escalating to eventual apoptotic cell death. The MCF-12A cell line did not show significant ultrastructural changes in response to 2ME-BM exposure, with only a minor increase in the amount of cytoplasmic processes (indicating cellular stress) being observed[227 228].

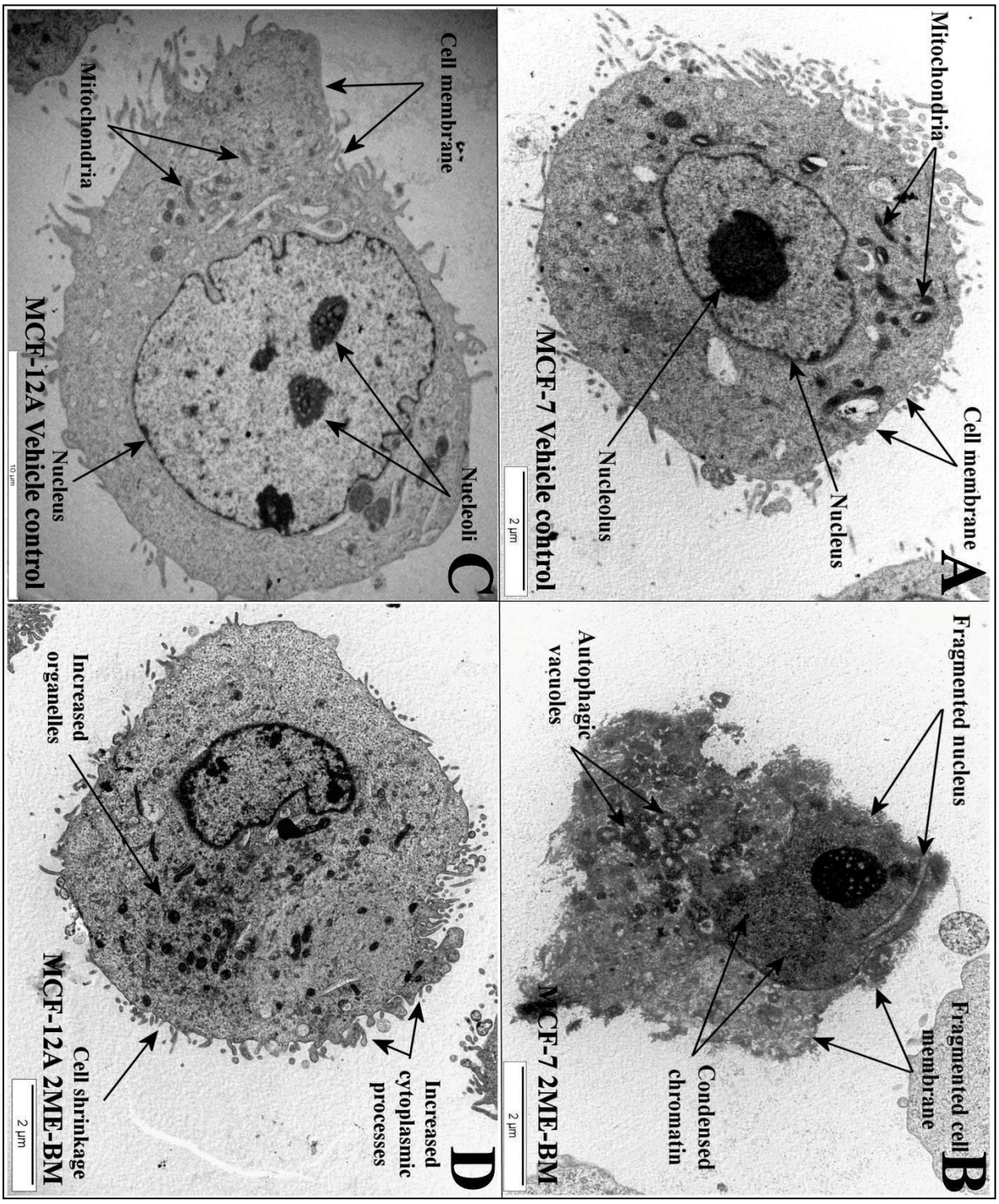

Figure 21: Transmission electron microscopic examination of the cellular ultrastructure of MCF-7 (A, B) and MCF-12A (C, D) exposed to DMSO as a vehicle control (A, C) and 2ME-BM (B, D)respectively. Photomicrographs revealed significant changes in 2ME-BM-exposed MCF-7 cells (B), with the observation of apoptotic characteristics (condensed or fragmented nuclei, apoptotic bodies) and indications of autophagy (intracellular autophagosomes or vesicles). The MCF-12A cell line showed an increase in cellular stress (increased cytoplasmic processes and smaller cell size) in response to 2ME-BM exposure (D).

3.3. Flow cytometry

3.3.1. Cell cycle progression - 2-methoxyestradiol-bis-sulphamate

Flow cytometry was used in order to confirm and quantify the observed cell cycle aberrations (G_2/M phase block). Flow cytometric analysis of cell cycle dynamics revealed a significant shift in distribution in exposed MCF-7 samples, with a distinct increase (33.14%) in the G_2/M-phase cell fraction (figure 22). This corresponds to previous data indicating that 2ME-BM causes metaphase arrest and subsequent apoptosis in MCF-7 cells. MCF-12A cells were less affected by comparison, showing a 6.17% increase in G_2/M-phase cells (figure 23) in response to 2ME-BM exposure. PI fluorescence was analyzed using a linear plot of the forward scatter 3 detector (FL3 Lin) and representative results are presented[227 228].

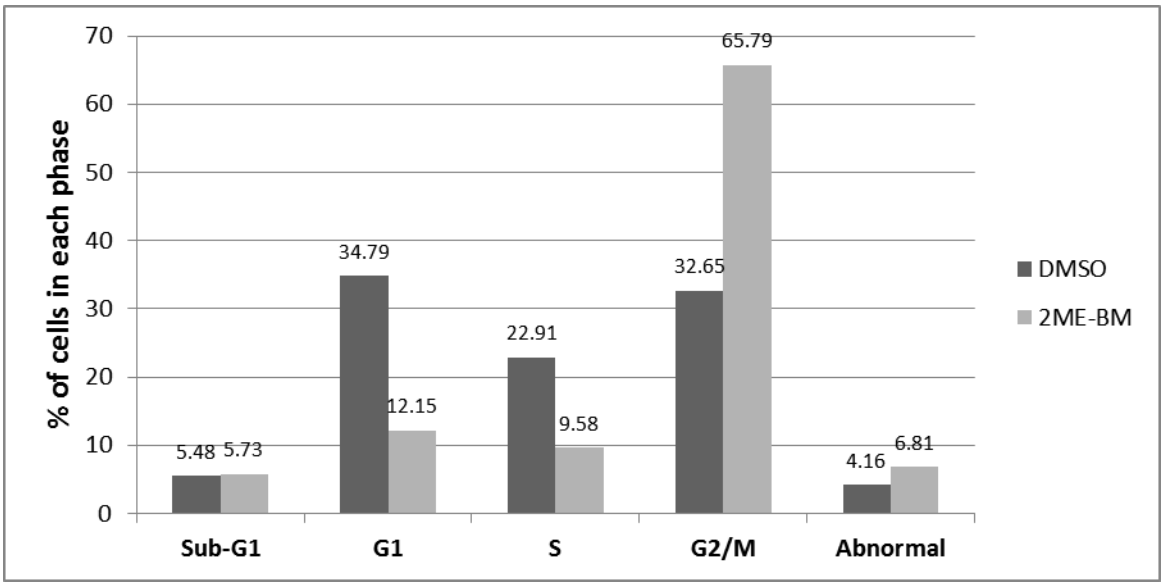

Figure 22: Flow cytometric analysis of the cell cycle dynamics of MCF-7 cells after exposure to vehicle control (DMSO) and 2ME-BM respectively. These analyses confirmed the G_2/M-phase blockade previously observed, with MCF-7 cells showing a 33.14% increase in the G_2/M-phase cell fraction in response to 2ME-BM exposure, with a subsequent decrease in G_1-and S-phase cells in addition to an increase in sub-G_1 and abnormal cell fractions.

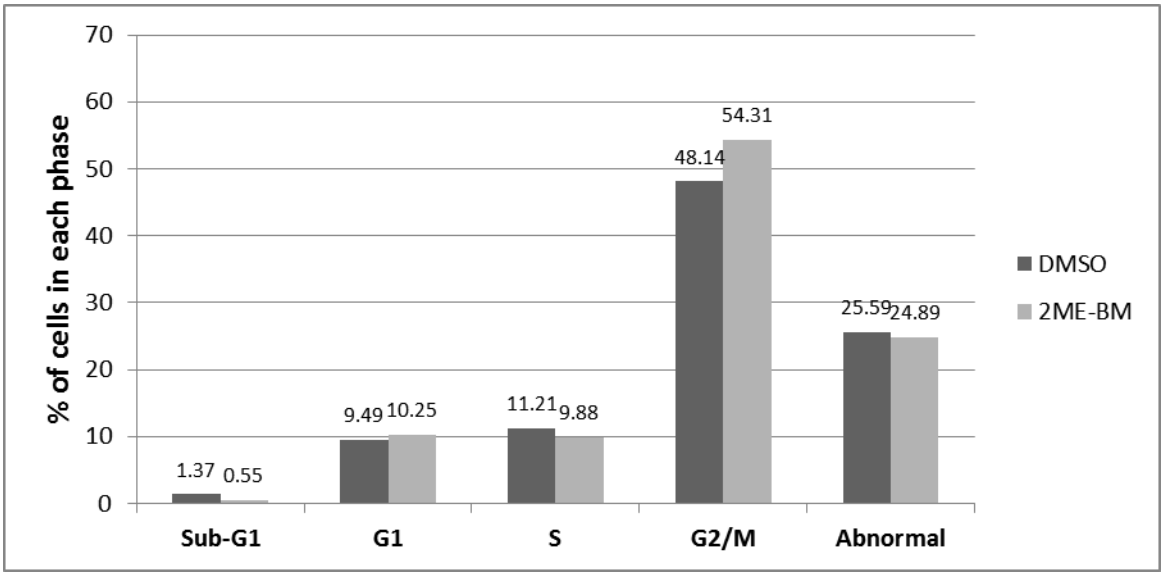

Figure 23: Flow cytometric analysis of the cell cycle dynamics of MCF-12A cells after exposure to vehicle control (DMSO) and 2ME-BM respectively. These results showed a 6.17% increase in G_2/M-phase cells in response to 2ME-BM exposure.

3.3.2. Cyclin B1 levels - 2-methoxyestradiol-bis-sulphamate

Flow cytometric analysis of cyclin B1 was used to confirm and quantify the observed G_2/M phase block, since the cell can only progress into the M-phase once the CDK1/cyclin B1 complex has been broken down. Analysis of intracellular cyclin B1 levels showed a 6.3% increase (from 5.0% in vehicle control cells to 11.3% in 2ME-BM-treated cells) in response to exposure of MCF-7 cells to 2ME-BM (figure 24), while MCF-12A samples showed a 4.25% decrease in cyclin B1 levels (from 6.49% in vehicle control cells to 1.7% in 2ME-BM-treated cells) (figure 25). Gating was conducted at a positive rate of 1% for isotypic control samples. Results are expressed as logarithmic histograms of the forward scatter 1 detector (FL1 Log)[227 228].

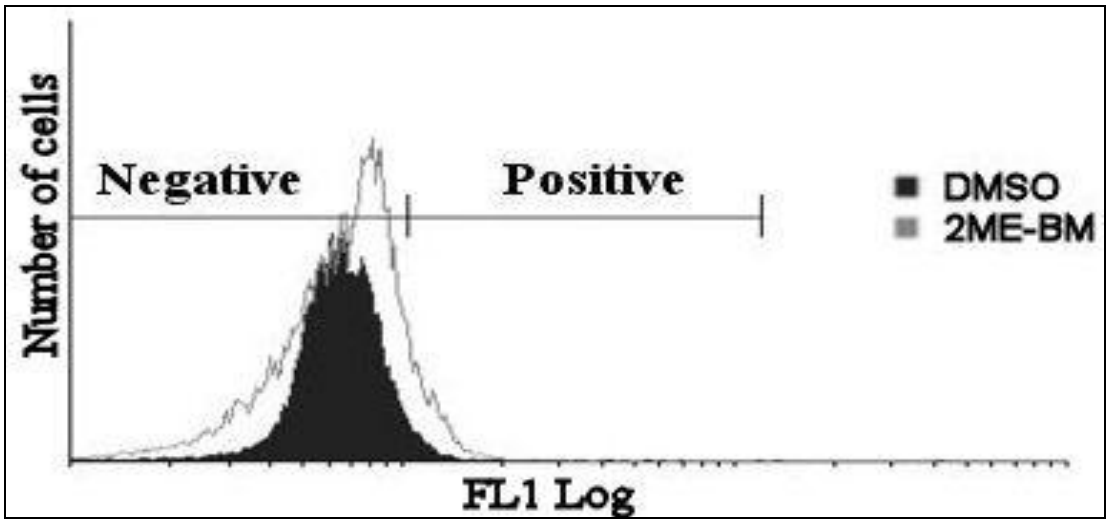

Figure 24: Flow cytometric evaluation of intracellular cyclin B1 levels in MCF-7 cells exposed to vehicle control (DMSO) and 2ME-BM respectively. Results revealed a 6.3% increase in cyclin B1 levels in cells exposed to 2ME-BM when compared to vehicle control samples. Results are presented as representative logarithmic histogram overlays of data collected by the forward scatter 1 detector (FL1).

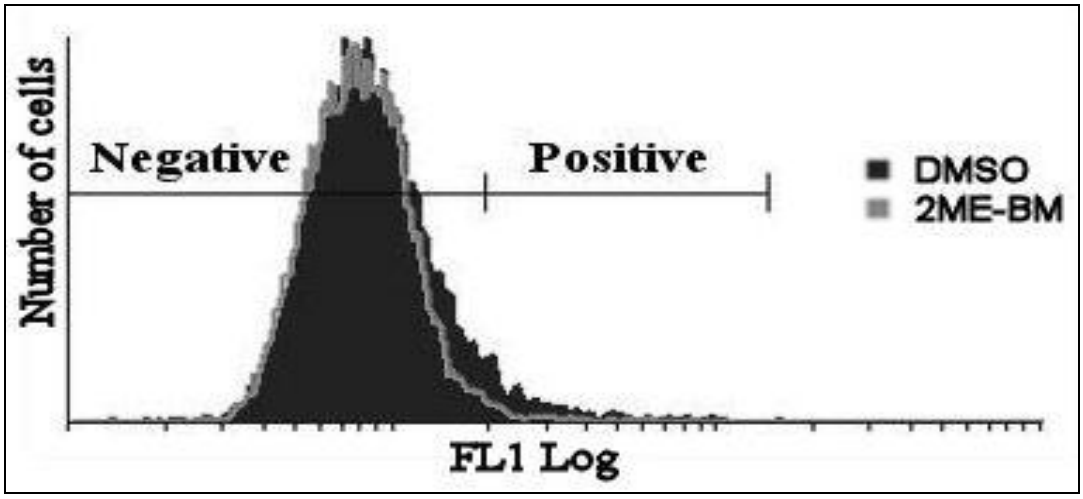

Figure 25: Flow cytometric evaluation of cyclin B1 levels in MCF-12A cells in response to exposure to vehicle control (DMSO) and 2ME-BM respectively. This revealed a 4.25% decrease in cyclin B1 levels after 2ME-BM exposure when compared to vehicle control samples. Results are presented as representative logarithmic histogram overlays of data collected by the forward scatter 1 detector (FL1).

3.3.3. Apoptosis detection - 2-methoxyestradiol-bis-sulphamate

After the induction of apoptosis, phosphatidylserine undergoes a flip-flop translocation from the inside to the outside of the plasma membrane. This effect can be quantified by using annexin V, which binds to phosphatidylserine on the outside of the cell membrane, and further information can be gained by coupling this observation to PI, which stains nuclear material but cannot cross intact cell membranes. During early apoptosis phosphatidylserine translocates, but the plasma membrane remains intact, leading to a positive annexin V-FITC signal without any PI signal. During the later stages of apoptosis the plasma membrane is compromised, manifesting as staining with both annexin V-FITC and PI. Exposure of the MCF-7 cell line to 2ME-BM resulted in a rise in annexin V-FITC binding, indicating a statistically significant 3.16% increase in the number of apoptotic cells (early and late apoptosis combined) as demonstrated in figure 26. Figure 27 shows that annexin V-FITC binding in the MCF-12A cell line was not significantly affected by 2ME-BM exposure (0.85% increase in total apoptotic cells). Neither cell line showed a significant change in the amount of necrotic cells after 24 hours of exposure to 2ME-BM.

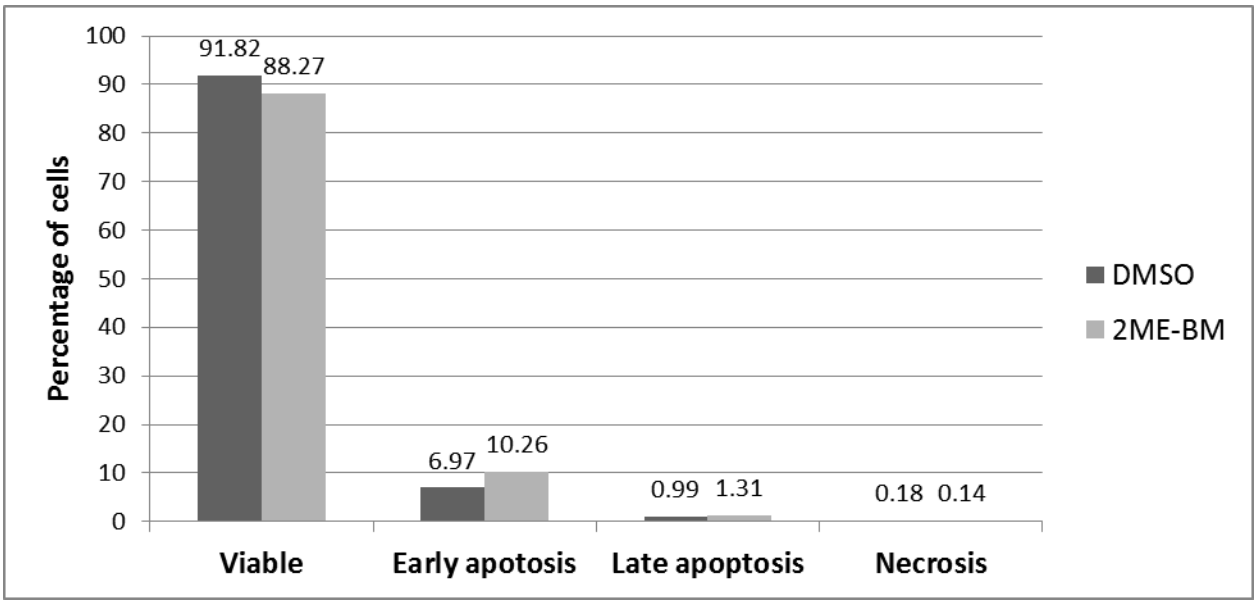

Figure 26: Flow cytometric comparison of annexin V-FITC binding, used as a measurement of apoptotic levels and progression in response to vehicle control (DMSO) and 2ME-BM exposure respectively in MCF-7 cells. This revealed a 3.55% decrease in viable cells and an increase of 3.29% in early apoptotic cells.

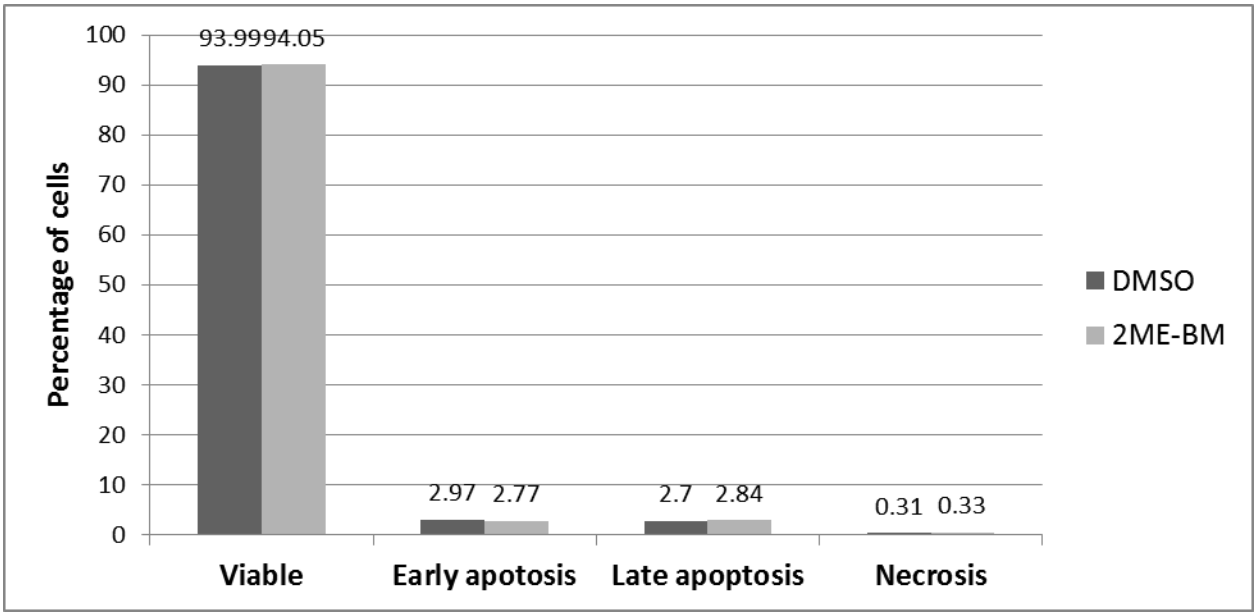

Figure 27: Flow cytometric comparison of annexin V-FITC binding as a measurement of apoptotic levels and progression in response to vehicle control (DMSO) and 2ME-BM exposure in MCF-12A cells. This revealed no significant changes in annexin V binding.

3.3.4. Autophagosome detection - 2-methoxyestradiol-bis-sulphamate

Autophagy is the process through which a cell can digest or recycle organelles, proteins and portions of cytoplasm by lysosomal degradation. As previously discussed, the level of autophagic activity can be quantified by measuring the amount of autophagosomes in a cell. This was achieved by using a fluorescent-labeled antibody to LC3, which is associated with autophagosomal membranes in the LC3-II isoform during autophagy. Figure 28 demonstrates a 35.9% increase (0.67% to 36.5%) in fluorescent-labeled LC3 antibody binding observed in the MCF-7 cancer cell line in response to 2ME-BM exposure. The MCF-12A cell line was showed a 12.79% decrease (16.92% to 4.13%) in fluorescent-labeled LC3 antibody binding (figure 29). Results indicate that 2ME-BM exposure causes an increase in the formation of autophagosomes and thus autophagic activity in the MCF-7 cell line and a decrease in these autophagic processes in the MCF-12A cell line.

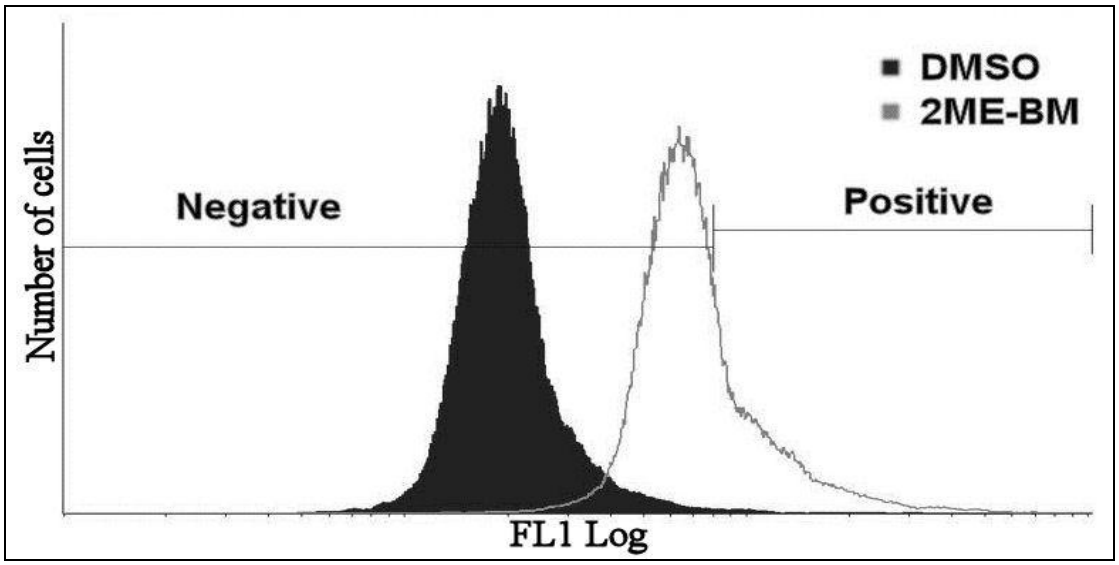

Figure 28: Flow cytometric analyses of LC3 binding in MCF-7 cell samples exposed to vehicle control (DMSO) and 2ME-BM respectively. Vehicle control samples showed a positive rate of 0.67%, while samples exposed to 2ME-BM showed a 36.5% positive rate. An increase in LC3 binding (35.9%) was observed when samples exposed to2ME-BM were compared to vehicle control samples, indicating a significant increase in autophagy induction.

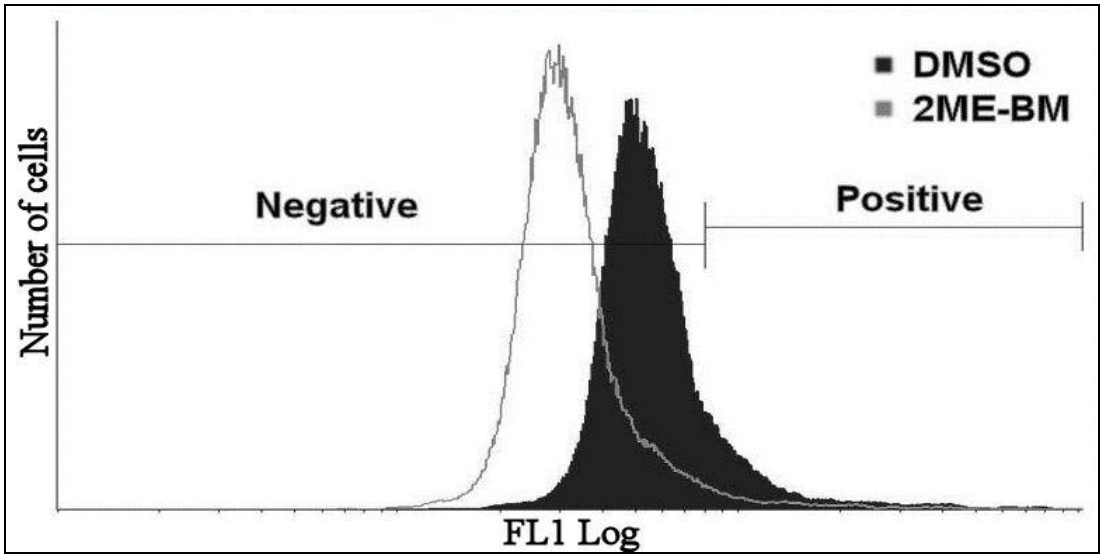

Figure 29: Flow cytometric analyses of LC3 binding in MCF-12A cell samples exposed to vehicle control (DMSO) and 2ME-BM respectively. Vehicle control samples showed a positive rate of 16.92%, while samples exposed to 2ME-BM showed a 4.13% positive rate, constituting a decrease in LC3 binding of 15.79%.

3.3.5. Mitochondrial permeability - 2-methoxyestradiol-bis-sulphamate

As previously discussed, there exist several avenues by which apoptosis can be induced including death receptor activation or the mitochondrial pathway. During apoptosis induction through the mitochondrial pathway, the membrane potential of the mitochondria is rapidly altered during an event known as the MPT or MOMP, leading to water entering and eventually rupturing the mitochondrial membrane. This causes pro-apoptotic factors (cytochrome *c*, endonuclease G etc.) to leak out. This effect was studied by utilizing a cationic dye which polymerizes in normal mitochondria but is released from permeabilized mitochondria, remaining in its monomeric form in the cytoplasm. Activation of the MPT would thus cause an increase in fluorescence in the monomeric, cytoplasmic component (FITC channel, measured with the forward scatter 1 detector). As demonstrated in figures 30 and 31 no significant evidence of a mitochondrial permeability transition was found by this study (indicated by a lack of increase in the amount of monomeric FITC-channel fluorescence) after 24 hours of exposure to 2ME-BM in either the MCF-7 (figure 29 - 0.09% change) or MCF-12A (figure 30 - 0.41% change) cell lines.

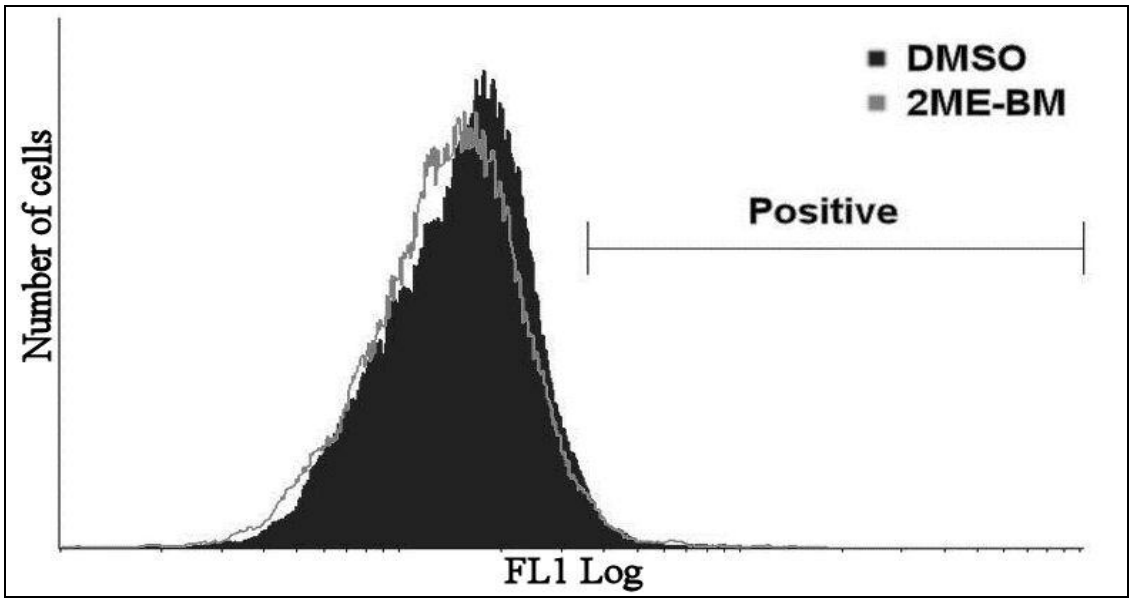

Figure 30: Flow cytometric analyses of mitochondrial permeability in MCF-7 cell samples exposed to vehicle control (DMSO) and 2ME-BM respectively. No significant changes were observed in response to 2ME-BM exposure (3.21% positive) when compared to vehicle control samples (3.12% positive).

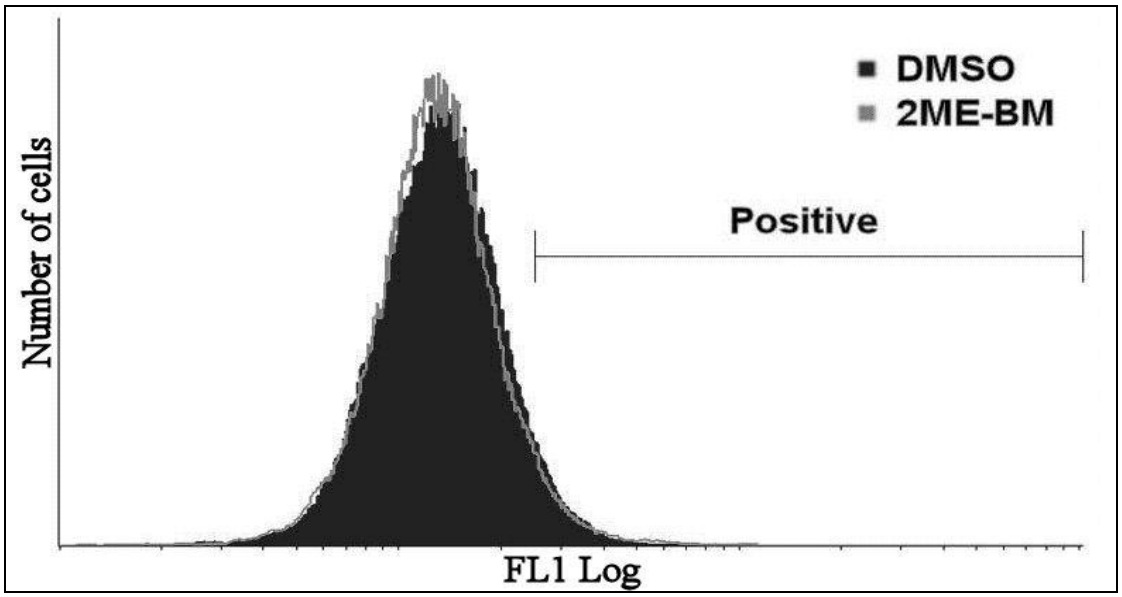

Figure 31: Flow cytometric analyses of mitochondrial permeability in MCF-12A cell samples exposed to vehicle control (DMSO) and 2ME-BM respectively. No significant changes were observed in response to 2ME-BM exposure (6.79% positive) when compared to vehicle control samples (7.2% positive).

3.3.6. Cell cycle progression - *S. frutescens*

Flow cytometry was used in order to confirm and quantify the previously observed cell cycle aberrations, and to confirm the absence of an S-phase cell cycle block (previously reported in studies using ethanolic extracts of *S. frutescens* [140]). Analyses of cell cycle dynamics showed a significant increase (12.19%) in G_1-phase cells in the MCF-7 cell line (39.57% to 51.76%), with a resulting decrease in actively cycling cells (S- and G_2/M-phase) in response to *S. frutescens* exposure, indicative of an inhibition of normal cellular replication (figure 32). The MCF-12A cell line followed the same pattern (to a lesser extent), showing a 4.82% increase in G_1-phase cells (37.65% to 42.47%) as shown in figure 33[229].

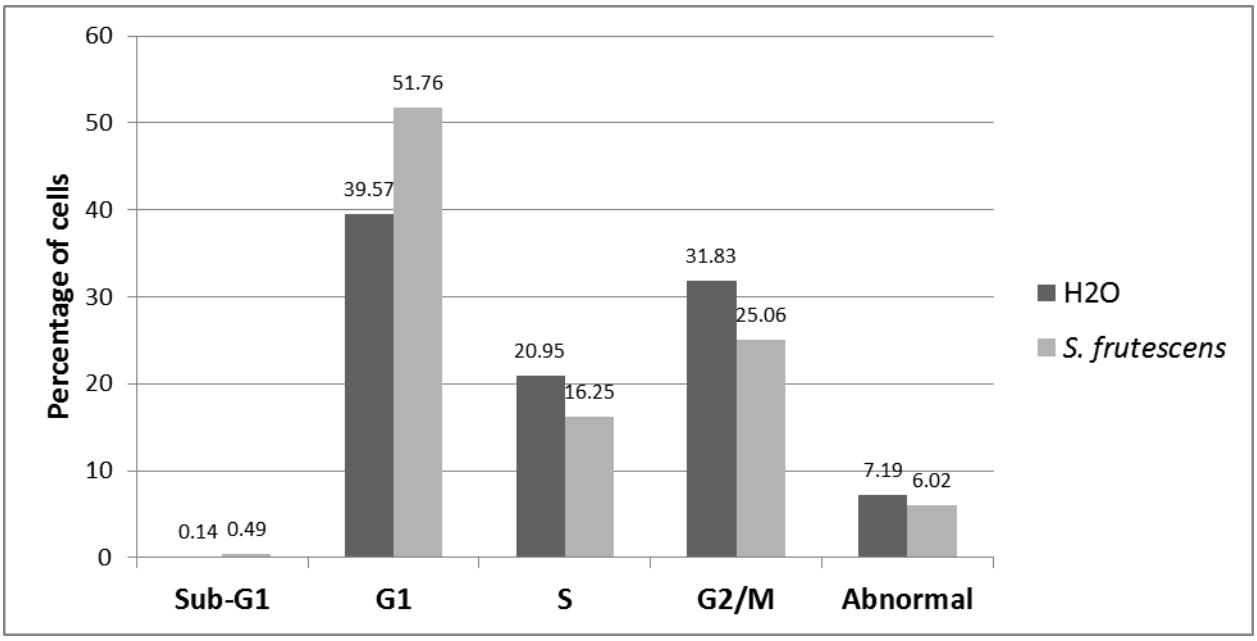

Figure 32: Flow cytometric analyses of cell cycle progression in MCF-7 cells after exposure to vehicle control (H_2O) and *S. frutescens* respectively, revealing a marked 12.19% decrease in actively cycling cells (denoted by S- and G_2/M-phase constituents).

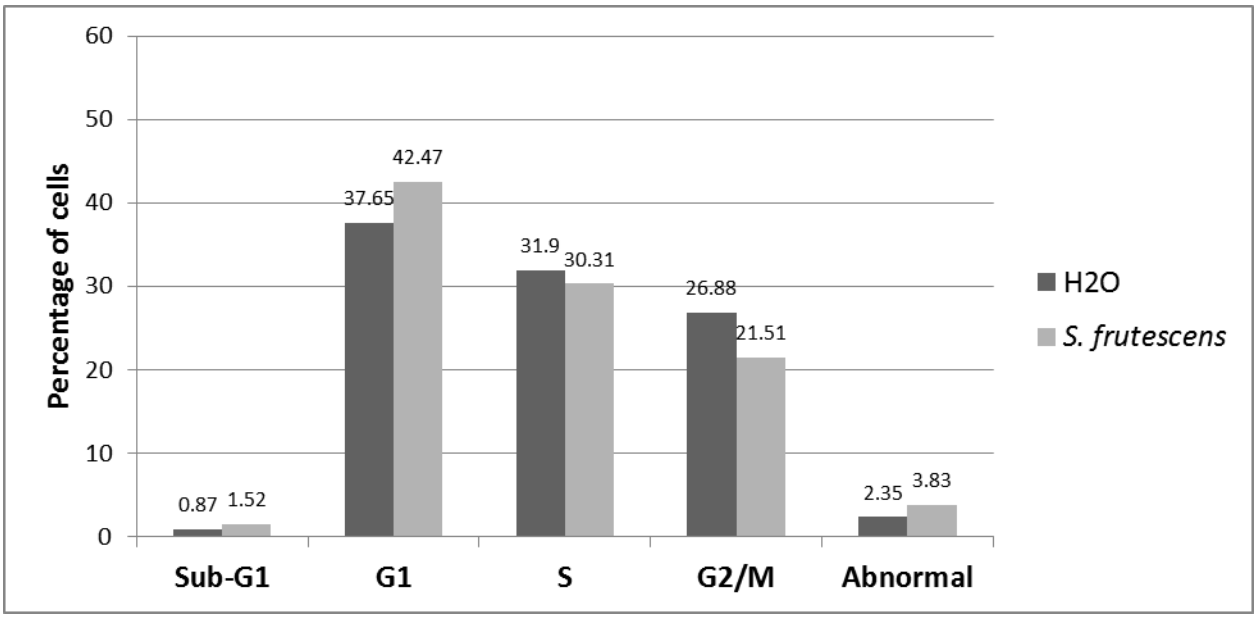

Figure 33: Flow cytometric analyses of cell cycle progression in MCF-12A cells after exposure to vehicle control (H_2O) and *S. frutescens* respectively, showing a mild decrease in actively cycling cells when compared to MCF-7 samples.

3.3.7. Apoptosis detection - *S. frutescens*

The flip-flop translocation of phosphatidylserine to the outside of the plasma membrane can be quantified by the binding of fluorescent-labeled annexin V to phosphatidylserine. Coupling this observation to the staining of nuclei by PI in cells with compromised cell membranes can yield additional information. Early apoptosis is thus indicated by a positive annexin V-FITC signal without PI signal (phosphatidylserine externalized, intact plasma membrane), and late apoptosis is indicated by positive signals for both annexin V-FITC and PI (externalized phosphatidylserine, compromised plasma membrane). Necrosis is observed as a negative annexin V-FITC signal with positive PI signal, as the structure of the plasma membrane is completely disrupted. Flow cytometric analyses of annexin V-FITC binding (indicating phosphatidylserine externalization) revealed a decrease (6.62%) in viable cells and increases in early apoptosis (1.88%), late apoptosis (2.44%) and necrosis (2.3%) in the MCF-7 cell line in response to *S. frutescens* exposure (figure 34). Annexin V-FITC binding was not affected to any significant level in the MCF-12A cell line when samples exposed to *S. frutescens* extracts were compared to vehicle control treated samples (figure 35)[229].

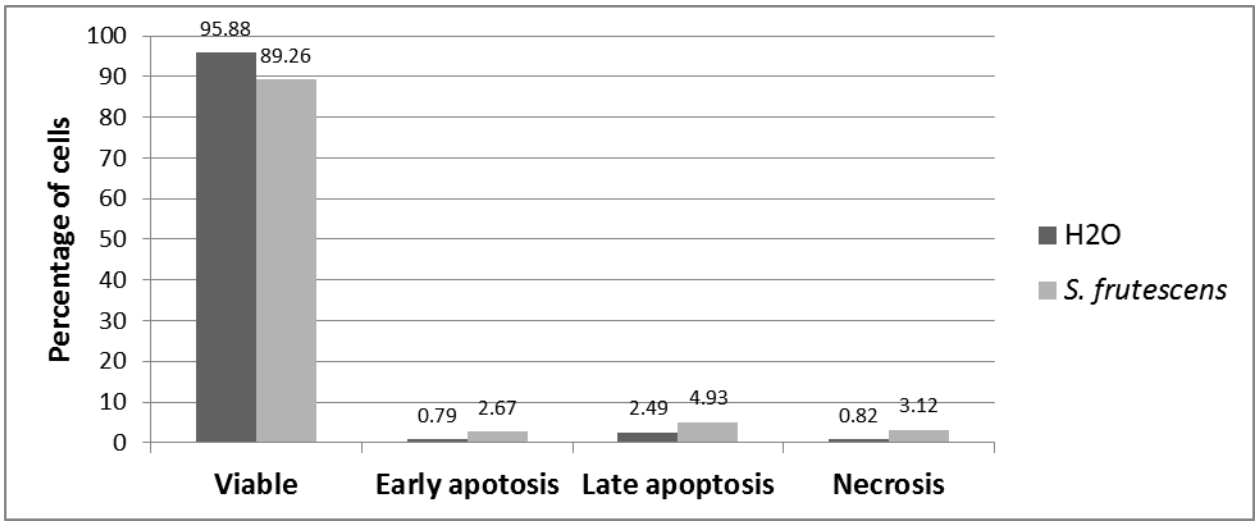

Figure 34: Flow cytometric analysis of annexin V-FITC binding in MCF-7 samples exposed to vehicle control (H_2O) and *S. frutescens* respectively. A decrease in viable cells was accompanied by an increase in apoptotic and necrotic cells in response to *S. frutescens* exposure.

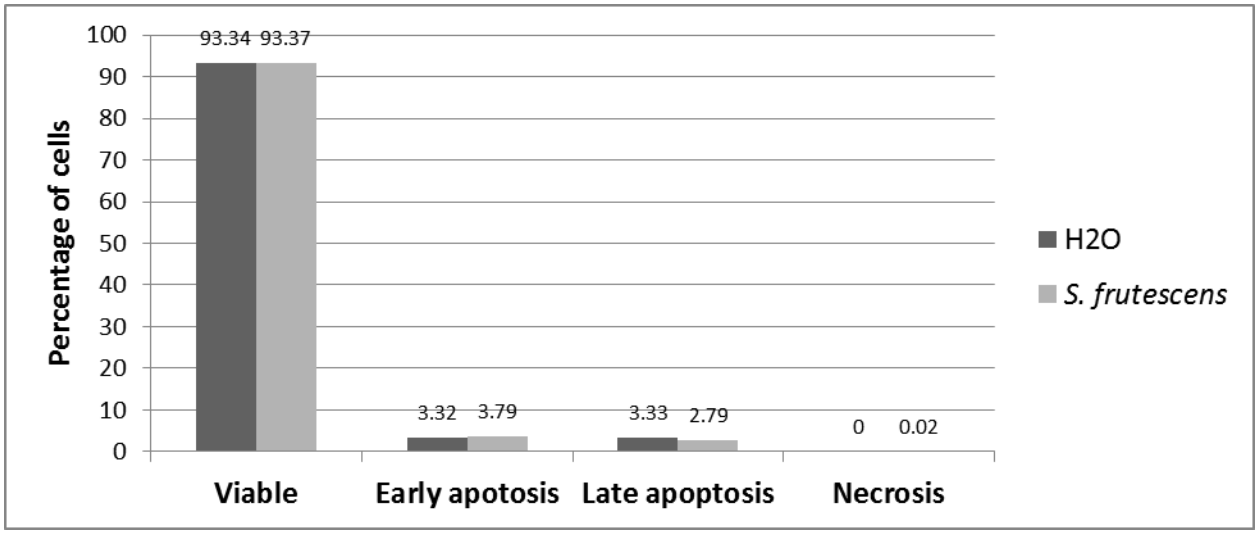

Figure 35: Flow cytometric analysis of annexin V-FITC binding in MCF-7 samples exposed to vehicle control (H_2O) and *S. frutescens* respectively. No significant changes in cell death were seen in response to *S. frutescens* exposure.

Chapter 4 - Discussion

4.1. 2-Methoxyestradiol-bis-sulphamate

One of the aims of this study entailed the *in vitro* evaluation of the potential anticancer compound 2-methoxyestradiol-bis-sulphamate (2ME-BM)'s differential effects on carcinogenic (MCF-7) and non-carcinogenic cell MCF-12A) lines derived from breast epithelial tissue. Additionally this study aimed to improve our understanding of the molecular processes involved in causing the effects of 2ME-BM on cell cycle dynamics and cell death.

Previous studies reported varying 2ME-BM concentrations (0.001µM to 10µM) and exposure times in a variety of cell lines [110, 111, 116]. It was thus decided to conduct proliferation assays in order to determine the optimal time- and dose parameters for this specific study. After exposure of cells to a series of concentrations of 2ME-BM for different time periods and analysis of crystal violet staining results, 0.4µM of 2ME-BM for 24 hours was chosen as the concentration to be utilized for further testing. This time- and dose combination showed growth inhibition by 2ME-BM to be approximately 44% in the MCF-7 cell line, compared to only 7% in the MCF-12A cell line. All further testing was conducted using these parameters, since they represented the best balance between pronounced intracellular effects and sufficient sample size for analysis, while also demonstrating the differential effects of 2ME-BM on carcinogenic MCF-7 *vs.* non-

carcinogenic MCF-12A cell lines. These experimental parameters are comparable to those used in previous *in vitro* studies by Raobaikady *et al*. (2003) [110], Suzuki *et al*. (2003) [116], Day *et al*. (2003) [119], Foster *et al*. (2008)[122], Utsumi *et al*. (2005)[118], Chander *et al*. (2007) [113 111], Visagie *et al*. (2011) [230] and Visagie *et al*. (2012) [231]. Raobaikady *et al*. (2003) [110] used dosages of 0.001-10µM for 72 hours for assessment of the *in vitro* effects of 2ME-BM on MCF-7 cell proliferation, morphology and STS activity, finding a dose-dependent inhibition of cell growth with an IC_{50} value of 0.4µM for 2ME-BM. Suzuki *et al*. (2003) [116], utilizing a 1µM 2ME-BM dosage for 5 days found cell growth inhibited to 12%, 6% and 23% in MCF-7, MCF-7 MR and MCF-7 DOX40 cell lines respectively when compared to control samples. Day *et al*. (2003) [119] conducted proliferation studies using a selection of cancer cell lines, exposing the cells to a concentration range of 0.1µM - 10µM 2ME-BM for 4 days. They reported irreversible, dose-dependent inhibition of proliferation and calculated IC_{50} values for LNCaP prostate carcinoma cells (0.53µM), androgen-independent PC3 prostate carcinoma cells (0.4µM), A2780 ovarian carcinoma cells (0.33µM), A2780adr adriamycin resistant ovarian carcinoma cells (0.87µM) and A2780cis cisplatin resistant ovarian carcinoma cells (0.38µM). Foster *et al*. (2008) [122] concluded that the *in vitro* IC_{50} values for 2ME-BM were 0.618µM in MDA-MB-231 cells and 0.04µM in HUVEC cells respectively after 96 hours of exposure, and found a 68% tumour volume regression in response to 20mg/kg/day of 2ME-BM during a 28 day treatment period in MF-1 nude mice inoculated with MDA-MB-231 cells. Utsumi *et al*. (2005)[118] found the IC_{50} value for 2ME-BM to be 0.25µM in MCF-7 cells, 0.23µM in MCF-7 cells transfected with steroid sulphatase cDNA and

0.29µM in MDA-MB-231 breast cancer cells. They also found a 52% *in vivo* tumour volume regression in ICFR nude mice inoculated with MCF-7 cells after 3 weeks of treatment with 2ME-BM at a dosage of 20mg/kg/day and significant levels of STS inhibition in liver and tumour tissues.

The study by Chander *et al*. (2007) [111] assessed the effects of 2ME-BM on *in vivo* xenografts of ER positive MCF-7 cells in female athymic mice, finding a 52% reduction in tumour volume (compared to control groups) when using 5mg/kg/day dosage and tumour regression (38%) when using a dosage of 20mg/kg/day after 3 weeks of treatment. This study also showed an apparent lack of *in vivo* toxicity (no reduction in animal weight over the 3 week test period) and a 44% reduction in tumour angiogenesis in response to 2ME-BM.

Using the time-and dose combination of 0.4µM of 2ME-BM for 24 hours revealed a significant decrease in microscopically observed cell density in both cell lines. Morphology was severely affected by 2ME-BM, as observed by means of various microscopic techniques, with an increase in the number of rounded, detached and/or visibly damaged cells. Literature has shown the effects of 2ME-BM on cellular morphology to be highly cell line-specific [119, 232] and the results from this study clearly demonstrated a significant difference in effect between the MCF-7 and MCF-12A cell lines. The MCF-7 cell line appeared to be more significantly affected by 2ME-BM exposure with regard to morphology and apoptotic characteristics when compared to MCF-12A samples. An increased amount of cellular fragments, blebbing cells and ultrastructural features (formation of apoptotic bodies) implicated apoptosis in the

mechanisms of cell death. These results are in concurrence with the findings of Raobaikady *et al*. (2003) [110], Ho *et al*. (2003)[232], Day *et al*. (2003) [119] and Suzuki *et al*. (2003) [116]. Raobaikady *et al*. (2003) [110] reported a significant increase in detached and rounded cells after exposure of MCF-7 cells to 1µM of 2ME-BM for 24 hours. Ho *et al*. (2003) [232] indicated that the exposure of human dermal fibroblasts to 0.1µM of 2ME-BM for 24 hours resulted in significant morphological changes without indications of apoptosis. Day *et al*. (2003) [119] showed rounded, detached cells displaying apoptotic characteristics in LNCaP, PC3 and normal- and drug-resistant A2780 ovarian carcinoma cell lines after 48 hours of treatment with 1µM of 2ME-BM. The study by Suzuki *et al*. (2003) [116] in MCF-7 and drug resistant MCF-7-MR and MCF-7 DOX40 cells revealed significant changes in cell adhesion and colony formation in response to 1µM 2ME-BM exposure for 5 days.

The involvement of apoptosis in the observed cell death was confirmed in this study by flow cytometric analyses of phosphatidylserine externalization (annexin V-FITC binding). It was furthermore shown by flow cytometric analyses that 2ME-BM does not cause a mitochondrial permeability transition (MPT) at the time- and dose parameters used. This result is supported by studies conducted in our laboratory by Visagie *et al*. (2011) [230] and Visagie *et al*. (2012) [231], demonstrating no statistically significant decrease in mitochondrial membrane potential after 48 hours of exposure to 0.4µM 2ME-BM in MCF-7 and MCF-12A cells. However, a study by Foster *et al*. (2008) [122] revealed significant depolarization of the inner mitochondrial membrane potential with concurrent cytochrome *c* release and phosphatidylserine externalization in MDA-MB-231 and

HUVEC cells after 72 hours of exposure to 0.5µM 2ME-BM, indicating that this effect may be dependent on cell line, exposure time and the dosage of 2ME-BM utilized.

Investigation of the cytoskeletal effects of 2ME-BM through fluorescence microscopy showed distinct disturbances in cytoskeletal organization in exposed cells of both cell lines. The microtubule network appeared to be severely disrupted by 2ME-BM, with the observation of shortened and malformed microtubule fibers and cellular shrinkage. This would lead to inhibition of effective intracellular protein and organelle translocation and cause the formation of unattached kinetochores during mitosis and subsequently prolonged activation of the spindle assembly checkpoint. Fluorescence microscopy to investigate autophagic processes furthermore revealed the novel finding of a significant increase in the number of acidic intracellular lysosomes, indicating the involvement of autophagic processes, an effect confirmed by the raised LC3 levels (indicating autophagosome formation) observed with flow cytometric analyses. The MCF-7 cell line was again more severely affected by 2ME-BM exposure when compared to the MCF-12A cell line.

Flow cytometric analyses showed a significant shift in cell cycle dynamics and progression after 2ME-BM exposure, with cells being trapped in the G_2/M phase transition (accompanied by cyclin B1 accumulation) and very few cells progressing through metaphase and into the subsequent cell cycle phases (confirmed by microscopy techniques). This observation is supported by the findings of studies by Suzuki *et al*.

(2003) [116], Foster *et al*. (2008)[122], Ho *et al*. (2003)[232], Visagie *et al*. (2011) [230] and Visagie *et al*. (2012) [231]. Suzuki *et al*. (2003) [116] indicated a significantly increaesed number of MCF-7, MCF-7-MR and MCF-7 DOX40 cells in the G_2/M phase after 5 days of exposure to 1µM 2ME-BM. Foster *et al*. (2008) [122] found a significant decrease in G_1 phase cells when exposing the MDA-MB-231 and HUVEC cell lines to 0.5µM 2ME-BM for 72 hours. Ho *et al*. (2003) [232] found a 21% increase in G_2/M phase cells and a concurrent 23% decrease in G_1/S phase cells in human dermal fibroblasts after 48 hours of exposure to 0.1µM of 2ME-BM. However, they found no significant change in HUVEC cell cycle dynamics after 24 hours of exposure to 0.1µM 2ME-BM. Visagie *et al*. (2011) [230] and Visagie *et al*. (2012) [231] found no significant G_2/M phase block after 48 hours of exposure to 0.4µM of 2ME-BM in the MCF7 and MCF-12A cell lines, but did show an increase in the sub-G_1 cell fraction of treated MCF-7 samples [230].

When the results of this study and previous studies related to 2ME-BM and other sulphamoylated derivatives of 2ME2 are considered and compared to literature regarding the parent 2ME2 molecule, it becomes clear that 2ME-BM exerts these effects at a much lower concentration.

In a study by Lee *et al*. (2008) [233] a concentration range of 1-10µM 2ME2 for 24 was used to induce a G_2/M phase block and subsequent apoptosis after 72 hours of exposure. Thaver *et al*. (2009) [234] found morphological changes, G_2/M phase block and 40% growth inhibition of WHCO3 cells after 72 hours using 1µM of 2ME2. Stander *et al*. (2010) showed G_2/M phase block, morphological changes and apoptosis induction when MCF-7 cells were exposed to 1µM of 2ME2 for 24 hours. It appears from these results that

sulphamoylation of the steroid nucleus of the parent 2ME2 molecule results in a more favorable protein binding profile. Added to these observations, are the benefits of sulphamoylation seen during *in vivo* studies, which showed 2ME-BM and other sulphamoylated 2ME2-derivatives to have increased bioavailability [118]. It has been suggested that this effect is due to the ability of the sulphamoylated derivatives to enter red blood cells, thus escaping first-pass elimination by the liver [109].

Mitosis can only progress past metaphase once the MPF has been dephosphorylated and translocated to the nucleus via the microtubule network and centrosomes. Analysis of the MPF-involved protein cyclin B1 showed a distinct increase in intracellular levels, possibly due to inhibition of the normal proteasomal degradation or 2ME-BM induced defects in microtubule dynamics. Cyclin B1 binds to Cdk-1 to form MPF which is held in an inactive state by phosphorylation by Wee1 kinase and Myt1 kinase. Activation is achieved through the dephosphorylation of the complex by Cdc25C, after which normal mitosis can occur. Rising cyclin B1 levels in conjunction with pre-mitotic cell cycle arrest would thus indicate an upstream cell cycle machinery blockade, which warrants further investigation. The up-regulation of cyclin B1 has also been observed in studies of 2ME2, and Choi *et al*. (2012) [107], who observed a strong up-regulation of cyclin B1 levels in MCF-7 cells in response to 2ME2 exposure, proposed that this effect is due to the microtubule disruption caused by 2ME2. When an overview of these results is taken this molecular mechanism of action for 2ME-BM appears probable.

It is thus possible that the effects on cell cycle progression and cell death are caused by the binding of 2ME-BM to the colchicine binding site of tubulin, thus depolymerizing the microtubule network, preventing chromosomal separation during mitosis and disrupting normal cellular structure and function in the same way as its parent compound, 2ME2 [107, 235]. Such a mechanism of action would also explain the differential effects observed in the fast-dividing carcinogenic MCF-7 cell line when compared to the relatively slow-dividing non-carcinogenic MCF-12A cell line. During the G_2/M-phase block, Mad2 can bind to the unattached kinetochores, activating the JNK1 pathway [107]. Tubulin polymerization has been shown to be linked to cell death signaling [125 236, 237], and prolonged disruption of microtubules would result in cytoprotective autophagy and eventual apoptotic cell death.

2ME-BM was found to negatively affect the carcinogenic MCF-7 cell line to a greater extent when results were compared to the non-carcinogenic MCF-12A cell line, encouraging further research into this potentially useful anticancer agent. Furthermore, in addition to the novel insights into the cellular mechanism of action of 2ME-BM's effects offered by these results (cyclin B1 levels, autophagy detection and visualization, cell cycle analysis, cytoskeletal investigation), 2ME-BM was found to potently inhibit cell proliferation in a time-and dose-dependent manner in concurrence with previous studies using different cell lines [111, 115, 118].

This study has thus shown that 2ME-BM disrupts the microtubule network, causes a G2/M-phase block and induces both apoptosis and autophagy. Furthermore, the differential action mechanisms of 2ME-BM on the MCF-7 and MCF-12A cell lines were

clearly demonstrated, confirming that 2ME-BM affects the fast-dividing carcinogenic cell line to a greater extent and these results pave the way to pursue 2ME-BM'S potential clinical application in cancer therapy.

4.2. *Sutherlandia frutescens*

The aim of this study was to investigate the influence of aqueous *S. frutescens* extracts on cell proliferation, cellular morphology and cell death, and to compare these effects in the carcinogenic MCF-7 and non-carcinogenic MCF-12A cell lines. Crude aqueous extracts were used in order to evaluate the *in vitro* pharmacological relevance of traditionally used ethnopharmacological preparations [125, 127] for support to future *in vivo* research and the possible isolation of novel therapeutic compounds.

This study has shown that aqueous *S. frutescens* extracts have differential effects on proliferation, morphology and cell cycle progression in the carcinogenic MCF-7 and non-carcinogenic MCF-12A cell lines.

Spectrophotometric techniques (crystal violet staining) were utilized to evaluate proliferation as a method to screen different time- and dose parameters. Results show that aqueous *S. frutescens* extracts inhibit cell proliferation in a time- and dose-dependent manner. It was determined that a time- and dose combination of 1mg/ml for 48 hours were the optimal parameters for this study. Using these parameters, growth inhibition was quantified at 48.2% for the MCF-7 cell line and 6.8% for the MCF-12A cell line (a difference of 41.43%). These values are comparable to those used in previous studies by Stander *et al*. (2007)[140] where

1.5mg/ml of ethanolic extract yielded a growth inhibition of 50% and 26% after 24 and 48 hours respectively in MCF-7 cells and Tai *et al.* (2004)[238] where ethanolic extracts of *S. frutescens* tablets were evaluated on MCF-7, MDA-MB-468, Jurkat and HL60 cell lines in concentrations ranging from 0.55mg/ml to 1.375mg/ml, resulting in significant growth inhibition. Stander *et al*. (2009) [239] used aqueous *S. frutescens* extracts in a concentration range of 2mg/ml to 10mg/ml for 72 hours to determine IC_{50} values in MCF-7 and MCF-12A cells and decided to conduct further studies with concentrations of 5mg/ml and 10mg/ml. Skerman *et al*. (2011) [240] evaluated the effects of ethanolic *S. frutescens* extracts (extracted from *S. frutescens* plants found in two different regions) on the growth of SNO esophageal cancer cells, and found IC_{50} values between 2.5mg/ml and 5mg/ml depending on plant origin. As shown in the studies by Albrecht *et al*. (2012) [241] and Mncwangi *et al*. (2012)[242], *S. frutescens* samples from different geographic origins show marked differences in chemical composition, possibly accounting for the wide range of IC_{50} values and variable effects reported in the literature.

Morphological investigations by means of light microscopy after haematoxylin and eosin staining and PlasDIC microscopy revealed defined apoptotic characteristics in cells exposed to aqueous *S. frutescens* extracts, with hypercondensed and fragmented chromatin, apoptotic blebbing and cellular disintegration being observed in both MCF-7 and MCF-12A cell line.

Mitotic index counts and flow cytometric analyses of cell cycle dynamics showed a distinct decrease in actively cycling cells in response to aqueous *S. frutescens* extracts. These results

are in accordance with previous studies by Chinkwo (2005)[128], Stander *et al*. (2007)[140] and Skerman *et al*. (2011)[240]. Chinkwo (2005) [126] observed vacuolization, nuclear condensation and membrane damage indicative of cell death after only 6 hours of exposure in the Chinese hamster ovary (CHO) and CaSki cervical carcinoma cell lines when using 3.5mg/ml aqueous *S. frutescens* extracts. Stander *et al*. (2007) [140] found decreased cell density and morphological indications of apoptosis after 24 hours in MCF-7 cells exposed to 1.5mg/ml ethanolic *S. frutescens* extracts, while Skerman *et al*. (2011) [240] showed that SNO cells exposed to 2.5mg/ml and 5mg/ml ethanolic *S. frutescens* extracts for 24 hours displayed membrane blebbing and detachment from culture dishes, indicative of apoptotic and necrotic cell death.

Fluorescence microcopy of intracellular lysosomes and flow cytometric analyses of cell cycle progression and the annexin V-FITC assay of PS externalization showed that aqueous *S. frutescens* extracts inhibit proliferation and induce autophagy with the carcinogenic MCF-7 cells to be more susceptible to these effects. These finding are supported by the results of Stander *et al*. (2009) [239] where exposure of MCF-7 and MCF-12A cells to 5mg/ml and 10mg/ml aqueous *S. frutescens* extracts for 72 hours resulted in increased cytoplasmic lysosomal staining with acridine orange, indicating increased autophagic activity.

These findings are in concurrence with previous studies [126, 140] which have demonstrated the cytostatic and cytotoxic effects of *S. frutescens* in cervical carcinoma, CHO Chinese hamster ovary cancer cells, DU-145 prostate cancer cells and MDA-MB-231 breast cancer cells.

However phosphatidylserine externalization, indicative of apoptosis, was observed to a much lesser extent in the current study than in previously studies utilizing ethanolic extracts [126, 239]. Chinkwo (2005)[126] showed positive results when investigating CHO cells for phosphatidylserine externalization in response to 3.5mg/ml aqueous *S. frutescens* extracts with fluorescence microscopy, and confirmed that approximately 70% of treated cells were undergoing apoptosis through flow cytometric investigation of phosphatidylserine externalization. Using 5mg/ml and 10mg/ml aqueous *S. frutescens* extracts Stander *et al*. (2009) [239] found phosphatidylserine externalization in MCF-7 cells to be elevated by 17.1% (5mg/ml) and 66.5% (10mg/ml) respectively. MCF-12A cells were similarly affected, showing a rise in apoptotic activity of 23.7% (5mg/ml) and 42.2% (10mg/ml) in response to *S. frutescens* treatment. Furthermore, no S-phase cell cycle arrest was observed in this study as previously reported by Stander *et al*. (2009)[239] when using ethanolic extracts of *S. frutescens* [239] and the cancer-specific cytotoxic effects previously reported in ethanolic extracts appear to be less pronounced when aqueous extracts are utilized. The carcinogenic MCF-7 cell line was, however, clearly more susceptible to the cytostatic effects described, as evidenced by the proliferation assay results.

Significant inroads into the chemical characterization of *S. frutescens* have recently been made. It has been shown by van Wyk *et al*. (2008) [125] that *S. frutescens* contains a complex mixture of amino acids, canavanine and pinitol. Furthermore, a study by Albrecht et al. (2012) [241] verified the presence of sutherlandin and sutherlandioside compounds and again confirmed the chemically heterogeneous nature of *S. frutescens* samples obtained from

different geographical locations. Mncwangi et al. (2012) investigated the variable amounts and types of amino acids in *S. frutescens* samples from 51 different locations, identifying proline, L-asparagine and alanine as the most abundant amino acids and confirming the presence of pinitol. They too found variation with regard to chemical composition in plants collected from different geographical locations, and found that amino acids made up 10% - 15% of dried plant material. Several of the compounds identified by these studies have effects on cellular function, leading to the hypothesis that the effects of *S. frutescens* extracts are mediated through the actions of a combination of several different chemicals instead of a single pharmacologically active agent. This would lead to several distinct, but interlinked, mechanisms of action, each corresponding to an active component of *S. frutescens.*

This study has shown that aqueous *S. frutescens* extracts inhibit cell proliferation and could induce autophagy and apoptosis. Differences between the responses of the carcinogenic MCF-7 and non-carcinogenic MCF-12A cell lines to aqueous *S. frutescens* extracts were not as pronounced, however clearly differential results were obtained with regard to inhibition of cell proliferation and observed cell density. Results of this study yielded valuable data in the search for a molecular mechanism of action for extracts of *S. frutescens*.

Chapter 5 - Conclusion

5.1. 2-Methoxyestradiol-bis-sulphamate

In conclusion, this study has revealed novel insights into the intracellular events which make 2ME-BM a potent inhibitor of MCF-7 breast adenocarcinoma cell growth by demonstrating previously undocumented characteristics of 2ME-BM-induced cell cycle arrest (cell cycle analysis, cyclin B1 levels) and subsequent autophagic processes and apoptotic cell death (autophagy detection and morphological investigations).

2ME-BM was shown to potently inhibit cell growth during proliferation assays and a GI_{50} value of 0.4µM was established after 24 hours of exposure. Morphological investigations showed decreased cell density, defined cell cycle disturbances, cytoskeletal disruption, distinct apoptotic characteristics and increased autophagic activity in response to 2ME-BM exposure. Flow cytometric analyses confirmed that a G_2/M-phase cell cycle block, apoptotic induction and autophagic processes were present in exposed samples and showed that mitochondrial permeability was unaffected by 2ME-BM at the time- and dose parameters used in this study. Furthermore, it was noted that the non-tumorigenic MCF-12A cell line was less severely affected by 2ME-BM exposure than the tumorigenic MCF-7 cell line,

indicating a certain degree of cancer specificity. This effect is probably, at least in part, due to the antimitotic actions of 2ME-BM, thus having more pronounced actions in fast-dividing cells, such as tumor cells.

This study has broadened our understanding of the underlying mechanisms involved in the cellular and molecular effects of 2ME-BM. However, several questions regarding the intracellular signaling events that lead to the observed cell death still remain unanswered. Elucidation of a detailed picture of the intracellular events that facilitate the actions of 2ME-BM could lead to the discovery of additional anticancer drug targets, and specific protein targets could help researchers to refine the structures surrounding the steroid nucleus of 2ME2, leading to greater and more targeted therapies. Further research into the mechanism of action of 2ME-BM could include *in silico*-binding screening used in conjunction with microarray and protein array analyses to identify the protein targets of 2ME-BM followed by biochemical studies to quantify such interactions. Given the therapeutic potential of 2ME-BM, future studies into these signaling mechanisms are warranted.

5.2. *Sutherlandia frutescens*

In conclusion, this study has shown that aqueous *S. frutescens* extracts exert clearly differential effects on cellular proliferation in the MCF-7 and MCF-12A cell lines. It was further shown that aqueous *S. frutescens* extracts can induce autophagy and apoptosis in these cells.

Single pharmacologically active ingredients in *S. frutescens* isolates *vs.* the differing efficacy of ethanolic and aqueous extracts, makes it probable that the cumulative combination of the plant's chemical ingredients are responsible for the promising anticancer effects. The finding that aqueous extracts appear to be less effective when compared to ethanolic extracts could indicate the ethanolic fractionalization of a key effector molecule leading to the promising cancer specific cytotoxic effects previously observed. While the studies of the chemical composition of *S. frutescens* plant material mentioned above have expanded our knowledge of the substances responsible for the observed effects, further research into the variable presence in plant material and the combined effects of these compounds is required before a mechanism of action can be hypothesized. Such research could lead to the development of new anticancer drugs and strategies utilizing the synergistic effects of diverse compounds. It is thus clear that additional study regarding the composition and effects of *S. frutescens* extracts will be of great merit in the continuing fight against cancer.

This study has broadened our understanding of the effects of aqueous *S. frutescens* extracts by showing that aqueous extracts have differential effects on proliferation in the carcinogenic MCF-7 breast adenocarcinoma cell line when compared to the non-carcinogenic MCF-12A cell line and demonstrated the effects of such extracts on morphology and cell death in these cell lines. Further *in vitro* research and biochemical analyses into the physiological and molecular mechanisms of this potentially useful natural product are warranted.

References

1. Ferlay J, Shin H, Bray F, Forman D, Mathers C, Parkin D. Estimates of worldwide burden of cancer in 2008: GLOBOCAN 2008. Int J Cancer. 2010; 127: p. 2893-2917.

2. Jemal A, Bray F, Center M, Ferlay J, Ward E, Forman D. Global Cancer Statistics. CA Cancer J Clin. 2011; 61: p. 69-90.

3. Jemal A, Bray F, Forman D, O'Brien M, Ferlay J, Center M, et al. Cancer Burden in Africa and Opportunities for Prevention. Cancer. 2012; 118(18): p. 4372-4384.

4. Statistics South Africa. Mortality and causes of death in South Africa, 2009: Findings from death notification. Pretoria:; 2011. Report No.: P0309.3.

5. Chen F, Wang W, El-Deiry W. Current strategies to target p53 in cancer. Biochem Pharmacol. 2010; 80(5): p. 724-730.

6. Staples O, Steele R, Lain S. p53 as a therapeutic target. Surgeon. 2008; 6(4): p. 240-243.

7. Quyn A, Steele R, Näthke I. Prognostic and therapeutic applications of APC mutations in colorectal cancer. Surgeon. 2008; 6(6): p. 350-356.

8. Manning A, Dyson N. pRB, a tumor suppressor with a stabilizing presence. Trends Cell Biol. 2011; 21(8): p. 433-441.

9. Larsson L. Oncogene- and tumor suppressor gene-mediated suppression of cellular senescence. Semin Cancer Biol. 2011; 21: p. 367-376.

10. Chelimo C, Wouldes T, Cameron L, Elwood J. Risk factors for and prevention of human papillomaviruses (HPV), genital warts and cervical cancer. J Infect. 2013; 66(3): p. 207-217.

11. Mu N, Zhu Y, Wang Y, Zhang H, Xue F. Insulin resistance: A significant risk factor of endometrial cancer. Gynecol Oncol. 2012; 125: p. 751-757.

12. Burger M, Catto J, Dalbagni G, Grossman H, Herr H, Karakiewicz P, et al. Epidemiology and Risk Factors of Urothelial Bladder Cancer. Eur Urol. 2013; 63(2): p. 234-241.

13. Meurman J. Infectious and dietary risk factors of oral cancer. Oral Oncol. 2010; 46: p. 411-413.

14. Asombang A, Kelly P. Gastric cancer in Africa: what do we know about incidence and risk factors? Trans R Soc Trop Med Hyg. 2012; 106: p. 69-74.

15. Puñal-Riobóo J, Varela-Lema L, Barros-Dios J, Juiz-Crespo M, Ruano-Raviñaa A. Occupation as a risk factor for oral and pharyngeal cancer. Acta Otorrinolaringol Esp.

2010; 61(5): p. 375-383.

16. Russo P, Cardinale A, Margaritora S, Cesario A. Nicotinic receptor and tobacco-related cancer. Life Sci. 2012; 91: p. 1087-1092.

17. Huang R, Chen G. Cigarette smoking, cyclooxygenase-2 pathway and cancer. Biochim Biophys Acta. 2011; 1815: p. 158-169.

18. Reidy J, McHugh E, Stassen L. A review of the relationship between alcohol and oral cancer. Surgeon. 2011; 9: p. 278-283.

19. Okona-Mensah K, Battershill J, Boobis A, Fielder R. An approach to investigating the importance of high potency polycyclic aromatic hydrocarbons (PAHs) in the induction of lung cancer by air pollution. Food Chem Toxicol. 2005; 43: p. 1103-1116.

20. Nilsson R. The molecular basis for induction of human cancers by tobacco specific nitrosamines. Regul Toxicol Pharmacol. 2011; 60: p. 268-280.

21. Jelski W, Szmitkowski M. Alcohol dehydrogenase (ADH) and aldehyde dehydrogenase (ALDH) in the cancer diseases. Clin Chim Acta. 2008; 395: p. 1-5.

22. Li M, Greenberg R. Links between genome integrity and BRCA1 tumor suppression. Trends Biochem Sci. 2012; 37(10): p. 418-424.

23. Tourvas A, Frangos C. Towards an extension of the two-variable model of

carcinogenesis through oncogenes and tumour suppressor genes. Med Hypotheses. 2011; 77: p. 956-958.

24. LLeonart M. A new generation of proto-oncogenes: Cold-inducible RNA binding proteins. Biochim Biophys Acta. 2010; 1805: p. 43-52.

25. Schäfer R, Sers C. RAS oncogene-mediated deregulation of the transcriptome: From molecular signature to function. Adv Enzyme Regul. 2011; 51: p. 126-136.

26. Lenz G. Transient oncogenes. Med Hypotheses. 2010; 75: p. 660-662.

27. Lee J. The good oncogene: When bad genes identify good outcome in cancer. Med Hypotheses. 2011; 76: p. 259-263.

28. Zhao J, Roberts T, Hahn W. Functional genetics and experimental models of human cancer. Trends Mol Med. 2004; 10(7): p. 344-350.

29. Wang Z, Ahmad A, Li Y, Kong D, Azmi A, Banerjee S, et al. Emerging roles of PDGF-D signaling pathway in tumor development and progression. Biochim Biophys Acta. 2010; 1806: p. 122-130.

30. Denley A, Cosgrove L, Booker G, Wallace J, Forbes B. Molecular interactions of the IGF system. Cytokine Growth Factor Rev. 2005; 16: p. 421-439.

31. Larsson L, Henriksson M. The Yin and Yang functions of the Myc oncoprotein in

cancer development and as targets for therapy. Exp Cell Res. 2010; 316: p. 1429-1437.

32. Dang C, O'Donnell K, Zeller K, Nguyen T, Osthus R, Li F. The c-Myc target gene network. Semin Cancer Biol. 2006; 16: p. 253-264.

33. Cowling V, Cole M. Mechanism of transcriptional activation by the Myc oncoproteins. Semin Cancer Biol. 2006; 16: p. 242-252.

34. Laurenti E, Wilson A, Trumpp A. Myc's other life: stem cells and beyond. Curr Opin Cell Biol. 2009; 21: p. 844-854.

35. Araki H. Cyclin-dependent kinase-dependent initiation of chromosomal DNA replication. Curr Opin Cell Biol. 2010; 22: p. 766-771.

36. Echalier A, Endicott J, Noble M. Recent developments in cyclin-dependent kinase biochemical and structural studies. Biochim Biophys Acta. 2010; 1804: p. 511-519.

37. Wells A. Cyclin-dependent kinases: Molecular switches controlling energy and potential therapeutic targets for tolerance. Semin Immunol. 2007; 19: p. 173-179.

38. Weigel N, Moore N. Cyclins, cyclin dependent kinases, and regulation of steroid receptor action. Mol Cell Endocrinol. 2007; 265-266: p. 157-161.

39. Mayer B. Perspective: Dynamics of receptor tyrosine kinase signaling complexes. FEBS Lett. 2012; 586: p. 2575-2579.

40. Lemmon M, Schlessinger J. Cell Signaling by Receptor Tyrosine Kinases. Cell. 2010; 141: p. 1117-1134.

41. Biarc J, Chalkley R, Burlingame A, Bradshaw R. Receptor tyrosine kinase signaling – a proteomic perspective. Adv Enzyme Regul. 2011; 51: p. 293-305.

42. Petrelli F, Borgonovo K, Cabiddu M, Barni S. Efficacy of EGFR Tyrosine Kinase Inhibitors in Patients With EGFR-Mutated Non–Small-Cell Lung Cancer: A Meta-Analysis of 13 Randomized Trials. Clin Lung Cancer. 2012; 13(2): p. 107-114.

43. Pines G, Köstler W, Yarden Y. Oncogenic mutant forms of EGFR: Lessons in signal transduction and targets for cancer therapy. FEBS Lett. 2010; 584: p. 2699-2706.

44. Foley J, Nickerson N, Nam S, Allen K, Gilmore J, Nephew K, et al. EGFR signaling in breast cancer: Bad to the bone. Semin Cell Dev Biol. 2010; 21: p. 951-960.

45. Lieu C, Kopetz S. The Src Family of Protein Tyrosine Kinases: A New and Promising Target for Colorectal Cancer Therapy. Clin Colorectal Cancer. 2010; 9(2): p. 89-94.

46. Zhang S, Yu D. Targeting Src family kinases in anti-cancer therapies: turning promise into triumph. Trends Pharmacol Sci. 2012; 33(3): p. 122-128.

47. Lavoie J, Landry M, Faure R, Champagne C. Src-family kinase signaling, actin-mediated membrane trafficking and organellar dynamics in the control of cell fate:

Lessons to be learned from the adenovirus E4orf4 death factor. Cell Signal. 2010; 22: p. 1604-1614.

48. Karlsson R, Pedersen E, Wang Z, Brakebusch C. Rho GTPase function in tumorigenesis. Biochim Biophys Acta. 2009; 1796: p. 91-98.

49. Barr F. Rab GTPase function in Golgi trafficking. Sem Cell Dev Biol. 2009; 20: p. 780-783.

50. Rajalingam K, Schreck R, Rapp U, Albert S. Ras oncogenes and their downstream targets. Biochim Biophys Acta. 2007; 1773: p. 1177-1195.

51. Buday L, Downward J. Many faces of Ras activation. Biochim Biophys Acta. 2008; 1786: p. 178-187.

52. Patra S. Ras regulation of DNA-methylation and cancer. Exp Cell Res. 2008; 314: p. 1193-1201.

53. Murugan A, Munirajan A, Tsuchida N. Ras oncogenes in oral cancer: The past 20 years. Oral Oncol. 2012; 48: p. 383-392.

54. Warmerdam D, Kanaar R. Dealing with DNA damage: Relationships between checkpoint and repair pathways. Mutat Res. 2010; 704: p. 2-11.

55. Poehlmann A, Roessner A. Importance of DNA damage checkpoints in the

pathogenesis of human cancers. Pathol Res Pract. 2010; 206: p. 591-601.

56. Zhang M, Yang H. Negative growth regulators of the cell cycle machinery and cancer. Pathophysiology. 2009; 16: p. 305-309.

57. Coin F, Oksenych V, Mocquet V, Groh S, Blattner C, Egly J. Nucleotide Excision Repair Driven by the Dissociation of CAK from TFIIH. Mol Cell. 2008; 31: p. 9-20.

58. Zhu Q, Wani G, Sharma N, Wani A. Lack of CAK complex accumulation at DNA damage sites in XP-B and XP-B/CS fibroblasts reveals differential regulation of CAK anchoring to core TFIIH by XPB and XPD helicases during nucleotide excision repair. DNA Repair. 2012; 11(12): p. 942-950.

59. Karlsson-Rosenthal C, Millar J. Cdc25: mechanisms of checkpoint inhibition and recovery. Trends Cell Biol. 2006; 16(6): p. 285-292.

60. Malumbres M. Oncogene-Induced Mitotic Stress: p53 and pRb Get Mad Too. Cancer Cell. 2011; 19: p. 691-692.

61. Dey A, Lane D, Verma C. Modulating the p53 pathway. Semin Cancer Biol. 2010; 20: p. 3-9.

62. Machado-Silva A, Perrier S, Bourdon J. p53 family members in cancer diagnosis and treatment. Semin Cancer Biol. 2010; 20: p. 57-62.

63. Price M, Monteiro A. Fine tuning chemotherapy to match BRCA1 status. Biochem Pharmacol. 2010; 80: p. 647-653.

64. Jung Y, Qian Y, Chen X. Examination of the expanding pathways for the regulation of p21 expression and activity. Cell Signal. 2010; 22: p. 1003-1012.

65. Zhang P, Chen J, Guo X. New insights into PTEN regulation mechanisms and its potential function in targeted therapies. Biomed Pharmacother. 2012; 66: p. 485-490.

66. Park K, Liu K, Hu Y, Kanter J, He Z. PTEN/mTOR and axon regeneration. Exp Neurol. 2010; 223: p. 45-50.

67. Hurst D, Welch D. Unraveling the enigmatic complexities of BRMS1-mediated metastasis suppression. FEBS Lett. 2011; 585: p. 3185-3190.

68. Galmarini D, Galmarini C, Galmarini F. Cancer chemotherapy: A critical analysis of its 60 years of history. Crit Rev Oncol Hematol. 2012; 84: p. 181-199.

69. Rieder E, Swanstrom L. Advances in cancer surgery: Natural orifice surgery (NOTES) for oncological diseases. Surg Oncol. 2011; 20: p. 211-218.

70. Reed M. Principles of cancer treatment by surgery. Surgery (Oxford). 2009; 27(4): p. 178-181.

71. Abraham J, Staffurth J. Hormonal therapy for cancer. Medicine. 2011; 39(12): p.

723-727.

72. Bossi A. Modern External-Beam Radiation Therapy for Prostate Cancer: How and When? European Urology Supplements. 2008; 7: p. 22-28.

73. Borchiellini D, Etienne-Grimaldi M, Thariat J, Milano G. The impact of pharmacogenetics on radiation therapy outcome in cancer patients. A focus on DNA damage response genes. Cancer Treat Rev. 2012; 38: p. 737-759.

74. Shuptrine C, Surana R, Weiner L. Monoclonal antibodies for the treatment of cancer. Semin Cancer Biol. 2012; 22: p. 3-13.

75. Rescigno M, Avogadri F, Curigliano G. Challenges and prospects of immunotherapy as cancer treatment. Biochim Biophys Acta. 2007; 1776: p. 108-123.

76. Ridky T. Nonmelanoma skin cancer. J Am Acad Dermatol. 2007; 57: p. 484-501.

77. Berry M, Gomez K. Surgical techniques in breast cancer. Surgery. 2009; 28(3): p. 135-139.

78. Cash J, Fay J, Dattoli M. Combined modality treatment for prostate cancer with dynamic adaptive radiation therapy using four-dimensional image-guided intensity-modulated radiation therapy and brachytherapy. J Radiol Nurs. 2009; 28: p. 87-95.

79. Geisler J, Lønning P. Aromatase inhibitors as adjuvant treatment of breast cancer.

Crit Rev Oncol Hematol. 2006; 57: p. 53-61.

80. Heredi-Szabo K, Lubke J, Toth G, Murphy R, Lovas S. Importance of the central region of lamprey gonadotropin-releasing hormone III in the inhibition of breast cancer cell growth. Peptides. 2005; 26: p. 419-422.

81. Wirth M, Hakenberg O, Froehner M. Antiandrogens in the Treatment of Prostate Cancer. Eur Urol. 2007; 51: p. 306-314.

82. Chua W, Kho P, Moore M, Charles K, Clarke S. Clinical, laboratory and molecular factors predicting chemotherapy efficacy and toxicity in colorectal cancer. Crit Rev Oncol Hematol. 2011; 79: p. 224-250.

83. Coley H. Mechanisms and strategies to overcome chemotherapy resistance in metastatic breast cancer. Cancer Treat Rev. 2008; 34: p. 378-390.

84. Borghaei H, Smith M, Campbell K. Immunotherapy of cancer. Eur J Pharmacol. 2009; 625: p. 41-54.

85. Speiser D, Romero P. Molecularly defined vaccines for cancer immunotherapy, and protective T cell immunity. Semin Immunol. 2010; 22: p. 144-154.

86. Lasaro M, Ertl H. Targeting inhibitory pathways in cancer immunotherapy. Curr Opin Immunol. 2010; 22: p. 385-390.

87. Binyamin L, Borghaei H, Weiner L. Cancer therapy with engineered monoclonal antibodies. Update Cancer Ther. 2006; 1: p. 147-157.

88. Weiner L, Dhodapkar M, Ferrone S. Monoclonal antibodies for cancer immunotherapy. Lancet. 2009; 373: p. 1033-1040.

89. Parks M, Tillhon M, Donà F, Prosperi E, Scovassi A. 2-Methoxyestradiol: New perspectives in colon carcinoma treatment. Mol Cell Endocrinol. 2011; 331: p. 119-128.

90. Pribluda V, Gubish E, LaVallee T, Treston A, Swartz G, Green S. 2-Methoxyestradiol: an endogenous antiangiogenic and antiproliferative drug candidate. Cancer Metastasis Rev. 2000; 19: p. 173-179.

91. Qadan L, Perez-Stable C, Anderson C, D'Ippolito G, Herron A, Howard G, et al. 2-Methoxyestradiol induces G2/M arrest and apoptosis in prostate cancer. Biochem Biophys Res Commun. 2001; 285: p. 1259-1266.

92. Bu S, Blaukat A, Fu X, Heldin N, Landström M. Mechanisms for 2-methoxyestradiol-induced apoptosis of prostate cancer cells. FEBS Lett. 2002; 531: p. 141-151.

93. Salama S, Diaz-Arrastia C, Patel D, Botting S, Hatch S. 2-Methoxyestradiol, an Endogenous Estrogen Metabolite, Sensitizes Radioresistant MCF-7/FIR Breast Cancer Cells Through Multiple Mechanisms. Int J Radiat Oncol Biol Phys. 2011; 80(1): p. 231-

239.

94. Nakagawa-Yagi Y, Ogane N, Inoki Y, Kitoh N. The endogenous estrogen metabolite 2-methoxyestradiol induces apoptotic neuronal cell death in vitro. Life Sci. 1996; 58: p. 1461-1467.

95. Klauber N, Parangi S, Flynn E, Hamel E, D'Amato R. Inhibition of angiogenesis and breast cancer in mice by the microtubule inhibitors 2-methoxyestradiol and taxol. Cancer Res. 1997; 1(57): p. 81-86.

96. Wang H, Myc A, Koenig R, Bretz J, Arscott P, Baker J. 2-Methoxyestradiol, an endogenous estrogen metabolite, induces thyroid cell apoptosis. Mol Cell Endocrinol. 2000; 165: p. 163-172.

97. Mooberry S. Mechanism of action of 2-methoxyestradiol: new developments. Drug Resist Updat. 2003; 6: p. 355-361.

98. Attalla H, Makela T, Adlercreutz H, Andersson L. 2-Methoxyestradiol Arrests Cells in Mitosis without Depolymerizing Tubulin. Biochem Biophys Res Commun. 1996; 228: p. 467-473.

99. Prakasham A, Shanker K, Negi A. A simple and convenient synthesis of 2-methoxyestradiol from estrone. Steroids. 2012; 77: p. 467-470.

100. Lakhani N, Sarkar M, Venitz J, Figg W. 2-Methoxyestradiol, a promising anticancer

agent. Pharmacotherapy. 2003;(23): p. 165-172.

101. James J, Murry D, Treston A, Storniolo A, Sledge G, Sidor C, et al. Phase I safety, pharmacokinetic and pharmacodynamic studies of 2-methoxyestradiol alone or in combination with docetaxel in patients with locally recurrent or metastatic breast cancer. Invest New Drugs. 2006; 25: p. 41-48.

102. Stubelius A, Andréasson E, Karlsson A, Ohlsson C, Tivesten A, Islander U, et al. Role of 2-methoxyestradiol as inhibitor of arthritis and osteoporosis in a model of postmenopausal rheumatoid arthritis. Clin Immunol. 2011; 140: p. 37-46.

103. Salama S, Diaz-Arrastia C, Kilic G, Kamel M. 2-Methoxyestradiol causes functional repression of transforming growth factor β3 signaling by ameliorating Smad and non-Smad signaling pathways in immortalized uterine fibroid cells. Fertil Steril. 2012; 98(1): p. 178-184.

104. Bàrdos J, Ashcroft M. Negative and positive regulation of HIF-1: A complex network. Biochim Biophys Acta. 2005; 1755: p. 107-120.

105. Strimpakos A, Karapanagiotou E, Saif M, Syrigos K. The role of mTOR in the management of solid tumors: An overview. Cancer Treat Rev. 2009; 35: p. 148-159.

106. Mueck A, Seeger H. 2-Methoxyestradiol - Biology and mechanism of action. Steroids. 2010; 75: p. 625-631.

107. Choi H, Zhu B. Critical role of cyclin B1/Cdc2 up-regulation in the induction of mitotic prometaphase arrest in human breast cancer cells treated with 2-methoxyestradiol. Biochim Biophys Acta. 2012; 1823: p. 1306-1315.

108. Wang Y, Guo R, Caob X, Shen M, Shi X. Encapsulation of 2-methoxyestradiol within multifunctional poly(amidoamine) dendrimers for targeted cancer therapy. Biomaterials. 2011; 32: p. 3322-3329.

109. Newman S, Ireson C, Tutill H, Day J, Parsons M, Leese M, et al. The role of 17b-hydroxysteroid dehydrogenase in modulating the activity of 2-methoxyestradiol in breast cancer cells. Cancer Res. 2006; 66: p. 324-330.

110. Raobaikady B, Purohit A, Chander S, Woo L, Leese M, Potter B, et al. Inhibition of MCF-7 breast cancer cell proliferation and in vivo steroid sulphatase activity by 2-methoxyoestradiol-bis-sulphamate. J Steroid Biochem Mol Biol. 2003; 84: p. 351-358.

111. Chander S, Foster P, Leese M, Newman S, Potter B, Purohit A, et al. In vivo inhibition of angiogenesis by sulphamoylated derivatives of 2-methoxyoestradiol. Br J Cancer. 2007; 96: p. 1368-1376.

112. Reed M, Purohit A. The development of steroid sulphatase inhibitors. Endocr Rel Cancer. 1996; 3: p. 9-23.

113. Woo L, Purohit A, Potter B. Development of steroid sulfatase inhibitors. Mol Cell

Endocrinol. 2011; 340: p. 175-185.

114. Maltais R, Poirier D. Steroid sulfatase inhibitors: A review covering the promising 2000-2010 decade. Steroids. 2011; 76: p. 929-948.

115. Purohit A, Woo L, Chander S, Newman S, Ireson C, Ho Y, et al. Steroid sulphatase inhibitors for breast cancer therapy. J Steroid Biochem Mol Biol. 2003; 86: p. 423-432.

116. Suzuki R, Newman S, Purohit A, Leese M, Potter B, Reed M. Growth inhibition of multi-drug-resistant breast cancer cells by 2-methoxyoestradiol-bis-sulphamate and 2-ethyloestradiol-bis-sulphamate. J Steroid Biochem Mol Biol. 2003; 84: p. 269-278.

117. Ireson C, Chander S, Purohit A, Perera S, Newman S, Parish D, et al. Pharmacokinetics and efficacy of 2-methoxyoestradiol and 2-methoxyoestradiol-bis-sulphamate in vivo in rodents. Br J Cancer. 2004; 90: p. 932-937.

118. Utsumi T, Leese M, Chander S, Gaukroger K, Purohit A, Newman S, et al. The effects of 2-methoxyoestrogen sulphamates on the in vitro and in vivo proliferation of breast cancer cells. J Steroid Biochem Mol Biol. 2005; 94: p. 219-227.

119. Day J, Newman S, Comninos A, Solomon C, Purohit A, Leese M, et al. The effects of 2-substituted oestrogen sulphamates on the growth of prostate and ovarian cancer cells. J Steroid Biochem Mol Biol. 2003; 84: p. 317-325.

120. Foster P, Ho Y, Newman S, Kasprzyk P, Leese M, Potter B, et al. 2-

MeOE2bisMATE and 2-EtE2bisMATE induce cell cycle arrest and apoptosis in breast cancer xenografts as shown by a novel ex vivo technique. Breast Cancer Res Treat. 2008; 111: p. 251-260.

121. MacCarthy-Morrogh L, Townsend P, Purohit A, Hejaz H, Potter B, Reed M, et al. Differential effects of estrone and estrone-3-O-sulfamate derivatives on mitotic arrest, apoptosis and microtuble assembly in human breast cancer cells. Cancer Res. 2000; 60: p. 5441-5450.

122. Castoria G, Migliaccio A, Giovannelli P, Auricchio F. Cell proliferation regulated by estradiol receptor: Therapeutic implications. Steroids. 2010; 75: p. 524-527.

123. da Rocha A, Lopes R, Schwartsmann G. Natural products in anticancer therapy. Curr Opin Pharmacol. 2001; 1: p. 364-369.

124. Balunas M, Kinghorn A. Drug discovery from medicinal plants. Life Sci. 2005;(78): p. 431-441.

125. van Wyk B, Albrecht C. A review of the taxonomy, ethnobotany, chemistry and pharmacology of Sutherlandia frutescens (Fabaceae). J Ethnopharmacol. 2008; 119: p. 620-629.

126. Chinkwo K. Sutherlandia frutescens extracts can induce apoptosis in cultured carcinoma cells. J Ethnopharmacol. 2005; 98: p. 163-170.

127. van Wyk B, Gericke N. People's plants - A guide to useful plants of southern Africa. Pretoria: Briza Publications; 2000.

128. Brown L, Heyneke O, Brown D, van Wyk J, Hamman J. Impact of traditional medicinal plant extracts on antiretroviral drug absorption. J Ethnopharmacol. 2008; 119: p. 588-592.

129. Harnett S, Oosthuizen V, van de Venter M. Anti-HIV activities of organic and aqueous extracts of Sutherlandia frutescens and Lobostemon trigonus. J Ethnopharmacol. 2005; 96: p. 113-119.

130. Grandi M, Roselli L, Vernay M. Lessertia (Sutherlandia frutescens) et la fatigue en cancérologie. Phytothérapie. 2005; 3: p. 110-113.

131. Morris K. Treating HIV in South Africa - a tale of two systems. The Lancet. 2001; 357: p. 1190.

132. Chadwick W, Roux S, van de Venter M, Louw J, Oelofsen W. Anti-diabetic effects of Sutherlandia frutescens in Wistar rats fed a diabetogenic diet. J Ethnopharmacol. 2007; 109: p. 121-127.

133. Katerere D, Eloff J. Antibacterial and Antioxidant Activity of Sutherlandia frutescens (Fabaceae), A Reputed Anti-HIV/AIDS Phytomedicine. Phytother Res. 2005; 19: p. 779-781.

134. Jang M, Jun D, Rue S, Han K, Park W, Kim Y. Arginine antimetabolite L-canavanine induces apoptotic cell death in human Jurkat T cells via caspase-3 activation regulated by Bcl-2 or Bcl-xL. Biochem Biophys Res Commun. 2002; 295: p. 283-288.

135. Pervin S, Singh R, Chaudhuri G. Nitric oxide, Nx-hydroxy-L-arginine and breast cancer. Nitric Oxide. 2008; 19: p. 103-106.

136. Sivakumar S, Palsamy P, Subramanian S. Impact of d-pinitol on the attenuation of proinflammatory cytokines, hyperglycemia-mediated oxidative stress and protection of kidney tissue ultrastructure in streptozotocin-induced diabetic rats. Chem Biol Interact. 2010; 188: p. 237-245.

137. Androutsopoulos V, Papakyriakou A, Vourloumis D, Tsatsakis A, Spandidos D. Dietary flavonoids in cancer therapy and prevention: Substrates and inhibitors of cytochrome P450 CYP1 enzymes. Pharmacol Ther. 2010;(126): p. 9-20.

138. Chan P. Acylation with diangeloyl groups at C21–22 positions in triterpenoid saponins is essential for cytotoxcity towards tumor cells. Biochem Pharmacol. 2007; 73: p. 341-350.

139. Jiang Z, Gallard J, Adeline M, Dumontet V, Tri M, Se´venet T, et al. Six triterpenoid saponins from Maesa laxiflora. J Nat Prod. 1999; 62: p. 873-876.

140. Stander B, Marais S, Steynberg T, Theron D, Joubert F, Albrecht C, et al. Influence of Sutherlandia frutescens extracts on cell numbers, morphology and gene expression in

MCF-7 cells. J Ethnopharmacol. 2007; 112: p. 312-318.

141. Varetti G, Musacchio A. The spindle assembly checkpoint. Curr Biol. 2008; 18(14): p. 591-595.

142. McGuinness B, Anger M, Kouznetsova A, Gil-Bernabe A, Helmhart W, Kudo N, et al. Regulation of APC/C Activity in Oocytes by a Bub1-Dependent Spindle Assembly Checkpoint. Curr Biol. 2009; 19: p. 369-380.

143. Nezi L, Musacchio A. Sister chromatid tension and the spindle assembly checkpoint. Curr Opin Cell Biol. 2009; 21: p. 785-795.

144. Wang Y, Tsai Y, Huang J, Lee K, Kuo C, Wang C, et al. Arecoline arrests cells at prometaphase by deregulating mitotic spindle assembly and spindle assembly checkpoint: Implication for carcinogenesis. Oral Oncol. 2010; 46: p. 255-262.

145. Rieder C, Maiato H. Stuck in Division or Passing through: What Happens When Cells Cannot Satisfy the Spindle Assembly Checkpoint. Dev Cell. 2004; 7: p. 637-651.

146. Sastre-Serra J, Nadal-Serrano M, Pons D, Roca P, Oliver J. Mitochondrial dynamics is affected by 17b-estradiol in the MCF-7 breast cancer cell line. Effects on fusion and fission related genes. Int J Biochem Cell Biol. 2012; 44: p. 1901-1905.

147. Portt L, Norman G, Clapp C, Greenwood M, Greenwood M. Anti-apoptosis and cell survival: A review. Biochim Biophys Acta. 2011; 1813: p. 238-259.

148. Galluzzi L, Morselli E, Kepp O, Vitale I, Rigoni A, Vacchelli E, et al. Mitochondrial gateways to cancer. Mol Aspects Med. 2010; 31: p. 1-20.

149. Mazzoni C, Falcone C. Caspase-dependent apoptosis in yeast. Biochim Biophys Acta. 2008; 1783: p. 1320-1327.

150. Kantari C, Walczak H. Caspase-8 and Bid: Caught in the act between death receptors and mitochondria. Biochim Biophys Acta. 2011; 1813: p. 558-563.

151. Würstle M, Laussmann M, Rehm M. The central role of initiator caspase-9 in apoptosis signal transduction and the regulation of its activation and activity on the apoptosome. Exp Cell Res. 2012; 318: p. 1213-1220.

152. Shikama Y, Shen L, Yonetani M, Miyauchi J, Miyashita T, Yamada M. Death Effector Domain-Only Polypeptides of Caspase-8 and -10 Specifically Inhibit Death Receptor-Induced Cell Death. Biochem Biophys Res Commun. 2002; 291: p. 484-493.

153. Zhao X, Sun Y, Yu H, Ye L, Zhang L, Lu J, et al. Apoptosis induced by BIK was decreased with RNA interference of caspase-12. Biochem Biophys Res Commun. 2007; 359: p. 896-901.

154. Elumalai P, Gunadharini D, Senthilkumar K, Banudevi S, Arunkumar R, Benson C, et al. Induction of apoptosis in human breast cancer cells by nimbolide through extrinsic and intrinsic pathway. Toxicol Lett. 2012; 215: p. 131-142.

155. Beurel E, Jope R. The paradoxical pro- and anti-apoptotic actions of GSK3 in the intrinsic and extrinsic apoptosis signaling pathways. Prog Neurobiol. 2006; 79: p. 173-189.

156. Sirbulescu R, Zupanc G. Inhibition of caspase-3-mediated apoptosis improves spinal cord repair in a regeneration-competent vertebrate system. Neuroscience. 2010; 171: p. 599-612.

157. Vaidya S, Velázquez-Delgado E, Abbruzzese G, Hardy J. Substrate-Induced Conformational Changes Occur in All Cleaved Forms of Caspase-6. J Mol Biol. 2011; 406: p. 75-91.

158. Lamkanfi M, Kanneganti T. Caspase-7: A protease involved in apoptosis and inflammation. Int J Biochem Cell Biol. 2010; 42: p. 21-24.

159. Karimpour S, Davoodi J, Ghahremani M. Integrity of ATP binding site is essential for effective inhibition of the intrinsic apoptosis pathway by NAIP. Biochem Biophys Res Commun. 2011; 407: p. 158-162.

160. Hüttemann M, Pecina P, Rainbolt M, Sanderson T, Kagan V, Samavati L, et al. The multiple functions of cytochrome c and their regulation in life and death decisions of the mammalian cell: From respiration to apoptosis. Mitochondrion. 2011; 11: p. 369-381.

161. Jeong H, Choi H, Lee E, Kim J, Jeon K, Lee H, et al. Involvement of caspase-9 in autophagy-mediated cell survival pathway. Biochim Biophys Acta. 2011; 1813: p. 80-

90.

162. Hardwick J, Chen Y, Jonas E. Multipolar functions of BCL-2 proteins link energetics to apoptosis. Trends Cell Biol. 2012; 22(6): p. 318-328.

163. Muilenburg D, Coates J, Virudachalam S, Bold R. Targeting Bcl-2-Mediated Cell Death as a Novel Therapy in Pancreatic Cancer. J Surg Res. 2010; 163: p. 276-281.

164. Lee H, Li T, Tsao J, Fong Y, Tang C. Curcumin induces cell apoptosis in human chondrosarcoma through extrinsic death receptor pathway. Int Immunopharmacol. 2012; 13: p. 163-169.

165. Ashkenazi A. Targeting the extrinsic apoptosis pathway in cancer. Cytokine Growth Factor Rev. 2008; 19: p. 325-331.

166. Martinez-Lostao L, Marzo I, Anel A, Naval J. Targeting the Apo2L/TRAIL system for the therapy of autoimmune diseases and cancer. Biochem Pharmacol. 2012; 83: p. 1475-1483.

167. Mellier G, Huang S, Shenoy K, Pervaiz S. TRAILing death in cancer. Mol Aspects Med. 2010; 31: p. 93-112.

168. Mahalingam D, Szegezdi E, Keane M, de Jong S, Samali A. TRAIL receptor signalling and modulation: Are we on the right TRAIL? Cancer Treat Rev. 2009; 35: p. 280-288.

169. Hangen E, Blomgren K, Benit P, Kroemer G, Modjtahedi N. Life with or without AIF. Trends Biochem Sci. 2010; 35(5): p. 278-287.

170. Urbano A, Lakshmanan U, Choo P, Kwan J, Ng P, Guo K, et al. AIF suppresses chemical stress-induced apoptosis and maintains the transformed state of tumor cells. EMBO J. 2005; 24(15): p. 2815-2826.

171. Lipton S, Bossy-Wetzel E. Dueling Activities of AIF in Cell Death versus Survival: DNA Binding and Redox Activity. Cell. 2002; 111: p. 147-150.

172. Apostolova N, Cervera A, Victor V, Cadenas S, Sanjuan-Pla A, Alvarez-Barrientos A, et al. Loss of apoptosis-inducing factor leads to an increase in reactive oxygen species, and an impairment of respiration that can be reversed by antioxidants. Cell Death Differ. 2006; 13: p. 354-357.

173. Cheung E, Joza N, Steenaart N, McClellan K, Neuspiel M, McNamara S, et al. Dissociating the dual roles of apoptosis inducing factor in maintaining mitochondrial structure and apoptosis. EMBO J. 2006; 25: p. 4061-4073.

174. Ye H, Cande C, Stephanou N, Jiang S, Gurbuxani S, Larochette N, et al. DNA binding as a structural requirement for the apoptogenic action of AIF. Nat Struct Biol. 2002; 9: p. 680-684.

175. Modjtahedi N, Giordanetto F, Madeo F, Kroemer G. Apoptosis-inducing factor:

vital and lethal. Trends Cell Biol. 2006; 16(5): p. 264-272.

176. Li J, Zhou J, Li Y, Qin D, Li P. Mitochondrial fission controls DNA fragmentation by regulating endonuclease G. Free Radic Biol Med. 2010; 49: p. 622-631.

177. Vaux D. Apoptogenic factors released from mitochondria. Biochim Biophys Acta. 2011; 1813: p. 546-550.

178. Yang Z, Klionsky D. Mammalian autophagy: core molecular machinery and signaling regulation. Curr Opin Cell Biol. 2010; 22: p. 124-131.

179. White E, Karp C, Strohecker A, Guo Y, Mathew R. Role of autophagy in suppression of inflammation and cancer. Curr Opin Cell Biol. 2010; 22: p. 212-217.

180. Kuma A, Mizushima N. Physiological role of autophagy as an intracellular recycling system: With an emphasis on nutrient metabolism. Semin Cell Dev Biol. 2010; 21: p. 683-690.

181. Chen N, Debnath J. Autophagy and tumorigenesis. FEBS Lett. 2010; 584: p. 1427-1435.

182. Chaachouay H, Ohneseit P, Toulany M, Kehlbach R, Multhoff G, Rodemann H. Autophagy contributes to resistance of tumor cells to ionizing radiation. Radiother Oncol. 2011; 99: p. 287-292.

183. Notte A, Leclere L, Michiels C. Autophagy as a mediator of chemotherapy-induced cell death in cancer. Biochem Pharmacol. 2011; 82: p. 427-434.

184. Lozy F, Karantza V. Autophagy and cancer cell metabolism. Semin Cell Dev Biol. 2012; 23: p. 395-401.

185. Hoare M, Young A, Narita M. Autophagy in cancer: Having your cake and eating it. Semin Cancer Biol. 2011; 21: p. 397-404.

186. Ryan K. p53 and autophagy in cancer: Guardian of the genome meets guardian of the proteome. Eur J Cancer. 2011; 47: p. 44-50.

187. Bellot G, Liu D, Pervaiz S. ROS, autophagy, mitochondria and cancer: Ras, the hidden master? Mitochondrion. 2013; 13(3): p. 155-162.

188. Xi G, Hu X, Wu B, Jiang H, Young C, Pang Y, et al. Autophagy inhibition promotes paclitaxel-induced apoptosis in cancer cells. Cancer Lett. 2011; 307: p. 141-148.

189. Zhou S, Zhao L, Kuang M, Zhang B, Liang Z, Yi T, et al. Autophagy in tumorigenesis and cancer therapy: Dr. Jekyll or Mr. Hyde? Cancer Lett. 2012; 323: p. 115-127.

190. Vicencio J, Galluzzi L, Tajeddine N, Ortiz C, Criollo A, Tasdemir E, et al. Senescence, apoptosis or autophagy? When a damaged cell must decide its path - A mini-review. Gerontology. 2008; 54(2): p. 92-99.

191. Levy J, Thorburn A. Targeting autophagy during cancer therapy to improve clinical outcomes. Pharmacol Ther. 2011; 131: p. 130-141.

192. Chen S, Rehman S, Zhang W, Wen A, Yao L, Zhang J. Autophagy is a therapeutic target in anticancer drug resistance. Biochim Biophys Acta. 2010; 1806: p. 220-229.

193. Coates J, Galante J, Bold R. Cancer Therapy Beyond Apoptosis: Autophagy and Anoikis as Mechanisms of Cell Death. J Surg Res. 2009; 2(164): p. 1-8.

194. Esteve J, Armengod M, Knecht E. BRCA1 negatively regulates formation of autophagic vacuoles in MCF-7 breast cancer cells. Exp Cell Res. 2010; 316: p. 2618-2629.

195. Jung C, Ro S, Cao J, Otto N, Kim D. mTOR regulation of autophagy. FEBS Lett. 2010; 584: p. 1287-1295.

196. Chakraborty A, Bodipati N, Demonacos M, Peddinti R, Ghosh K, Roy P. Long term induction by pterostilbene results in autophagy and cellular differentiation in MCF-7 cells via ROS dependent pathway. Mol Cell Endocrinol. 2012; 355: p. 25-40.

197. Chen N, Karantza-Wadsworth V. Role and regulation of autophagy in cancer. Biochim Biophys Acta. 2009; 1793: p. 1516-1523.

198. Kanchan R, Tripathi C, Baghel K, Dwivedi S, Kumar B, Sanyal S, et al. Estrogen receptor potentiates mTORC2 signaling in breast cancer cells by upregulating

superoxide anions. Free Radic Biol Med. 2012; 53: p. 1929-1941.

199. Inoki K, Zhu T, Guan K. TSC2 mediates cellular energy response to control cell growth and survival. Cell. 2003; 115: p. 577-590.

200. Sofer A, Lei K, Johannessen C, Ellisen L. Regulation of mTOR and cell growth in response to energy stress by REDD1. Mol Cell Biol. 2005; 25: p. 5834-5845.

201. Yang Z, Klionsky D. An Overview of the Molecular Mechanism of Autophagy. Curr Top Microbiol Immunol. 2009; 335: p. 1-32.

202. Noda T, Suzuki K, Ohsumi Y. Yeast autophagosomes: de novo formation of a membrane structure. Trends Cell Biol. 2002; 12: p. 231-235.

203. Kim J, Huang W, Stromhaug P, Klionsky D. Convergence of multiple autophagy and cytoplasm to vacuole targeting components to a perivacuolar membrane compartment prior to de novo vesicle formation. J Biol Chem. 2002; 277: p. 763-773.

204. Suzuki K, Kirisako T, Kamada Y, Mizushima N, Noda T, Ohsumi Y. The pre-autophagosomal structure organized by concerted functions of APG genes is essential for autophagosome formation. EMBO J. 2001; 20: p. 5971-5981.

205. Yamada T, Carson A, Caniggia I, Umebayashi K, Yoshimori T, Nakabayashi K, et al. Endothelial nitric-oxide synthase antisense (NOS3AS) gene encodes an autophagy-related protein (APG9-like2) highly expressed in trophoblast. J Biol Chem. 2005; 280:

p. 18283-18290.

206. Young A, Chan E, Hu X, Köchl R, Crawshaw S, High S, et al. Starvation and ULK1-dependent cycling of mammalian Atg9 between the TGN and endosomes. J Cell Sci. 2006; 119: p. 3888-3900.

207. Mari M, Tooze S, Reggiori F. The puzzling origin of the autophagosomal membrane. F1000 Biol Rep. 2011; 3(25): p. 1-9.

208. He C, Klionsky D. Regulation Mechanisms and Signaling Pathways of Autophagy. Annu Rev Genet. 2009; 43: p. 67-93.

209. Wang C, Klionsky D. The Molecular Mechanism of Autophagy. Mol Med. 2003; 9(3/4): p. 65-76.

210. Tanida I, Ueno Y, Kominami E. LC3 conjugation system in mammalian autophagy. Int J Biochem Cell Biol. 2004; 36: p. 2503-2518.

211. Yoshimori T, Noda T. Toward unraveling membrane biogenesis in mammalian autophagy. Curr Opin Cell Biol. 2008; 20: p. 401-407.

212. Xie Z, Klionsky D. Autophagosome formation: core machinery and adaptations. Nat Cell Biol. 2007; 9(10): p. 1102-1109.

213. Gillies R, Didier N, Denton M. Determination of cell number in monolayer cultures.

Anal Biochem. 1986; 159(1): p. 109-113.

214. Kueng W, Silber E, Eppenberger U. Quantification of cells cultured on 96-well plates. Anal Biochem. 1989; 182(1): p. 16-19.

215. Hayat M. Biological Applications - Principles and techniques of electron microscopy. Baltimore: University Park Press; 1981.

216. Beyer H, Riesenberg H. Handbuch der Mikroskopie. Berlin: VEB Verlag Technik; 1988.

217. Kiernan J. Histological Staining in One or Two Colours. In Histological and Histochemical Methods. 4th ed. Oxfordshire: Scion Publishing Ltd; 2008.

218. Kiernan J, Horobin R. A special issue devoted to hematoxylin, hematein, and hemalum. Biotech Histochem. 2010; 85(1): p. 5-6.

219. Kiernan J. Anionic counterstains. CSH Protoc. 2008; doi: 10.1101/pdb.top51.

220. Freshney R. Animal cell cultures. 3rd ed. Oxford: URL Press; 1995.

221. Sukumaran V, Ramalingam A. Spectral characteristics and nonlinear studies of acridine orange dye. Phys Lett A. 2005; 341: p. 454-458.

222. Krolenko S, Adamyan S, Belyaeva T, Mozhenok T. Acridine orange accumulation in acid organelles of normal and vacuolated frog skeletal muscle fibres. Cell Biol Int.

2006; 30: p. 933-939.

223. Pjura P, Grzeskowiak K, Dickerson R. Binding of Hoechst 33258 to the minor groove of B-DNA. J Mol Biol. 1987; 197: p. 257-271.

224. Haugland R. Handbook of Fluorescent Probes and Research Chemicals. 8th ed. Eugene, OR: Molecular Probes; 2001.

225. Vermes I, Haanen C, Steffens-Nakken H, Reutelingsperger C. A novel assay for apoptosis. Flow cytometric detection of phosphatidylserine expression on early apoptotic cells using fluorescein labelled Annexin V. J Immunol Methods. 1995; 184: p. 39-51.

226. Moore A, Donahue C, Bauer K, Mather J. Simultaneous measurement of cell cycle and apoptotic cell death. Methods Cell Biol. 1998; 57: p. 265-278.

227. Vorster C, Joubert A. In vitro effects of 2-methoxyestradiol-bis-sulphamate on cell growth, morphology and cell cycle dynamics in the MCF-7 breast adenocarcinoma cell line. Biocell. 2010; 34(2): p. 71-79.

228. Vorster C, Joubert A. In vitro effects of 2-methoxyestradiol-bis-sulphamate on the non-tumorigenic MCF-12A cell line. Cell Biochem Funct. 2010; 28(5): p. 412-419.

229. Vorster C, Stander A, Joubert A. Differential signaling involved in Sutherlandia frutescens-induced cell death in MCF-7 and MCF-12A cells. J Ethnopharmacol. 2012;

140: p. 123-130.

230. Visagie M, Joubert A. In vitro effects of 2-methoxyestradiol-bis-sulphamate on reactive oxygen species and possible apoptosis induction in a breast adenocarcinoma cell line. Cancer Cell Int. 2011; 11(1): p. 43.

231. Visagie M, Joubert A. 2-Methoxyestradiol-bis-sulphamate refrains from inducing apoptosis and autophagy in a non-tumorigenic breast cell line. Cancer Cell Int. 2012; 12(1): p. 37.

232. Ho Y, Newman S, Purohit A, Leese M, Potter B, Reed M. The effects of 2-methoxy oestrogens and their sulphamoylated derivatives in conjunction with TNF-alpha on endothelial and fibroblast cell growth, morphology and apoptosis. J Steroid Biochem Mol Biol. 2003; 86: p. 189-196.

233. Lee Y, Ting C, Cheng Y, Fan T, Wong R, Lung M, et al. Mechanisms of 2-methoxyestradiol-induced apoptosis and G2/M cell-cycle arrest of nasopharyngeal carcinoma cells. Cancer Lett. 2008; 268: p. 295-307.

234. Thaver V, Lottering M, van Papendorp D, Joubert A. In vitro effects of 2-methoxyestradiol on cell numbers, morphology, cell cycle progression, and apoptosis induction in oesophageal carcinoma cells. Cell Biochem Funct. 2009; 27: p. 205-210.

235. Gireesh K, Rashid A, Chakraborti S, Panda D, Manna T. CIL-102 binds to tubulin at colchicine binding site and triggers apoptosis in MCF-7 cells by inducing monopolar

and multinucleated cells. Biochem Pharmacol. 2012; 84: p. 633-645.

236. Sherwood S, Sheridan J, Schimke R. Induction of apoptosis by the anti-tubulin drug Colcemid: relationship of mitotic checkpoint control to the induction of apoptosis in HeLa S3 cells. Exp Cell Res. 1994; 215: p. 373-379.

237. Hwang J, Takagi M, Murakami H, Sekido Y, Shin-ya K. Induction of tubulin polymerization and apoptosis in malignant mesothelioma cells by a new compound JBIR-23. Cancer Lett. 2011; 300: p. 189-196.

238. Tai J, Cheung S, Hasman D. In vitro culture studies of Sutherlandia frutescens on human tumor cell lines. J Ethnopharmacol. 2004; 93(1): p. 9-19.

239. Stander A, Marais S, Stivaktas V, Vorster C, Albrecht C, Lottering M, et al. In vitro effects of Sutherlandia frutescens water extracts on cell numbers, morphology, cell cycle progression and cell death in a tumorigenic and a non-tumorigenic epithelial breast cell line. J Ethnopharmacol. 2009; 124: p. 45-60.

240. Skerman N, Joubert A, Cronjé M. The apoptosis inducing effects of Sutherlandia spp. extracts on an oesophageal cancer cell line. J Ethnopharmacol. 2011; 137: p. 1250-1260.

241. Albrecht C, Stander M, Grobbelaar M, Colling J, Kossmann J, Hills P, et al. LC–MS-based metabolomics assists with quality assessment and traceability of wild and

cultivated plants of Sutherlandia frutescens (Fabaceae). SA J Bot. 2012; 82: p. 33-45.

242. Mncwangi N, Viljoen A. Quantitative variation of amino acids in Sutherlandia frutescens (Cancer bush)—towards setting parameters for quality control. SA J Bot. 2012; 82: p. 46-52.

243. Luo S, Garcia-Arencibia M, Zhao R, Puri C, Toh P, Sadiq O, et al. Bim Inhibits Autophagy by Recruiting Beclin 1 to Microtubules. Mol Cell. 2012; 47: p. 359-370.